

Thiophene-Based Polymers and Oligomers for Organic Semiconductor Applications

Dissertation

zur Erlangung des akademischen Grades

Doktor der Naturwissenschaften
(Dr. rer. nat.)

eingereicht im Fachbereich C – Mathematik und Naturwissenschaften der
Bergischen Universität Wuppertal

von

Torsten W. Bünnagel

aus Düsseldorf

Wuppertal, April 2008

Die Dissertation kann wie folgt zitiert werden:

urn:nbn:de:hbz:468-20080738

[<http://nbn-resolving.de/urn/resolver.pl?urn=urn%3Anbn%3Ade%3Ahbz%3A468-20080738>]

Berichte aus der Chemie

Torsten W. Bünnagel

**Thiophene-Based Polymers and Oligomers for
Organic Semiconductor Applications**

Shaker Verlag
Aachen 2008

Bibliographic information published by the Deutsche Nationalbibliothek

The Deutsche Nationalbibliothek lists this publication in the Deutsche Nationalbibliografie; detailed bibliographic data are available in the Internet at <http://dnb.d-nb.de>.

Zugl.: Wuppertal, Univ., Diss., 2008

Copyright Shaker Verlag 2008

All rights reserved. No part of this publication may be reproduced, stored in a retrieval system, or transmitted, in any form or by any means, electronic, mechanical, photocopying, recording or otherwise, without the prior permission of the publishers.

Printed in Germany.

ISBN 978-3-8322-7793-2

ISSN 0945-070X

Shaker Verlag GmbH • P.O. BOX 101818 • D-52018 Aachen

Phone: 0049/2407/9596-0 • Telefax: 0049/2407/9596-9

Internet: www.shaker.de • e-mail: info@shaker.de

Meinen Eltern in Dankbarkeit

Stets findet Überraschung statt
Da, wo man's nicht erwartet hat.

Wilhelm Busch

Musik wird oft nicht schön gefunden,
weil sie stets mit Geräusch verbunden.

Wilhelm Busch

contact: torsten@buennagel.net

info & CV: <http://www.buennagel.net>

Die hier zugrunde liegende Arbeit wurde in der Zeit vom Juli 2004 bis April 2007 am Lehrstuhl für Makromolekulare Chemie des Fachbereiches C – Mathematik und Naturwissenschaften der Bergischen Universität Wuppertal unter Anleitung von Prof. Dr. U. Scherf angefertigt.

Mein besonderer Dank gilt Herrn Prof. Dr. U. Scherf für die Überlassung des interessanten und fruchtbaren Themas dieser Arbeit, seine stete Diskussionsbereitschaft sowie seine vielfältige persönliche Unterstützung.

1. Gutachter:	Prof. Dr. U. Scherf (Wuppertal)
2. Gutachter:	Prof. Dr. D. Vanderzande (Hasselt, Belgium)
Eingereicht am:	16. April 2008
Mündliche Prüfung am:	04. Juli 2008

Abstract

Conjugated oligomers and polymers have been the subject of extensive academic and industrial research efforts due to their promising potential for use as active semiconducting components, which has led to their use in the fabrication of optoelectronic and electronic devices, photovoltaic cells, chemical and biosensors. In these various applications it has been found that, in addition to the intrinsic chemical and physical properties of the polymers and additives, the device performance is strongly dependent on the morphology of the film in which the polymer is cast. This work presents several synthetic approaches to alter the electronic properties of various thiophene-containing oligomers and polymers. Special attention was, therefore, given to synthetic attempts to flatten the backbone structure of the molecules.

Chapter 2 describes the incorporation of phenylene and naphthalene moieties into novel thiophene-based step-ladder polymers. The optical and electronic properties have been investigated both for the homopolymers and corresponding, alternating copolymers containing additional oligothiophene units. Further investigations were performed on the temperature dependency of their optical properties. Oligomeric model compounds have been generated to obtain a deeper insight into structure-property relations of the novel polymers and copolymers. Some of the polymers (phenylene-based step-ladder materials) have been investigated as the active layer of organic field effect transistors (OFETs).

Chapter 3 presents a series of novel phenylene-vinylene-oligothiophene-based oligomers synthesized via a final formation of the vinylene double bonds. The optical properties of the oligomers have been investigated with respect to their behavior at different temperatures and in solution/solid state. The electronic properties of the materials as active layers in OFETs have been examined utilizing variations of substrates and processing methods. Finally, the surface morphology of oligomer films has been examined by AFM measurements.

A full planarization of dialkyl cyclopentadithiophene-based homo polymers (cyclopentadithiophene = CPDT) was accomplished by introduction of an olefinic substituent in the 4-position of the system. In Chapter 4 different polymerization methods are reported as well as characterization of the optical and electronic properties of the resulting poly(alkylidene-cyclopentadithiophene)s.

The last chapter presents an outlook towards cross-coupling reactions of the prior described CPDT and new thiophene/carbazole-based monomers (dithienopyrrole) with dibromo benzothiadiazole to give novel donor-acceptor copolymers.

Inhaltsangabe

Konjugierte Oligomere und Polymere wurden in den letzten Jahren intensiv sowohl in der akademischen als auch in der industriellen Forschung als viel versprechende, halbleitende Materialien im Bereich der Optoelektronik, Photovoltaik, Transistortechnik und Sensorik untersucht. In diesen Untersuchungen wurde herausgefunden, dass die Qualität der Bauelemente nicht nur von den chemischen und physikalischen Eigenschaften der Polymere und der weiteren verwendeten Materialien (Additive) abhängt, sondern besonders auch von der Morphologie der Polymere im Film. In dieser Arbeit werden verschiedene Methoden vorgestellt, um sowohl die elektronischen Eigenschaften von Thiophen-basierten, polymeren Materialien zu modifizieren als auch die Strukturbausteine der Polymere in eine planare Konfiguration einzubinden.

In Kapitel 2 werden Phenyl- und Naphthalin-Bausteine enthaltende Oligothiophen-basierte Stufenleiterpolymere vorgestellt. Die optischen und elektronischen Eigenschaften der Homopolymere und analoger, alternierender Copolymere mit zusätzlichen Oligothiophen-Einheiten werden beschrieben und diskutiert. Weitere Untersuchungen wurden in Bezug auf die Temperaturabhängigkeit der optischen Eigenschaften durchgeführt. Die Synthese von Modelverbindungen ermöglichte eine detaillierte Strukturanalyse der Monomerbausteine. Die Phenyl-basierten Stufenleiterpolymere wurden auf ihre Eignung als halbleitende Schicht in organischen Feld-Effekt-Transistoren (OFETs) getestet.

In Kapitel 3 wird eine Serie von Phenyl-Vinyl-Oligothiophen-basierten Oligomeren vorgestellt und ihre optischen Eigenschaften bei verschiedenen Temperaturen und in Lösung/Film berichtet. Darüber hinaus wurden die elektrischen Eigenschaften der Oligomere als aktive Halbleiterschicht in OFETs unter Verwendung von verschiedenen Substraten und Fabrikationsbedingungen getestet. Ebenfalls erfolgt eine Charakterisierung der Morphologie der Filme unter Verwendung der AFM (atomic force microscopy).

Eine vollständige Planarisierung von Dialkylcyclopentadithiophen-Bausteinen (CPDT) für entsprechende Homopolymere erfolgt durch die Einführung eines exocyclischen, olefinischen Substituenten in 4-Position des CPDT-Ringsystems. In Kapitel 4 werden sowohl verschiedene Synthesemethoden für Poly(alkyliden-cyclopentadithiophen)e als auch die optischen und elektronischen Eigenschaften dieser Materialien diskutiert.

Das letzte Kapitel gibt einen Ausblick auf Aryl-Aryl-Kreuzkupplungen der zuvor beschriebenen CPDT sowie neu synthetisierter Thiophen/Carbazol-basierter Monomere (Dithienopyrrol) mit Dibrombenzothiadiazol zu neuartigen Donor-Akzeptor Copolymeren.

Table of Contents

1 GENERAL INTRODUCTION	1
1.1 CONJUGATED POLYMERS AS ORGANIC SEMICONDUCTORS: CONTROLLING THE BAND GAP	2
1.2 POLYTHIOPHENES	5
1.3 SYNTHETIC METHODS	6
1.3.1 <i>Metal Catalyzed Cross-Coupling Reactions</i>	6
1.3.2 <i>Microwave Assisted Synthesis</i>	10
1.4 AIM AND SCOPE	12
1.5 REFERENCES AND NOTES.....	14
2 THIOPHENE-PHENYLENE/NAPHTHALENE-BASED STEP-LADDER COPOLYMERS.....	21
2.1 INTRODUCTION AND MOTIVATION	21
2.2 THIOPHENE-PHENYLENE-BASED MATERIALS: RESULTS AND DISCUSSION.....	22
2.2.1 <i>Monomer and Polymer Synthesis</i>	22
2.2.2 <i>Optical Spectroscopy</i>	26
2.3 SYNTHESIS AND CHARACTERIZATION OF MODEL COMPOUNDS	29
2.3.1 <i>Optical Spectroscopy</i>	30
2.3.2 <i>Crystallographic Investigations</i>	31
2.3.3 <i>OFET Investigations</i>	32
2.3.4 <i>Thermal Properties</i>	34
2.4 THIOPHENE-NAPHTHALENE-BASED MATERIALS: RESULTS AND DISCUSSION	34
2.4.1 <i>Monomer and Polymer Synthesis</i>	34
2.4.2 <i>Optical Spectroscopy</i>	36
2.5 CONCLUSION.....	40
2.6 EXPERIMENTAL SECTION	41
2.6.1 <i>Monomer Synthesis</i>	41
2.6.2 <i>Polymer Synthesis</i>	48
2.6.3 <i>Synthesis of Model Compounds</i>	53
2.7 REFERENCES AND NOTES.....	55

3	PHENYLENE-THIENYLENE-VINYLENE-BASED OLIGOMERS.....	59
3.1	INTRODUCTION AND MOTIVATION	59
3.2	RESULTS AND DISCUSSION	60
3.2.1	<i>Precursor Synthesis</i>	60
3.2.2	<i>Oligomer Synthesis</i>	61
3.2.3	<i>Optical Spectroscopy</i>	62
3.2.4	<i>OFET Investigations</i>	67
3.2.5	<i>AFM Investigations</i>	70
3.3	CONCLUSION.....	72
3.4	EXPERIMENTAL SECTION	73
3.5	REFERENCES AND NOTES.....	78
4	ALKYLIDENECYCLOPENTADITHIOPHENE - HOMOPOLYMERS.....	83
4.1	INTRODUCTION AND MOTIVATION	83
4.2	RESULTS AND DISCUSSION	84
4.2.1	<i>Monomer and Polymer Synthesis</i>	84
4.2.2	<i>Alkylidenecyclopentadithiophene monomers via a Gignard-type reaction</i>	84
4.2.3	<i>Alkylidenecyclopentadithiophene via a Horner-Wittig-type reaction</i>	85
4.2.4	<i>Alkylidenecyclopentadithiophene via a Knoevenagel-type reaction</i>	86
4.2.5	<i>Successful Synthesis of Alkylidenecyclopentadithiophene via a Dimethylated Thioacetal Intermediate</i>	86
4.2.6	<i>Optical Spectroscopy</i>	88
4.2.7	<i>Electrical Properties</i>	89
4.3	CONCLUSION.....	90
4.4	EXPERIMENTAL SECTION	90
4.5	REFERENCES AND NOTES.....	95
5	FUSED-RING DITHIOPHENES – ALTERNATING DONOR- ACCEPTOR COPOLYMERS... 99	
5.1	INTRODUCTION AND MOTIVATION	99
5.2	RESULTS AND DISCUSSION	100
5.2.1	<i>Monomer and Polymer Synthesis</i>	100
5.3	CONCLUSION.....	104
5.4	EXPERIMENTAL SECTION	104
5.5	REFERENCES AND NOTES.....	108
6	ACKNOWLEDGEMENTS	113

1 General Introduction

As a novel and very promising class of materials, conjugated semiconducting polymers combine the optical and electronic properties of semiconductors with the processing advantages and special mechanical properties of polymers. As a result, the research devoted to the synthesis of conjugated oligomers and polymers has experienced a dramatic increase in the past years.^[1-6] The development of substituted conjugated polymers has been the focus of much synthetic research and allows for tuning of the electronic properties by molecular engineering. The synthetic flexibility, the potential ease of processing, e.g. after attaching solubilizing side chains and the possibility of an exact tailoring of the electronic and mechanical properties to accomplish a desired function makes semiconducting organic oligomers and polymers attractive candidates for future applications in electronic devices.^[2, 7-13]

Variation of the conjugated backbone structure of poly(*para*-phenylene)s, poly(*para*-phenylenevinylene)s, polythiophenes or polyfluorenes has been shown to dramatically influence the polymers' electronic properties. For instance, a large number of polythiophenes with varying side chain structure have been synthesized and structure-property relationships investigated with a focus on solubility/processability issues and the environmental stability. Minor changes in the design of the polymeric backbone as well as the structure of the side chains can dramatically influence the characteristics of the polymer. Changes in the substituents are often made to make the materials more suitable for applications, e.g. in polymer electronic devices such as organic field effect transistors (OFET),^[13-15] organic light emitting diodes (OLED),^[16, 17] and photovoltaic devices.^[18-21]

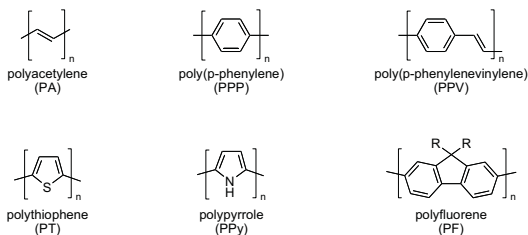


Figure 1.1. Chemical structure of some common π -conjugated polymers.

Apart from the structure-property discussion with regard to potential applications in devices, there are also scientific questions with regard to basic physical and chemical concepts.^[22, 23] One problem concerns the relation of the materials' electronic properties, such as charge carrier mobility and size

of the electronic band gap, to the geometry of the molecules. Special attention is paid to the band gap energy as it is considered to be a crucial factor in tuning the intrinsic electronic and optical properties. Therefore, it is of particular importance to understand the evolution of the band gap energy of conjugated materials based on their chemical structure.

1.1 Conjugated Polymers as Organic Semiconductors: Controlling the Band Gap

As conjugated polymers have their electrons organized in bands rather than in discrete energy levels and their ground state energy bands are either completely filled or completely empty, organic semiconductors hardly differ from inorganic *semiconductors* with respect to their electronic energy levels. The band structure of conjugated polymers originates from an interaction of the π -orbitals within the repeat unit throughout the main chain, which was shown by theoretical studies comparing the calculated energy levels as a function of oligomer length for oligothiophenes with $n = 1-4$ and polythiophene.^[24]

Starting from a single “monomer” unit addition of each new repeat unit causes additional hybridization of the energy levels until the overlap of the energetic levels results in bands rather than discrete levels (Figure 1.2). As is the case for inorganic semiconductors, the highest occupied band is called the valence band, while the lowest unoccupied band is called the conduction band, originating from the HOMO and the LUMO levels of the monomer units respectively, while the energy difference E_g is called the band gap. Due to the delocalization of the π -electrons, conjugated polymers display semiconducting properties in their electro-neutral state and the ability to support the transport of charge carriers. When the molecular structure is considered, both oligomers and polymers with a narrow band gap (1.5 - 3.0 eV) represent a fruitful approach towards novel materials for electronic applications.^[25]

A versatile variation of the band gap energy can be obtained by smart modification of the macromolecular structure, e. g. by tuning the electronic properties a) towards small band gaps suitable for so-called synthetic metals or infrared emitting polymers, or b) towards a larger band gap for a use as UV or blue emitting polymers. By changing subtle structural features of the oligomer or polymer, like the regioregularity or arrangement and distribution of the chromophoric units, it is possible to design a broad range of polymers with different band gap energies from a basic conjugated structure. Polythiophenes are one of the most prominent of the investigated examples, their band gap energy can be tuned throughout the whole UV/Vis spectrum from the UV

to the near IR (NIR) by variation of the substituents attached in 3 and/or 4 - position of the thiophene ring, depending on the inductive/ mesomeric effects towards the main chain.^[26, 27]

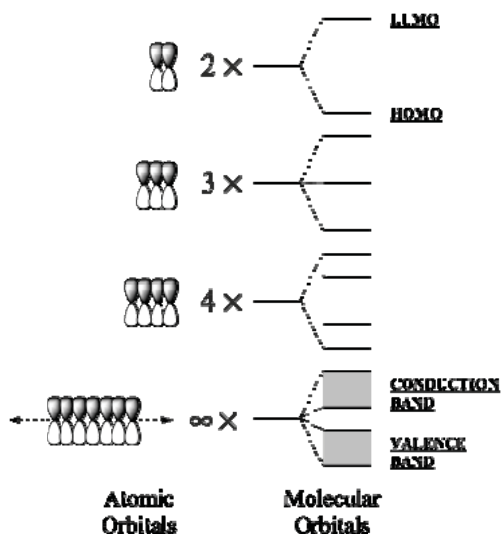


Figure 1.2. Energy band structure of conjugated polymers emerging from the energetic splitting upon addition of an increasing number of atomic orbitals.

In addition to the imminent influence of substituents, the so-called effective conjugation length is an important factor determining the electronic and electrochemical properties of organic semiconductors. Extended conjugation implies wider bands and a narrower band gap in the resulting semiconducting polymer. Therefore, the absorption of a conjugated polymer is red-shifted with an increasing degree of polymerization (DP) up to a certain DP above which no further red shift is observed. This threshold is described as the effective conjugation length. The convergence of the band gap energy for oligothiophenes was investigated by Bäuerle *et al* amongst others. They observed no further changes of the optical properties once the chain had reached 16 repeat units.^[28, 29]

Furthermore, the band gap energy is strongly dependent on the so-called bond length alternation (BLA), which refers to the energetic difference between single and double bonds.^[30-34] As a result, polyaromatic polymers differ from their non-aromatic counterparts (CH)_x as they have a non degenerate ground state. The competing benzoic and quinoid energy states are energetically

inequivalent, resulting in a smaller resonance energy for the quinoid form. Stabilization of the quinoid resonance structure of conjugated oligomers and polymers is of particular importance since it underlies most of the attempts to synthesize low band gap polymers.

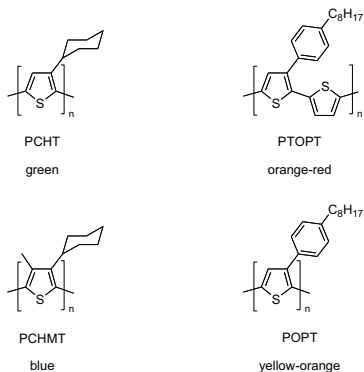


Figure 1.3. Examples of band gap energy tuning for polythiophenes (the photoluminescence emission color of the polymers is given underneath).

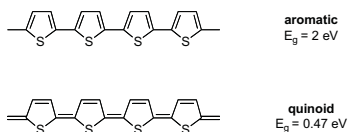


Figure 1.4. The aromatic form allows the thiophenes to rotate with a certain degree of rotational freedom while the quinoid form forces the rings to align in a planar conformation.

One of the factors determining the energy levels of conjugated polymers is the rotation between neighboring aromatic units around the single bonds with its distinct influence on the effective conjugation length. In the aromatic resonance state (ground state), the repulsion of (bulky) ortho-side groups often leads to a non-planar backbone. The consequent reduced overlap of the π -orbitals, which is proportional to the cosine of the twist angle (\angle), results in an increased band gap energy.^[35, 36] A second factor is the aromaticity of the monomeric units, which results in a competition between confinement of the π -electrons within the aromatic rings and delocalization along the π -conjugated chain.^[37] Therefore, to obtain a low band gap energy it is desirable to induce coplanarity of the building blocks along the π -conjugated chain, which can be achieved by an appropriate choice of substituents, fused ring systems, or the introduction of additional covalent bonds to rigidify the conjugated backbone in so-called step-ladder or ladder-type structures.

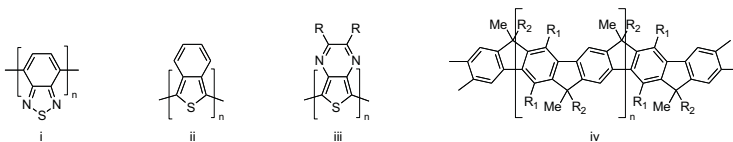


Figure 1.5. Common fused-ring systems for low bandgap-polymers: (i) poly-(benzothiadiazole), (ii) poly(isothianaphthalene) (PITN),^[38, 39] (iii) poly(thieno-pyrazine),^[40] as well as a ladder-type poly(*para*-phenylene): (iv) methyl-substituted ladder-type poly(*para*-phenylene) (MeLPPP)^[41]

1.2 Polythiophenes

Polythiophenes (PTs) represent one of the most important classes of π -conjugated polymers, because they meet the essential requirements of solubility and processability and offer the possibility of structural modifications by incorporation of a wide variety of side-chain functionalities.^[42] Furthermore, they exhibit an acceptable environmental stability. The intrinsically low aromatic resonance energy of the thiophene ring allows for distinct variations of the band gap energy. Many examples of synthetic approaches to accomplish this have been developed during the last decade. As mentioned before, the band gap of a PT is strongly influenced by the molecular structure (geometry). Favoring the quinoid resonance structure of polythiophenes (e.g. in fused-ring systems as PITN) leads to an increasing rigidification and planarization of the backbone since the rotation between the rings becomes more and more restricted (Figure 1.4).

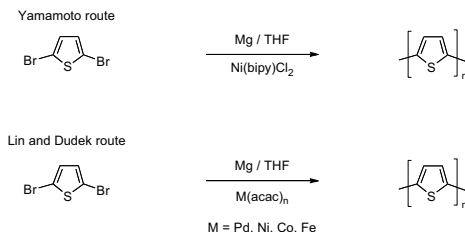
The extent of the effective π -conjugation along the PT-backbone is also much dependent on the length and structural regularity of the polymer chain.^[43-51] In summary, the amount of π -overlap is influenced both by the synthesis as well as the processing methods applied during material and device fabrication since the formation of π -stacks in the solid state is strongly influenced by the processing procedure during device fabrication.^[22]

1.3 Synthetic Methods

1.3.1 Metal Catalyzed Cross-Coupling Reactions

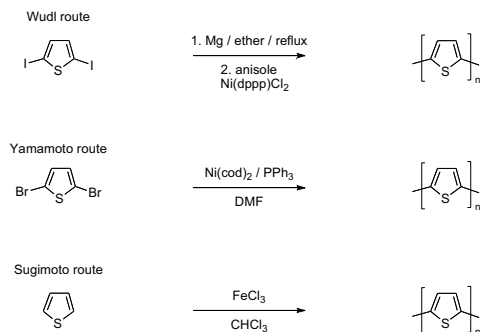
While much early effort was devoted to optimize the processes for electrochemical polymerization of thiophenes,^[52-59] most of the now commercially available polythiophenes (PT) are prepared by a wide variety of chemical pathways utilizing metal-catalyzed coupling strategies. In 1980 two research groups reported independently on the first chemical preparation of unsubstituted PT.^[60, 61] Both groups used an extension of the Kumada coupling of Grignard reagents with aryl halides,^[62] treating

2,5-dibromo-thiophene with stoichiometric amounts of Mg in THF to yield the appropriate mono-Grignard reagent followed by subsequent homo-coupling of the difunctional intermediate utilizing a) Ni(bipy)Cl₂ as a catalyst in the route proposed by Yamamoto *et al.*^[61] or b) Ni(acac)₂, Pd(acac)₂, Co(acac)₂, or Fe(acac)₃ as reported by Lin and Dudek.^[60] These routes gave unsubstituted PT with only the low molecular weight fraction being soluble in common organic solvents and significant amounts up to 3% of residual metal impurities.



Scheme 1.1. The first chemical synthesis of unsubstituted polythiophene.

Much work was then undertaken to improve the purity and molecular weight by variation of the solvent and reagents' concentrations, catalysts and reaction conditions.^[62-68] A major improvement was reported by Wudl *et al.* as the poorly soluble Grignard reagent was simply isolated and afterwards redissolved in hot anisole to carry out the Kumada-type reaction utilizing Ni(dppp)Cl₂ as a catalyst.^[69] A second approach to minimize the metal content was carried out using a Yamamoto-type coupling reaction starting from 2,5-dibromothiophene and Ni(COD)₂/triphenylphosphine as the catalytic system in DMF.^[67] Both strategies gave PTs in good yields and high purities with less than 50 ppm residual metal. However, the applied reaction conditions led to a certain amount of desulfurization which then resulted in a significant drop of the conductivity for solid PT films.^[62]



Scheme 1.2. Additional approaches towards unsubstituted polythiophene.

To increase the solubility and, therefore, improve the molecular weight and processability, the introduction of solubilizing side chains longer than butyl was necessary.^[70-72] The first successful synthesis of poly(alkylthiophene)s was reported by Elsenbaumer *et al.* (Scheme 1.3) and again achieved via a Kumada-type cross-coupling protocol similar to the previously described methods used for unsubstituted polythiophenes.^[70-72]

A second approach was reported by Sugimoto *et al.* via oxidative polymerization of unsubstituted, as well as 3-alkyl-substituted, thiophene monomers, utilizing FeCl_3 as oxidizing agent in chloroform and subsequent dedoping of the material after isolation.^[73-75] Although, this strategy produces soluble poly(alkylthiophene)s (PAT) in moderate yields and high molecular weight with sufficient purity, the oxidative coupling method did not show good reproducibility.^[75]

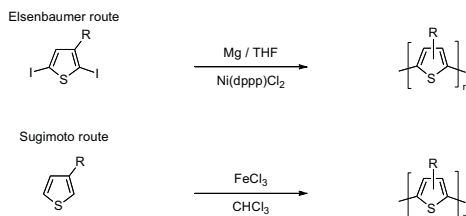
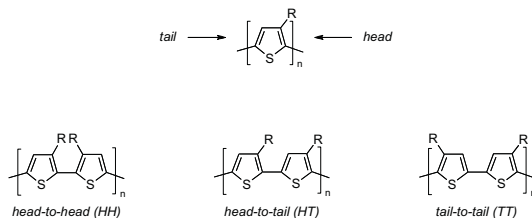


Figure Scheme 1.3. Synthetic pathways towards poly(3-alkylthiophene) (PAT).

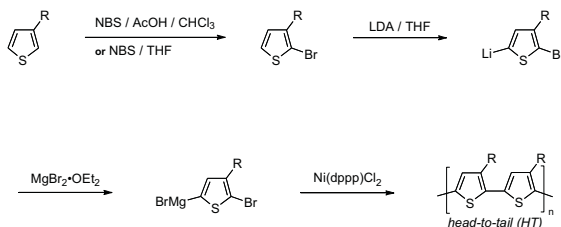
Further structural investigations revealed that the methods described above produce 2,5-linked PATs, exclusively, which should lead to high performance conjugated materials without 2,4-links as structural defects, which interrupt the main-chain conjugation. As 3-alkylthiophene is not a symmetrical molecule, three variations of the relative orientation of the building blocks are possible

for the coupling of two 3-alkyl-thiophene rings. In a stereoirregular coupling, the resulting polymer randomly contains head-to-head (HH), head-to-tail (HT), and tail-to-tail (TT) coupled repeat units.^[76, 77]



Scheme 1.4. Regiochemical dyads of regioregular poly(alkylthiophene)s (PATs).

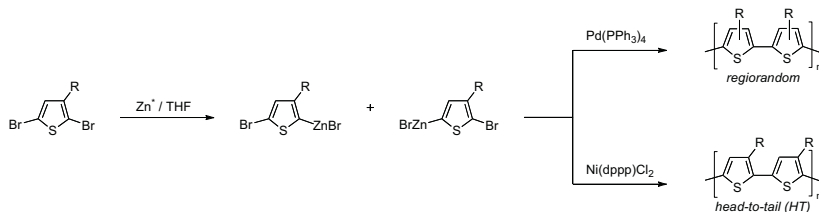
Electrochemical polymerization experiments using alkylthiophene dimers with predefined substitution patterns performed by Wudl *et al.* revealed that a higher degree of regioregularity within the resulting PATs is superior in its electronic performance (electrical conductivity of doped polymers) over the irregular material.^[78] The results were explained by a minimization of the sterical repulsion of ortho-substituents resulting in a less-twisted polymer backbone and therefore, as mentioned before, a higher degree of π -conjugation along the main chain.^[79-81] Consequently, fully HT-coupled PATs, denoted as regioregular PAT or P3AT, should be preferred over stereoirregular PAT to give a coplanar conformation.^[82, 83]



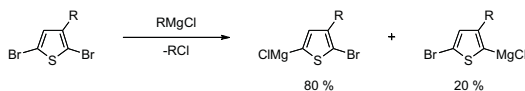
Scheme 1.5. The first method for the synthesis of regioregular poly(3-alkylthiophene)s after McCullough *et al.*

The generation of regioregular PATs has been demonstrated in the pioneering work of McCullough *et al.*, who reported their first synthesis via a generation of regiodefined 2-bromo-5-(bromomagnesio)-3-alkylthiophene followed by a Kumada-type cross-coupling protocol, resulting in P3ATs with nearly 100 % HT coupled repeat units.^[84] Further attempts were published by Rieke *et al.* by modifying the organometallic substituent utilizing activated “Rieke-zinc” (Zn^*) as

metalating agent.^[85-88] The choice of the catalyst used in the aryl-aryl-coupling can either lead to regiorandom $[\text{Pd}(\text{PPh}_3)_4]$ or regioregular $[\text{Ni}(\text{dppf})\text{Cl}_2]$ PATs.^[89]



Scheme 1.6. The Rieke method produces either regiorandom or HT-PATs depending on the choice of the utilized catalyst.

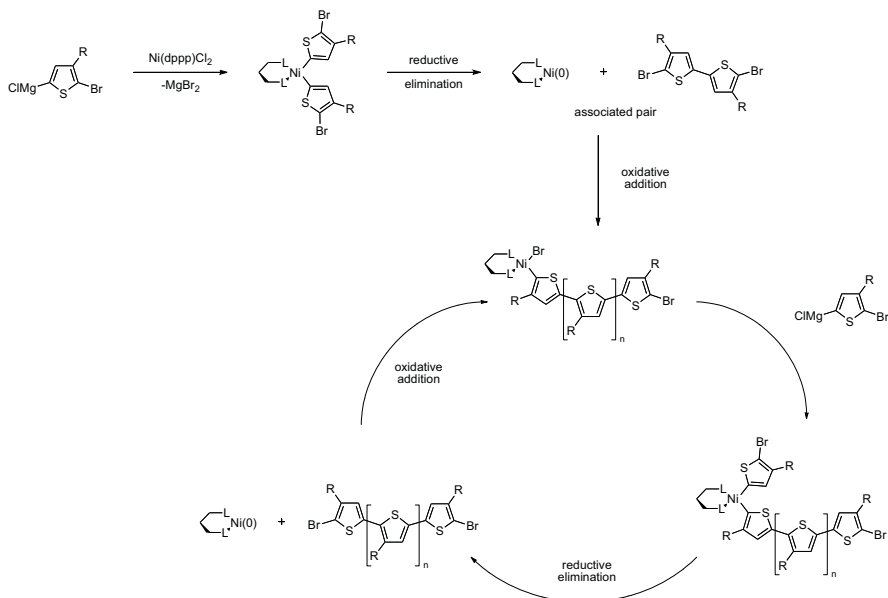


Scheme 1.7. Halogen-metal exchange reaction in the Grignard metathesis (GRIM) procedure after McCullough *et al.*

To overcome the drawbacks of these methods (multistep procedure in the case of the McCullough method, use of dangerous “Rieke-zinc” in the Rieke method) McCullough *et al.* developed the so-called GRIM (Grignard metathesis) scheme which allows for the generation of regioregular PATs with high molecular weight (M_n up to 40,000 g/mol) and narrow polydispersity in a relatively simple fashion.^[90-92] Similar to the Rieke method, the Grignard metathesis procedure starts from 2,5-dibromo-3-alkylthiophene, which undergoes a halogen-metal exchange reaction when treated with 1 eq. of RMgCl (R = alkyl) (Scheme 1.7).^[90] The reaction proceeds with a moderate degree of regioselectivity (80 : 20) at room temperature regardless of the Grignard reagent employed.^[91, 92]

Further studies revealed that only the Grignard reagent metalated in the 5-position is involved in the polymerization sequence while the other isomer is not consumed.^[90] Utilizing a nickel-based coupling catalyst and bulky ligands favors the transformation of the less sterically hindered 5-position and results in 95-99% HT-couplings. In the initial reaction step of the catalytic cycle 2-bromo-5-chloro-magnesium-3-alkylthiophene undergoes reductive elimination resulting in the formation of 5,5'-dibromobithienyl (TT-coupling) and $\text{Ni}(0)$ (Scheme 1.8).^[90] The dimer undergoes a fast oxidative addition to a $\text{Ni}(0)$ center followed by transmetalation with another molecule of the Grignard reagent and chain-forming reductive elimination. Due to the highly regioselective HT-

type fashion of the GRIM reaction, the formation of the initial TT-dyad remains the only structural defect within a single polymer chain.^[90]



Scheme 1.8. Mechanism of the so-called Grignard metathesis (GRIM) coupling in the synthesis of regioregular poly(3-alkylthiophene) (P3HT).

1.3.2 Microwave Assisted Synthesis

Within the last years, the use of microwave radiation as a heat source has become increasingly popular in organic synthesis,^[93] since the first successful syntheses were reported in 1986 by the groups of Giguere and Gedye.^[94, 95] Especially in the field of polymer synthesis, speeding up the reaction time from hours or days to minutes to produce the polymeric materials in high yields with a minimized rate of side products by employing microwave radiation is an undeniable advantage over conventional methods. The use of modern monomode microwave reactors that allow monitoring of temperature, pressure, stirring, and radiation levels has proven superior over multimode microwave sources in respect of controlling the reaction and furthermore, increasing security and reproducibility. A schematic setup of the monomode microwave reactor “Discover[®]” fabricated by CEM is depicted in Figure 1.6.

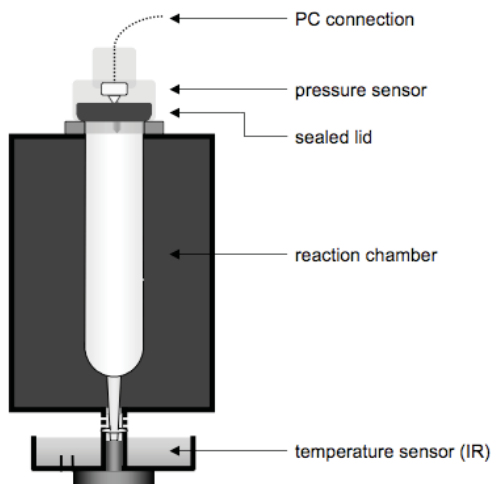
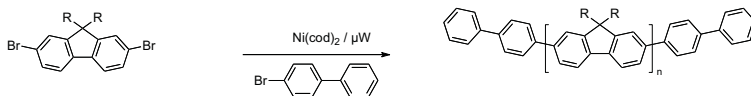


Figure 1.6. Schematic design of a monomode microwave reactor.

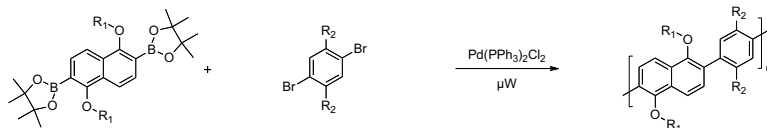
Microwave assisted chemistry gives access to high operating temperatures and elevated pressures that can be reached within a fraction of the time needed by conventional heating. Sealed vessels allow the reaction to be driven under conditions well above the boiling temperature of the solvent under atmospheric conditions. The method allows a broad variety of common organic solvents that are well established in the conventional procedures to be utilized, as long as they are amenable to microwave heating, which is determined by their (high) dielectric constant.^[96] The response to microwave heating can also be increased by polar additives like ionic liquids or - if the reaction conditions allow - simply water.^[97] To prevent the formation of “hot nuclei” and therefore, non-uniform heating within the vessel efficient stirring is essential.

The first microwave-assisted aryl-aryl coupling reaction was published in 2002 by Ken Carter *et al.* 2,7-Dibromo-9,9-dihexylfluorene was reacted in a Ni(0)-mediated Yamamoto-type coupling protocol and gave the polymer [poly(9,9-dihexylfluorene)] with high molecular weights (M_n up to 100,000 g/mol) in a very short reaction time of only 10 min.^[98] For comparison, the conventional synthesis utilizes reaction times of several days. Later optimizations by the groups of Yamamoto and Scherf achieved a further improvement in molecular weights by changing the solvent from DMF to THF.^[99, 100] In 2004 Scherf *et al.* reported the first synthesis of aromatic polymers via Pd-catalyzed Suzuki-type and Stille-type cross-coupling reactions utilizing a microwave reactor as a heat source.

Yamamoto-type coupling, Carter, 2002



Suzuki-type coupling, Scherf, 2004



Stille-type coupling, Scherf, 2004



Stille-type coupling, McCulloch, 2005



Scheme 1.9. First examples of microwave-assisted cross-coupling reactions via modification of the standard cross-coupling protocols.

They demonstrated that the modified reaction conditions had no effect on the quality of the produced materials.^[101] McCulloch *et al.* extended this method to the synthesis of soluble polythiophenes in 2005. The procedure allowed the polymer to be obtained in higher molecular weight (>15,000) and narrower polydispersity when compared to conventional heating methods without a loss of the materials' performance in OFET devices.^[102]

1.4 Aim and Scope

The main focus of this work was the synthetic incorporation of various thiophene building blocks into oligomeric and polymeric π -conjugated systems with the intention to generate novel semiconducting materials for organic field effect transistors (OFETs) or organic photovoltaic devices (OPV devices).

Chapter 2 describes the synthesis of new step-ladder copolymers based on double-stranded phenylene-thiophene building blocks. The optical properties of these copolymers were investigated with respect to their thiophene content in a series of alternating copolymers composed of step-ladder and (oligo)thiophene building blocks with varied oligothiophene lengths. The novel

materials were then studied to determine their electronic properties in organic field effect transistors (OFETs). A related model compound has also been synthesized and characterized by X-ray crystallography in order to get a deeper insight into the molecular structure of step-ladder building blocks.

Chapter 2 also presents related step-ladder copolymers, where the 1,4-phenylene units have been replaced by 1,5-naphthylene moieties. The incorporation of naphthylene units was anticipated to allow some tuning of the optical and electronic properties of the material whilst maintaining the π -conjugation in the polymer chain.

The oligomers described in Chapter 3 represent a series of novel oligomeric materials based on phenylene and thiophene building blocks that are connected by vinylene bridges. The optical properties of these materials were determined as well as their characteristics in “small molecule”-based OFETs. The solid state structure in thin vacuum-deposited films has been investigated by AFM measurements.

In Chapter 4 the synthesis of a novel planarized derivative of the well-known 4,4-dialkyl-cyclopentadithiophene (CPDT) is reported. The oxidative coupling of the 4-alkylidene-cyclopentadithiophene monomers led to novel CPDT-type polymers with an improved solid state ordering as consequence of the fully planar backbone structure.

The final chapter (Chapter 5) presents an initial investigation into the development of dithienopyrrole monomers related to CPDT. Further coupling experiments using these monomers should lead to novel donor-acceptor-type copolymers suitable as active component of organic photovoltaic devices.

1.5 References and Notes

1. Grimdale, A. C.; Müllen, K., *Macromol. Rapid Commun.* **2007**, 28, (17), 1676.
2. Coropceanu, V.; Cornil, J.; da Silva, D. A.; Olivier, Y.; Silbey, R.; Bredas, J. L., *Chem. Rev.* **2007**, 107, (4), 926.
3. Gierschner, J.; Cornil, J.; Egelhaaf, H. J., *Adv. Mater.* **2007**, 19, (2), 173.
4. Chang, M. H.; Frampton, M. J.; Anderson, H. L.; Herz, L. M., *Phys. Rev. Lett.* **2007**, 98, (2), 027402.
5. Mart, H., *Des. Monom. Polym.* **2006**, 9, (6), 551.
6. Gholami, M.; Tykwinski, R. R., *Chem. Rev.* **2006**, 106, (12), 4997.
7. Roncali, J.; Leriche, P.; Cravino, A., *Adv. Mater.* **2007**, 19, (16), 2045.
8. Li, L. G.; Lu, G. H.; Yang, X. N.; Zhou, E. L., *Chin. Sci. Bull.* **2007**, 52, (2), 145.
9. Bag, D. S.; Rao, K. U. B., *J. Polym. Mater.* **2006**, 23, (3), 225.
10. Roncali, J., *Macromol. Rapid Commun.* **2007**, 28, (17), 1761.
11. Liang, Y. Y.; Wang, H. B.; Yuan, S. W.; Lee, Y. G.; Yu, L. P., *J. Mater. Chem.* **2007**, 17, (21), 2183.
12. Murphy, A. R.; Frechet, J. M. J., *Chem. Rev.* **2007**, 107, (4), 1066.
13. Facchetti, A., *Materials Today* **2007**, 10, (3), 28.
14. Bilge, A.; Zen, A.; Forster, M.; Li, H. B.; Galbrecht, F.; Nehls, B. S.; Farrell, T.; Neher, D.; Scherf, U., *J. Mater. Chem.* **2006**, 16, (31), 3177.
15. Park, Y. D.; Lim, J. A.; Lee, H. S.; Cho, K., *Materials Today* **2007**, 10, (3), 46.
16. Grigalevicius, S.; Ma, L.; Xie, Z. Y.; Scherf, U., *J. Polym. Sci., Part A* **2006**, 44, (20), 5987.
17. Koch, N., *ChemPhysChem* **2007**, 8, (10), 1438.

18. Gunes, S.; Neugebauer, H.; Sariciftci, N. S., *Chem. Rev.* **2007**, 107, (4), 1324.
19. Koppe, M.; Scharber, M.; Brabec, C.; Duffy, W.; Heeney, M.; McCulloch, I., *Adv. Funct. Mater.* **2007**, 17, (8), 1371.
20. Tsami, A.; Bunnagel, T. W.; Farrell, T.; Scharber, M.; Choulis, S. A.; Brabec, C. J.; Scherf, U., *J. Mater. Chem.* **2007**, 17, (14), 1353.
21. Waldauf, C.; Morana, M.; Denk, P.; Schilinsky, P.; Coakley, K.; Choulis, S. A.; Brabec, C. J., *Appl. Phys. Lett.* **2006**, 89, (23).
22. Zen, A.; Pflaum, J.; Hirschmann, S.; Zhuang, W.; Jaiser, F.; Asawapirom, U.; Rabe, J. P.; Scherf, U.; Neher, D., *Adv. Funct. Mater.* **2004**, 14, (8), 757.
23. Patil, A. O.; Heeger, A. J.; Wudl, F., *Chem. Rev.* **1988**, 88, (1), 183.
24. Salzner, U.; Lagowski, J. B.; Pickup, P. G.; Poirier, R. A., *Synth. Met.* **1998**, 96, (3), 177.
25. Thompson, B. C.; Kim, Y. G.; Reynolds, J. R., *Macromolecules* **2005**, 38, (13), 5359.
26. Granstrom, M.; Inganas, O., *Appl. Phys. Lett.* **1996**, 68, (2), 147.
27. Roncali, J., *Chem. Rev.* **1997**, 97, (1), 173.
28. Bäuerle, P.; Fischer, T.; Bidlingmeier, B.; Stabel, A.; Rabe, J. P., *Angew. Chem. - Int. Ed.* **1995**, 34, (3), 303.
29. Bäuerle, P., *Adv. Mater.* **1992**, 4, (2), 102.
30. Zhang, Q. T.; Tour, J. M., *J. Am. Chem. Soc.* **1997**, 119, (21), 5065.
31. Ajayaghosh, A., *Chem. Soc. Rev.* **2003**, 32, (4), 181.
32. Karikomi, M.; Kitamura, C.; Tanaka, S.; Yamashita, Y., *J. Am. Chem. Soc.* **1995**, 117, (25), 6791.
33. Kastner, J.; Kuzmany, H.; Vegh, D.; Landl, M.; Cuff, L.; Kertesz, M., *Macromolecules* **1995**, 28, (8), 2922.
34. Hung, T. T.; Chen, S. A., *Polymer* **1999**, 40, (13), 3881.
35. Mulliken, R. S.; Rieke, C. A.; Brown, W. G., *J. Am. Chem. Soc.* **1941**, 41.

36. Bredas, J. L.; Street, G. B.; Themans, B.; Andre, J. M., *J. Chem. Phys.* **1985**, 83, (3), 1323.
37. Hernandez, V.; Castiglioni, C.; Delzoppo, M.; Zerbi, G., *Phys. Rev. B* **1994**, 50, (14), 9815.
38. Wudl, F.; Kobayashi, M.; Heeger, A. J., *J. Org. Chem.* **1984**, 49, (18), 3382.
39. Meyer, R.; Kleinert, H.; Richter, S.; Gewald, K., *J. Prakt. Chem.* **1963**, 244.
40. Pomerantz, M.; Chaloner-Gill, B.; Harding, L. O.; Tseng, J. J.; Pomerantz, W. J., *Chem. Commun.* **1992**, (22), 1672.
41. Hertel, D.; Bäessler, H.; Scherf, U.; Hörhold, H.-H., *J. Chem. Phys.* **1999**, 110, (18), 9214.
42. Skotheim, T. A., *Handbook of Conducting Polymers*. 2nd ed.; Marcel Dekker: New York, 1997.
43. Furukawa, Y.; Akimoto, M.; Harada, I., *Synth. Met.* **1987**, 18, (1-3), 151.
44. Delabouglise, D.; Garreau, R.; Lemaire, M.; Roncali, J., *New J. Chem.* **1988**, 12, (2-3), 155.
45. Roncali, J.; Garnier, F., *New J. Chem.* **1986**, 10, (4-5), 237.
46. Roncali, J.; Yassar, A.; Garnier, F., *Chem. Commun.* **1988**, (9), 581.
47. Yassar, A.; Roncali, J.; Garnier, F., *Macromolecules* **1989**, 22, (2), 804.
48. Hotta, S., *Synth. Met.* **1987**, 22, (2), 103.
49. Sato, M.-A.; Tanaka, S.; Kaeriyama, K., *Synth. Met.* **1986**, 14, (4), 279.
50. Sauvajol, J. L.; Chenouni, D.; Lere-Porte, J. P.; Chorro, C.; Moukala, B.; Petrisans, J., *Synth. Met.* **1990**, 38, (1), 1.
51. Roncali, J.; Lemaire, M.; Garreau, R.; Garnier, F., *Synth. Met.* **1987**, 18, (1-3), 139.
52. Roncali, J., *J. Mater. Chem.* **1999**, 9, (9), 1875.
53. Ballarin, B.; Seeber, R.; Tassi, L.; Tonelli, D., *Synth. Met.* **2000**, 114, (3), 279.
54. Zanardi, C.; Scanu, R.; Pigani, L.; Pilo, M. I.; Sanna, G.; Seeber, R.; Spano, N.; Terzi, F.; Zucca, A., *Electrochim. Acta* **2006**, 51, (23), 4859.

55. Brisset, H.; Navarro, A.-E.; Moggia, F.; Jusselme, B.; Blanchard, P.; Roncali, J., *J. Electroanal. Chem.* **2007**, 603, (1), 149.
56. Ballarin, B.; Lanzi, M.; Paganin, L.; Cesari, G., *Electrochim. Acta* **2007**, 52, (28), 7849.
57. Talu, M.; Kabasakaloglu, M.; Yildirim, F.; Sari, B., *Appl. Surf. Sci.* **2001**, 181, (1-2), 51.
58. Demeter, D.; Blanchard, P.; Allain, M.; Grosu, I.; Roncali, J., *J. Org. Chem.* **2007**, 72, (14), 5285.
59. Galal, A.; Lewis, E. T.; Ataman, O. Y.; Zimmer, H.; Mark, H. B., *J. Polym. Sci., Part A* **1989**, 27, (6), 1891.
60. Lin, J. W. P.; Dudek, L. P., *J. Polym. Sci., Part A* **1980**, 18, (9), 2869.
61. Yamamoto, T.; Sanechika, K.; Yamamoto, A., *J. Polym. Sci., Polym. Lett.* **1980**, 18, (1), 9.
62. Tamo, K.; Sumitani, K.; Kumada, M., *J. Am. Chem. Soc.* **1972**, 4376.
63. Hotz, C. Z.; Kovacic, P.; Khoury, I. A., *J. Polym. Sci., Polym. Chem.* **1983**, 21, (9), 2617.
64. Yamamoto, T.; Maruyama, T.; Zhou, Z. H.; Miyazaki, Y.; Kanbara, T.; Sanechika, K., *Synth. Met.* **1991**, 41, (1-2), 345.
65. Yamamoto, T.; Morita, A.; Maruyama, T.; Zhou, Z. H.; Kanbara, T.; Sanechika, K., *Polym. J.* **1990**, 22, (2), 187.
66. Yamamoto, T.; Osakada, K.; Wakabayashi, T.; Yamamoto, A., *Makromol. Chem. - Rapid Commun.* **1985**, 6, (10), 671.
67. Yamamoto, T.; Morita, A.; Miyazaki, Y.; Maruyama, T.; Wakayama, H.; Zhou, Z.; Nakamura, Y.; Kanbara, T.; Sasaki, S.; Kubota, K., *Macromolecules* **1992**, 25, (4), 1214.
68. Colon, I.; Kwiatkowski, G. T., *J. Polym. Sci., Part A* **1990**, 28, (2), 367.
69. Kobayashi, M.; Chen, J.; Chung, T. C.; Moraes, F.; Heeger, A. J.; Wudl, F., *Synth. Met.* **1984**, 9, (1), 77.
70. Jen, K. Y.; Miller, G. G.; Elsenbaumer, R. L., *Chem. Commun.* **1986**, (17), 1346.
71. Jow, T. R.; Jen, K. Y.; Elsenbaumer, R. L.; Shacklette, L. W.; Angelopoulos, M.; Cava, M. P., *Synth. Met.* **1986**, 14, (1-2), 53.

72. Elsenbaumer, R. L.; Jen, K. Y.; Oboodi, R., *Synth. Met.* **1986**, 15, (2-3), 169.
73. Sugimoto, R.; Takeda, S.; Yoshino, K., *Chem. Express* **1986**, 635.
74. Yoshino, K.; Hayashi, S.; Sugimoto, R., *Jpn. J. Appl. Phys.* **1984**, 23, (12), L899.
75. Pomerantz, M.; Tseng, J. J.; Zhu, H.; Sproull, S. J.; Reynolds, J. R.; Uitz, R.; Arnott, H. J.; Haider, M. I., *Synth. Met.* **1991**, 41, (3), 825.
76. Sato, M. A.; Morii, H., *Polym. Commun.* **1991**, 32, (2), 42.
77. Sato, M. A.; Morii, H., *Macromolecules* **1991**, 24, (5), 1196.
78. Maior, R. M. S.; Hinkelmann, K.; Eckert, H.; Wudl, F., *Macromolecules* **1990**, 23, (5), 1268.
79. Siringhaus, H.; Brown, P. J.; Friend, R. H.; Nielsen, M. M.; Bechgaard, K.; Langeveld-Voss, B. M. W.; Spiering, A. J. H.; Janssen, R. A. J.; Meijer, E. W.; Herwig, P.; de Leeuw, D. M., *Nature* **1999**, 401, (6754), 685.
80. McCullough, R. D., *Adv. Mater.* **1998**, 10, (2), 93.
81. Barbarella, G.; Bongini, A.; Zambianchi, M., *Macromolecules* **1994**, 27, (11), 3039.
82. McCullough, R. D.; Lowe, R. D.; Jayaraman, M.; Anderson, D. L., *J. Org. Chem.* **1993**, 58, (4), 904.
83. McCullough, R. D.; Lowe, R. D.; Jayaraman, M.; Ewbank, P. C.; Anderson, D. L.; Trisramnagle, S., *Synth. Met.* **1993**, 55, (2-3), 1198.
84. Barbarella, G.; Zambianchi, M.; Bongini, A.; Antolini, L., *Adv. Mater.* **1994**, 6, (7-8), 561.
85. Wu, X. M.; Chen, T. A.; Rieke, R. D., *Macromolecules* **1995**, 28, (6), 2101.
86. Chen, T. A.; Rieke, R. D., *J. Am. Chem. Soc.* **1992**, 114, (25), 10087.
87. Chen, T. A.; O'Brien, R. A.; Rieke, R. D., *Macromolecules* **1993**, 26, (13), 3462.
88. Chen, T. A.; Rieke, R. D., *Synth. Met.* **1993**, 60, (2), 175.
89. Chen, T. A.; Wu, X. M.; Rieke, R. D., *J. Am. Chem. Soc.* **1995**, 117, (1), 233.

90. Iovu, M. C.; Sheina, E. E.; Gil, R. R.; McCullough, R. D., *Macromolecules* **2005**, 38, (21), 8649.
91. Loewe, R. S.; Ewbank, P. C.; Liu, J. S.; Zhai, L.; McCullough, R. D., *Macromolecules* **2001**, 34, (13), 4324.
92. Loewe, R. S.; Khersonsky, S. M.; McCullough, R. D., *Adv. Mater.* **1999**, 11, (3), 250.
93. Adam, D., *Nature* **2003**, 421, (6923), 571.
94. Giguere, R. J.; Bray, T. L.; Duncan, S. M.; Majetich, G., *Tetrahedron Lett.* **1986**, 27, (41), 4945.
95. Gedye, R.; Smith, F.; Westaway, K.; Ali, H.; Baldisera, L.; Laberge, L.; Rousell, J., *Tetrahedron Lett.* **1986**, 27, (3), 279.
96. Stass, D. V.; Woodward, J. R.; Timmel, C. R.; Hore, P. J.; McLauchlan, K. A., *Chem. Phys. Lett.* **2000**, 329, (1-2), 15.
97. Pringle, J. M.; Forsyth, M.; MacFarlane, D. R.; Wagner, K.; Hall, S. B.; Officer, D. L., *Polymer* **2005**, 46, (7), 2047.
98. Carter, K. R., *Macromolecules* **2002**, 35, (18), 6757.
99. Yamamoto, T.; Fujiwara, Y.; Fukumoto, H.; Nakamura, Y.; Koshihara, S. Y.; Ishikawa, T., *Polymer* **2003**, 44, (16), 4487.
100. Galbrecht, F.; Yang, X. H.; Nehls, B. S.; Neher, D.; Farrell, T.; Scherf, U., *Chem. Commun.* **2005**, (18), 2378.
101. Nehls, B. S.; Asawapirom, U.; Fuldner, S.; Preis, E.; Farrell, T.; Scherf, U., *Adv. Funct. Mater.* **2004**, 14, (4), 352.
102. McCulloch, L.; Bailey, C.; Giles, M.; Heeney, M.; Love, I.; Shkunov, M.; Sparrowe, D.; Tierney, S., *Chem. Mater.* **2005**, 17, (6), 1381.

Based on these phenylene-thiophene-based step-ladder copolymers, similar copolymers with a 1,5-naphthylene moiety instead of the phenylene unit have been generated (Figure 2.2). 1,5-Naphthylene, with its larger energy difference between the benzoic and quinoid resonance structure compared to 1,4-phenylene, should lead to a hypsochromic shift in the optical spectra and somewhat modified electronic properties.^[20]

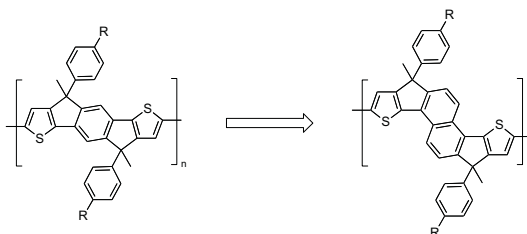
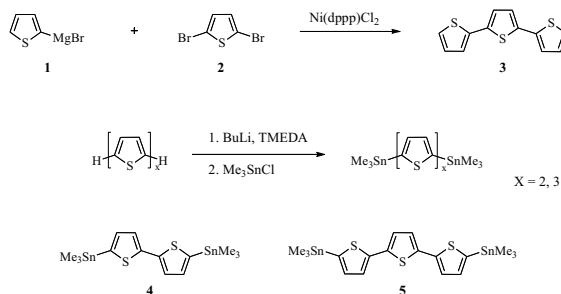


Figure 2.2. Modification of the 1,4-phenylene-based building block by exchange with 1,5-naphthylene.

2.2 Thiophene-Phenylene-Based Materials: Results and Discussion

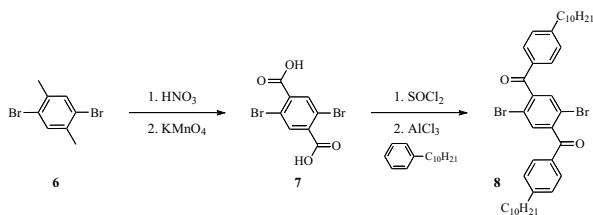
2.2.1 Monomer and Polymer Synthesis

The synthesis of the step-ladder copolymers with varying thiophene content first required the preparation of different oligothiophene monomers. While bithiophene is commercially available, terthiophene **3** was prepared via a Nickel-mediated aryl-aryl-coupling following a Kumada protocol.^[21] Deprotonation of the oligothiophenes using *n*-butyl lithium followed by treatment with trimethyltin chloride afforded the corresponding distannylated monomers **4** and **5**, respectively.



Scheme 2.1: Synthesis of the distannylated thiophene monomers **4** and **5**.

The central building block was synthesized by twofold oxidation of commercially available 2,5-dibromo-1,4-dimethylbenzene **6** yielding the corresponding 2,5-dibromo-terephthalic acid **7**.^[22] The diacid was converted into the corresponding diacid dichloride by treatment with thionyl chloride and then reacted in a Friedel-Crafts acylation to give 1,4-bis(4',4''-decylbenzoyl)-2,5-dibromobenzene **8**.^[9]

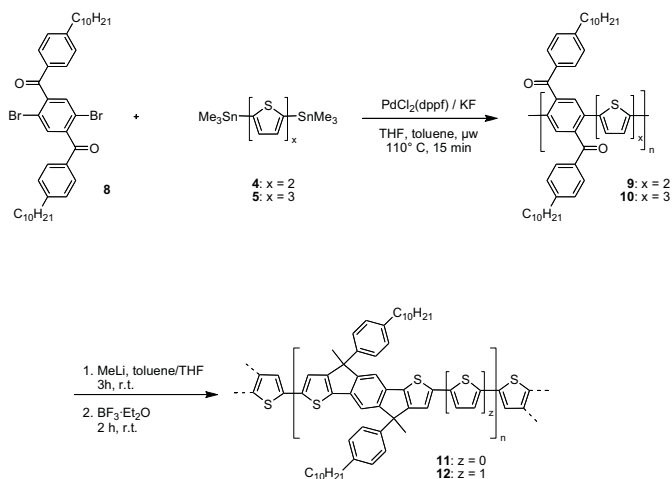


Scheme 2.2. Synthesis of monomer **8**.

The initial polymeric intermediates towards the desired step-ladder copolymers were the polyketones **9** and **10** shown in Scheme 2.3, which were synthesized in a microwave-assisted Stille-type cross-coupling reaction from monomer **8** and the corresponding bis(trimethyl)stannyl oligothiophenes utilizing PdCl₂(dppf) as catalyst.^[23, 24] The resulting single-stranded polyketones **9** and **10** were purified by Soxhlet extraction with ethanol to remove low molecular weight fractions and gave the polyketones in 44 and 47% yield, respectively. The second step was a polymer-analogous transformation of the keto groups into tertiary alcohols by reaction with methyl lithium.^[25] The progress of the conversion was monitored via IR-spectroscopy using the disappearance of the carbonyl band (and appearance of alcohol bands). The final Friedel-Crafts-type ring closure was achieved by addition of an excess of BF₃·Et₂O to a solution of the polyalcohol in dichloromethane.^[26] This ring closure sequence allows for the introduction of a broad variety of substituents ranging from alkyl to alkylphenyl side groups at the conjugated backbone via addition of different lithium organyls. To remove low molecular weight fractions all step-ladder polymers were again extracted with ethanol and subsequently precipitated into methanol to afford the polymers **11** and **12** in yields of 76 and 71%, respectively.

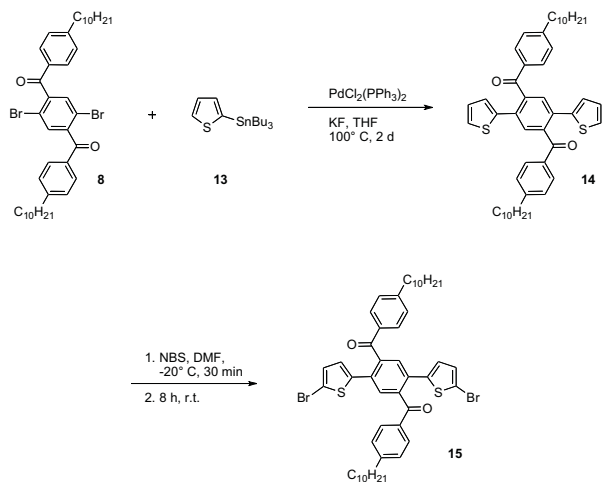
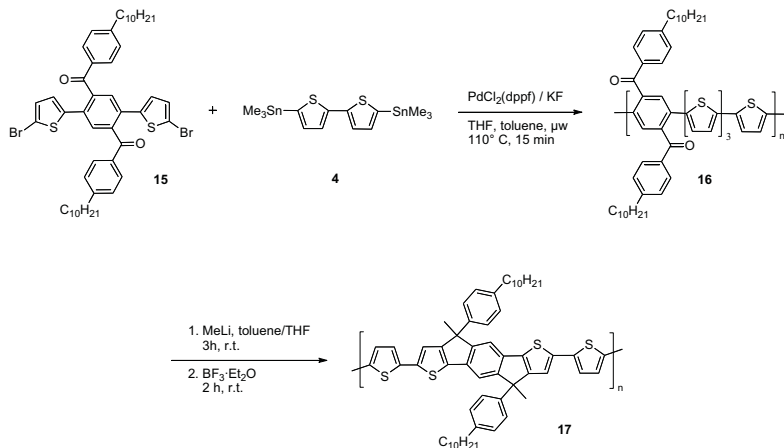
The polymers were soluble in many organic solvents like toluene, chloroform or dichloromethane; this allowed a full spectroscopic characterization. GPC analysis revealed that polymers **11** and **12** possess M_n values of 12,000 g/mol (PD = 2.0) and 16,200 g/mol (PD = 2.9), respectively. The polymers were fully characterized by IR and ¹H/¹³C NMR spectroscopy. In the ¹³C NMR spectrum of the polyketone precursor **9**, the carbon resonance of the carbonyl group was observed at δ =

196.7 ppm. Upon cyclization to **11**, the disappearance of the keto resonance and the appearance of a signal at $\delta = 53.2$ ppm assigned to the newly formed quarternary carbon of the methylene bridge proved the complete formation of the step-ladder structure. Similar features could be observed for polymers **10/12** with corresponding carbon signals at $\delta = 194.2$ ppm (**10**) and $\delta = 54.1$ ppm (**12**), respectively.



Scheme 2.3. Synthesis of the step-ladder polymers **11** and **12** using a microwave-assisted Stille-type cross-coupling reaction followed by a Friedel-Crafts-type ring closure.

Due to the very low solubility of unsubstituted 2,2':5',2''':5'',2'''-quaterthiophene, generation of the appropriate distannylated derivative was unfeasible. Therefore, another synthetic route to synthesize the step-ladder derivative bearing four thiophene rings per repeat unit was established. The synthesis of monomer **14** is depicted in Scheme 2.4 and started from monomer **8** which was reacted with 2-(tributyl)stannyl thiophene **13** following a microwave-assisted Stille-type coupling protocol as described previously.^[27] Bromination of the monomer precursor with NBS gave the dibromo monomer **15**,^[28] which was copolymerized with bis(trimethyl)stannyl oligothiophene **4** to the corresponding polyketone **16** and afterwards reduced and cyclized with (i) methyl lithium and (ii) $\text{BF}_3 \cdot \text{Et}_2\text{O}$, respectively, as described before to give step-ladder copolymer **17** (Scheme 2.5).^[26] After Soxhlet extraction with ethanol, GPC analysis revealed that polymer **17** possesses a M_n value of 14,200 g/mol (PD = 3.1). The polymer was fully characterized by IR and $^1\text{H}/^{13}\text{C}$ NMR spectroscopy.

Scheme 2.4. Synthesis of the dibrominated monomer **15**.Scheme 2.5. Synthesis of the step-ladder copolymer **17** using a microwave-assisted Stille-type cross-coupling reaction followed by a Friedel-Crafts-type ring closure.

2.2.2 Optical Spectroscopy

The UV-Vis absorption spectra of the copolymers **11**, **12** and **17** in dilute chloroform solution are shown in Figure 2.3. All polymers were completely soluble in chloroform. The UV-Vis spectrum of **11** shows a broad featureless long wavelength absorption band peaking at 490 nm with a steep absorption edge, consistent with the presence of a nearly coplanar backbone structure. The incorporation of additional thiophene rings between the step-ladder subunits leads to a 15 nm red-shift of the absorption maximum for **12** and 16 nm for **17**, respectively. The bathochromic shift of **12** when compared to copolymer **11** reflects the lower band gap energy of polythiophenes in comparison to polyphenylenes. However, further incorporation of thiophene units (as seen in the transition of **12** to **17**) seems to have only a minor influence on the absorption characteristics.

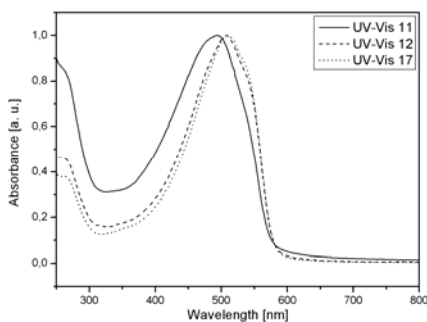


Figure 2.3. UV-Vis spectra of the step-ladder copolymers **11**, **12**, and **17**.

The photoluminescence (PL) emission spectra of the novel step-ladder polymers were recorded in dilute chloroform solution and are depicted in Figure 2.4. Polymer **11** again exhibits the highest energy PL, with a maximum at 570 nm and a vibronic side-band at 600 nm. Polymers **12** and **17** show a slight red-shift and slightly better resolved vibronic side-bands. As already shown for the absorption spectra, the PL spectra of the two copolymers with the larger oligothiophene segments do not show any significant differences. Therefore, it can be expected that a further elongation of the oligothiophene segments will not lead to significant changes of the optical properties of the copolymers.

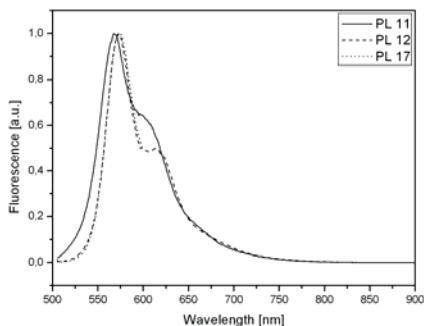


Figure 2.4: PL emission spectra of the step-ladder copolymers **11**, **12**, and **17** (excitation wavelength: 500 nm).

Investigations of the temperature dependence of absorption and PL emission in dilute toluene solution were performed in the group of Prof. H. Burrows, University of Coimbra, Portugal. At room temperature the spectra of the copolymer materials contained similar features to those described before for dilute chloroform solutions (Figure 2.5). Upon lowering the temperature to 77 K the absorption spectra became more structured and demonstrated well-resolved 0-1 transitions and, in case of copolymer **11**, also the second vibronic progression (0-2). The solid state absorption spectra of films again showed a loss of information about the vibronic transitions and a noticeable broadening of the absorption spectra. The spectroscopic data are listed in Table 2.1.

Table 2.1. Spectroscopic data of the step-ladder-type copolymers in toluene at room temperature (293 K), low temperature (77 K) and in the solid state (thin films). The underlined wavelengths are the maxima with the highest intensity.

Polymer	λ_{\max}^{Abs}	λ_{\max}^{Abs}	λ_{\max}^{Abs}	λ_{\max}^{Fluo}	λ_{\max}^{Fluo}	λ_{\max}^{Fluo}	$\lambda_{\max}^{T_1 \rightarrow T_n}$
	[nm], 293	[nm], 77 K	[nm], Film	[nm], 293 K	[nm], 77 K	[nm], Film	[nm]
11	480	470, <u>505</u> , 540	495	<u>562</u> , 600	<u>569</u> , 612	563, 590	660
12	505	<u>520</u>	510	<u>569</u> , 615	<u>578</u> , 627	576, <u>610</u>	690
17	508	525, 558	515	<u>572</u> , 620	<u>580</u> , 630	581, <u>615</u>	750

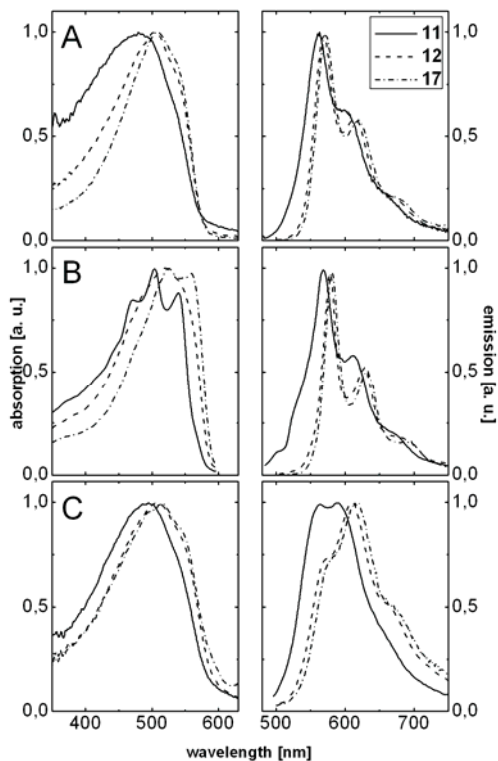


Figure 2.5. Absorption and fluorescence emission spectra for polymers **11**, **12**, and **17** in dilute toluene solution at room temperature (A, 293 K), at low temperature (B, 77 K), and as thin films (C) (for the PL spectra: excitation wavelength: 500 nm).

The maxima of the PL emission spectra experience a slight bathochromic shift by 7-9 nm for all polymers at low temperatures and also an improvement in the resolution of the vibronic progressions. This result can be related to a more rigid structure at lower temperature leading to absorption and emission spectra of better resolution. Thin films of the copolymer materials show broadened and unresolved PL emission bands, which may be the result of solid state interchain interactions accompanied by a fast spectral diffusion to the lowest energy chromophores in the tail of the density of states (DOS)*. The thin film spectra show only small bathochromic shifts if compared to the spectra in dilute toluene solutions. This implies that the copolymers in the solid state only show a low degree of interchain order. The amount of interchain order, leading to

* Density of states (DOS): A function quantifying how many allowed, distinct energy states (so-called eigenstates) exist at (or very near) a given energy level. A high density of states indicates either very small energy gaps or a high degree of degeneracy.

characteristic interchain π -interactions, is assumed to be responsible for the frequently observed red shifts of the optical spectra of conjugated polymers, especially oligothiophenes, in the solid state. The low intensity of the 0-0 PL transitions of the copolymers **11**, **12** and **17** in the solid state is likely to be caused by self-absorption effects.

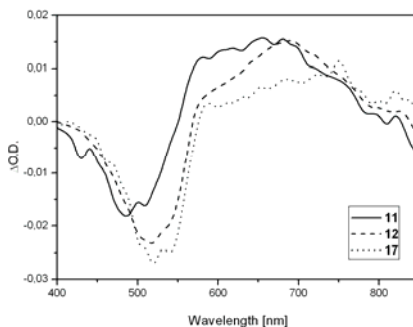


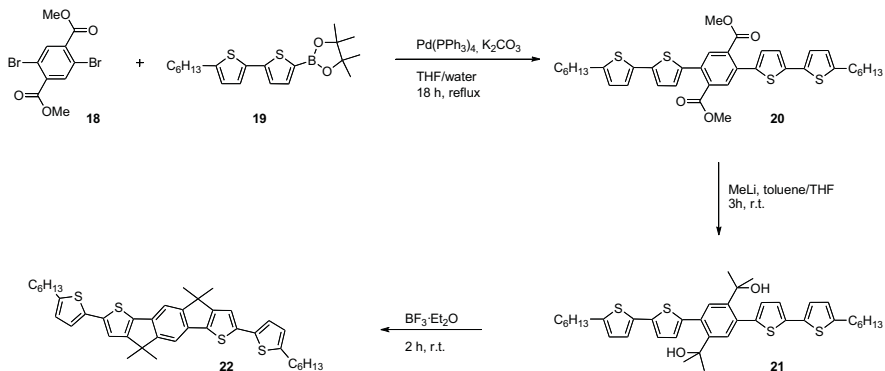
Figure 2.6. Transient singlet-triplet difference absorption spectra for **11**, **12**, and **17** in toluene at room temperature (delay interval between excitation and observation: 1.8 μ s).

Transient singlet-triplet difference absorption spectra in solution with a time delay of 1.8 μ s between excitation and observation are depicted in Figure 2.6. In the area of 400 to ca. 560 nm all spectra show the typical ground state bleaching and the occurrence of polaronic absorptions (p^+/p^-) at higher wavelength (\sim 600 nm). The spectra peak in barely observable maxima for the $T_1 \rightarrow T_n$ transition at 660, 690, and 750 nm for **11**, **12**, and **17**, respectively. The poor $T_1 \rightarrow T_n$ performance might be due to so-called geminate pair recombination of excited states, which can only be suppressed in low temperature measurements.^[29-33]

2.3 Synthesis and Characterization of Model Compounds

To investigate the molecular structure of the bridged bis(2-thienyl)-benzene repeat units of these copolymers in more detail, synthesis and characterization of related model compounds seemed appropriate. Scheme 2.6 depicts the synthesis of a model compound composed of a dithienyl-substituted step-ladder thiophene-benzene-thiophene core unit. Diethyl 2,5-dibromoterephthalate **18** was reacted with 2.5 eq. of 2,2'-bithiophene-5-pinacol boronate **19** utilizing $\text{Pd}(\text{PPh}_3)_4$ as catalyst and K_2CO_3 as base in a microwave assisted Suzuki-type cross-coupling reaction yielding the diketo

compound **20** in 76 % yield.^[27] Cyclization to afford the model compound **22** was achieved by utilizing the methyl lithium / $\text{BF}_3 \cdot \text{Et}_2\text{O}$ -mediated reaction sequence described previously.^[26]



Scheme 2.6. Synthetic route towards the model compound **22**.

2.3.1 Optical Spectroscopy

Figure 2.7 shows the UV-Vis absorption spectrum of the precursor **21** as well as of the cyclized model compound **22** in dilute chloroform solution. The cyclization of **21** to **22** is accompanied by a drastic change of the optical properties. The precursor shows a featureless long-wavelength absorption band peaking at 389 nm, whereas upon ring-closure the absorption maximum is red-shifted to 424 nm. Furthermore, **22** displays a much steeper absorption edge and better resolved vibronic side-bands due to the increased rigidity of the molecule. The corresponding PL spectrum exhibits two well-resolved peaks for the 0-0 and 0-1 transitions at 475 and 502 nm, respectively, as well as a shoulder at 523 nm for the 0-2 transition.

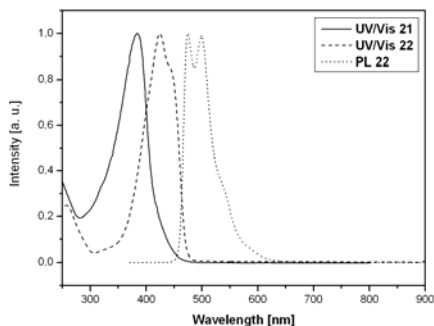


Figure 2.7. UV-Vis absorption spectra solution of **21** and model compound **22** in dilute chloroform; as well as the PL spectra of **22** in dilute chloroform solution (excitation wavelength: 445 nm).

2.3.2 Crystallographic Investigations

The molecular structure of model compound **22** was also determined by X-ray crystallography (Figures 2.8 and 2.9). The figures show that the π -conjugated core segment that is bridged by two sp^3 -hybridized carbon atoms is planar. The four methyl side-groups are positioned orthogonal to this plane. The attached thiophene substituents exhibit a slight out-of-plane twist of 20.05° relative to the planar core segment, suggesting that the copolymers **12** and **17** should also show a similar weak distortion of the individual segments. The relatively small distortion is similar to the situation in unsubstituted poly(*para*-phenylene)s (distortion angle: ca. 19°).^[34] In contrast, a higher distortion angle is observed in P3HT (ca. 30°).^[35, 36] The weak distortion in oligomer **22** and the corresponding copolymers **12** and **17** should allow a sufficient conjugative interaction along the oligomer and copolymer backbones. Within the unit cell of **22** some intermolecular π -stacking between the planarized oligomer molecules occurs (mean distance between molecular planes: 4.2 Å). It can be concluded that a significant interchain π - π -interaction within the copolymers **12** and **17** should also occur.

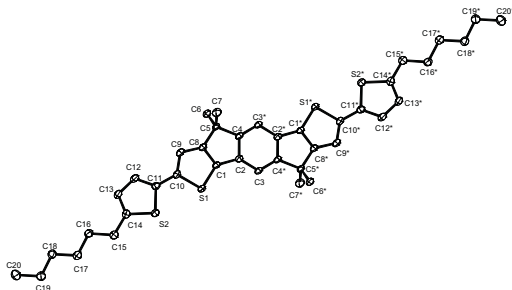


Figure 2.8: ORTEP plot of the model compound **22**.



Figure 2.9: View in-plane and perpendicular to the plane of the planarized core segment of **22**.

2.3.3 OFET Investigations

The charge carrier mobilities of the copolymers **11**, **12** and **17** in OFET devices have been determined in the group of Prof. Dr. E. List at the Technical University of Graz, Austria; the HOMO energy levels were measured in the group of Dr. H. Thiem, Evonik Degussa, Marl.

First, OFET devices fabricated with the step-ladder copolymers **11**, **12** and **17** as the active semiconducting layer showed the typical output characteristics of an OFET device but did not show the typical linear rise of the source-drain current with increasing drain voltage and experienced no clear saturation regime for high gate voltages. As an example, Figure 2.10 depicts the output characteristic of an OFET device utilizing copolymer **12**; performing in a similar fashion to the copolymers **11** and **17**.

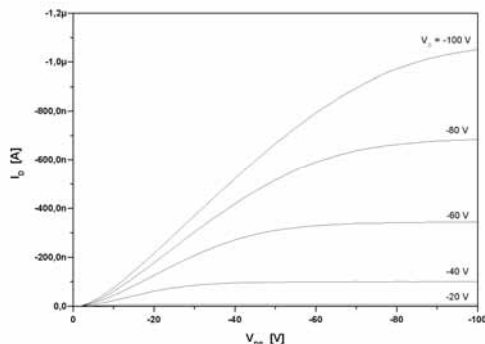


Figure 2.10. Output characteristics of an OFET device utilizing copolymer **12** in a bottom-gate/bottom-contact OFET architecture.

The copolymer materials gave low charge-carrier mobilities, being 3 - 4 orders of magnitude lower than that of regioregular poly(3-hexyl thiophene) P3HT, with moderate on/off ratios 1 - 2 orders of magnitude lower than that of P3HT.^[37] The comparison of the different polymers showed a decrease of the mobility as well as on/off ratio with increasing thiophene content. As indicated in the prior section, the extension of the more flexible oligothiophene segments induces an increased conformational freedom and may lead to less interchain π -stacking.

The optical band gap energies of the step-ladder copolymers were found to be in the region of 2.4 - 2.55 eV and decreases slightly with increasing thiophene content. The HOMO level of copolymer **11** was measured by photoelectron spectroscopy to be 5.25 eV with an offset of ca. +0.13 eV compared to P3HT. Further increase of the thiophene content subsequently reduces the offset by ca. 0.01 eV per additional thiophene unit.

Table 2.2: Electronic properties of copolymers **11**, **12**, and **17**.

polymer	11	12	17
mobility μ [cm^2/Vs]	$8 \cdot 10^{-5}$	$5 \cdot 10^{-5}$	$9 \cdot 10^{-6}$
on/off ratio	10^5	$10^{4.5}$	10^4
band gap energy E_g [eV]	2.53	2.45	2.42
HOMO level [eV]	5.25	5.23	5.22

A HOMO level > 5.2 eV is believed to ensure sufficient air stability.^[38] To confirm this, repeated measurements of the optical spectra and OFET properties after exposure to light under ambient conditions for several days showed no differences in the PL spectra and the electronic parameters (charge carrier mobility).

2.3.4 Thermal Properties.

One basic requirement for organic materials in any novel technology is providing adequate device stability for the intended application. In general, the degradation of organic electronic devices appears in the form of a decrease of the device luminance for OLEDs or the occurrence of current leakages in OFETs. Morphological changes are believed to be the main reason for these failures of the organic material within the active layers. These morphological changes are often related to heating of the devices under operation.

To investigate the potential stability of the devices, the thermal properties of the copolymers **11**, **12** and **17** were investigated by Differential Scanning Calorimetry (DSC) in the temperature range of -20 to 250 °C. The heating and cooling rates used throughout the experiments were constant at 10 K/min.

No first or second order transitions were found in the DSC traces for polymers **11** and **12**, indicating the absence of melting or glass transitions. Differently from these two copolymers, copolymer **17** with its higher thiophene content showed a second order glass transition at a temperature of 93 °C during the first heating cycle. Upon cooling to room temperature, the material exhibited the reverse transition.

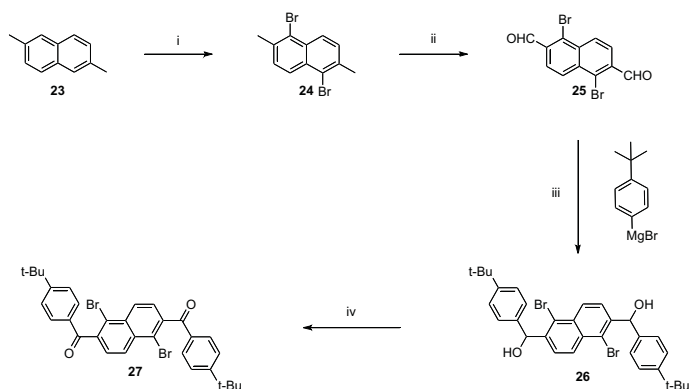
2.4 Thiophene-Naphthalene-Based Materials: Results and Discussion

2.4.1 Monomer and Polymer Synthesis

The synthesis of the 1,5-naphthylene monomer **27** was recently described by Scherf *et al.* and is depicted in Scheme 2.7.^[39] Bromination of commercially available 2,6-dimethylnaphthalene **23** with bromine gave the corresponding 1,5-dibromo-2,6-dimethyl-naphthalene **24**.^[40] Further side-chain bromination of the methyl groups with NBS, and hydrolysis of the bromomethyl to hydroxy methyl groups, followed by a selective oxidation with pyridinium chlorochromate (PCC) resulted in 1,5-dibromonaphthalene-2,6-dicarbaldehyde **25**.^[41] The dicarbaldehyde **25** was then reacted with

4-*tert*-butylphenylmagnesium bromide in a Grignard-type reaction to give the racemic 1,5-dibromo-2,6-bis(4-*tert*-butylphenylhydroxymethyl)naphthalene **26**. The aromatic alcohol was oxidized in a final reaction step by treatment with manganese dioxide to yield the diketo derivative 1,5-dibromo-2,6-bis(4-*tert*-butylbenzoyl)naphthalene **27**.

The diketo monomer **27** was then coupled with the distannylated bithiophene monomer **4** in a microwave-assisted Stille-type cross-coupling reaction utilizing PdCl₂(dppf) as catalyst (Scheme 2.8).^[23, 24] The reaction gave the single-stranded precursor polymer **28**, which was purified by Soxhlet extraction with ethanol to remove low molecular weight fractions leaving the polyketone in 49% yield after precipitation into methanol.

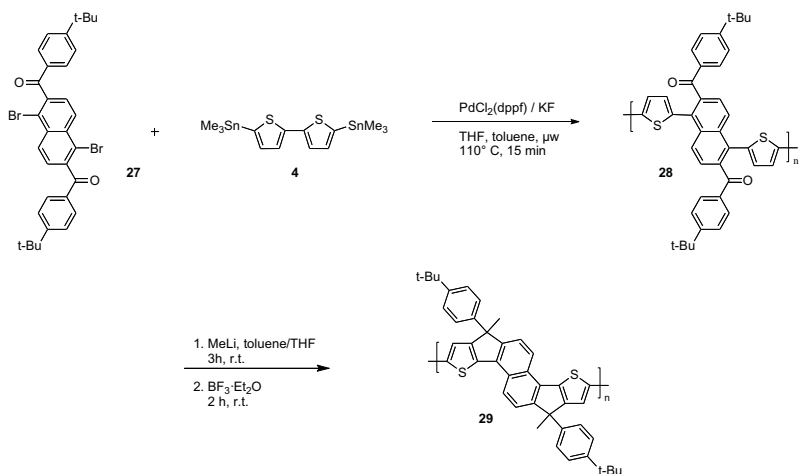


Scheme 2.7: Synthesis of the naphthalene monomer **27**. reagents: i) Br₂/CH₃COOH, ii) a) NBS/CCl₄, b) CaCO₃/dioxane, c) pyridinium chlorochromate (PCC)/CH₂Cl₂, iii) 4-*tert*-butylphenylmagnesium bromide/Et₂O, iv) MnO₂/toluene.

Subsequently, the polyketone was reacted in a polymer-analogous reaction with methyl lithium to convert the keto functions into tertiary alcohols.^[25] The progress of the reaction was monitored by IR spectroscopy by following the disappearance of the carbonyl band and the growth of alcohol-related bands. In the last reaction step a Friedel-Crafts-type ring-closing reaction was performed by treatment with an excess of BF₃•Et₂O in dichloromethane.^[26] Again, the progress of the transformation was monitored by IR and NMR spectroscopy.

After a final purification of the newly formed step-ladder copolymer by Soxhlet extraction with ethanol and reprecipitation from chloroform into methanol the polymer **29** was afforded in a yield of 82%. A *M_n* value of 13,500 g/mol (PD = 2.1) was confirmed by GPC analysis and the polymer

characterized by IR, ^1H and ^{13}C NMR spectroscopy. The carbon signal of the carbonyl groups in the ^{13}C NMR spectrum of **28** at $\delta = 197.4$ ppm completely vanished during the polymer analogous cyclization and a new carbon signal for the quaternary carbon of the formed methylene bridge in **29** could be found at $\delta = 55.4$ ppm.



Scheme 2.8: Synthesis of the 1,5-naphthylene containing precursor polymer **28** via microwave-assisted Stille-type cross-coupling reaction and its subsequent polymer-analogous cyclization leading to the step-ladder copolymer **29**.

2.4.2 Optical Spectroscopy

The UV-Vis absorption spectrum of the newly formed 1,5-naphthylene-based step-ladder copolymer **29** as well as its precursor **28** were recorded in dilute chloroform solution and are shown in Figure 2.11. While the precursor **28** shows a long wavelength absorption maximum peaking at 473 nm, the step-ladder copolymer shows a slightly red-shifted absorption maximum at 485 nm together with a slightly steeper absorption edge. Another feature of the rigidified π -conjugated system of **29** is the formation of a longer wavelength absorption shoulder at 515 nm which can be assigned to the 0-0 transition.

No PL emission spectra in chloroform have been recorded as the material showed only very weak photoluminescence.

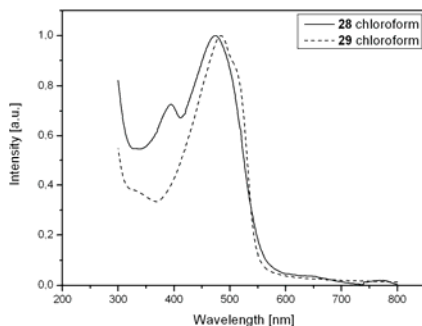


Figure 2.11. UV-Vis absorption of the precursor polymer **28** and the cyclized step-ladder copolymer **29** in dilute chloroform solution.

In Figure 2.12 the absorption spectrum of the 1,5-naphthylene-based copolymer **29** is compared with its 1,4-phenylene-based counterpart **11**. A distinct blue shift of 25 nm could be observed for **29** (λ_{max} **11**: 510 nm; λ_{max} **29**: 485 nm). This finding can be explained by an increase of the energy difference between the benzoid and quinoid resonance structures when switching from 1,4-phenylene to 1,5-naphthylene. As described previously, this leads to a higher excitation energy between the dominantly benzoid ground state and the excited state with its increased participation of quinoid resonance states for **29**. Interestingly, the spectral shapes of the long wavelength absorption bands of **11** and **29** are nearly identical.

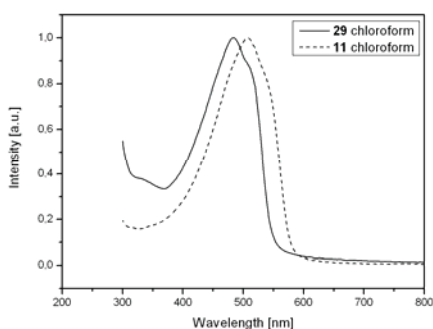


Figure 2.12. Comparison of the UV-Vis absorption spectra of the 1,5-naphthylene-based copolymer **29** and its 1,4-phenylene analogue **11** in dilute chloroform solution.

Temperature-dependant absorption and PL emission spectra of the 1,5-naphthylene-based copolymer **29** were recorded in the group of Prof. H. Burrows, University of Coimbra, Portugal and compared with the data of the 1,4-phenylene-based step-ladder copolymer **11**. In toluene solution at room temperature copolymer **29** gives a much more structured long wavelength absorption band compared to **11** with its significantly broadened absorption band. This result might be explained by a partial aggregation of the less soluble **11** in toluene. Upon cooling to 77 K both absorption spectra become clearly structured and well-resolved 0-0, 0-1, and 0-2 transitions are visible together with the already discussed blue shift for **11**. The thin films absorption spectra of the two copolymers display less structured and broad absorption bands. Additionally, the typical absorption tail indicates a certain disorder of the copolymer chains in the solid state.

Table 2.3. Spectroscopic data of the step-ladder-type copolymers **11** and **29** in toluene at room temperature (293 K), at low temperature (77 K) and in the solid state (thin films). The underlined wavelengths are the absorption and PL emission maxima with the highest intensity.

Polymer	λ_{\max}^{Abs}	λ_{\max}^{Abs}	λ_{\max}^{Abs}	λ_{\max}^{Fluo}	λ_{\max}^{Fluo}	λ_{\max}^{Fluo}	$\lambda_{\max}^{T_1 \rightarrow T_n}$
	[nm], 293	[nm], 77 K	[nm], Film	[nm], 293 K	[nm], 77 K	[nm], Film	[nm]
29	482	<u>490</u> , 525	485	<u>533</u> , 570	<u>536</u> , 577	535, <u>572</u>	660
11	480	470, <u>505</u> , 540	495	<u>562</u> , 600	<u>569</u> , 612	563, 590	660

The spectroscopic data are listed in Table 2.3. The PL emission spectrum of the 1,5-naphthylene-based copolymer **29** in toluene shows a similar spectral shape to its 1,4-phenylene-based counterpart **11** apart from the slight blue-shift of the emission maximum of **29** of ca. 30 nm. Again measurements at lower temperature (77 K) improved the resolution of the vibronic progressions due to an increased molecular order. Different from its 1,4-phenylene-based counterpart, copolymer **29** shows well-resolved solid state PL emission bands with the 0-0 emission at 535 and its first vibronic progression at 572 nm. The 0-0 emission is significantly reduced due to self-absorption effects.

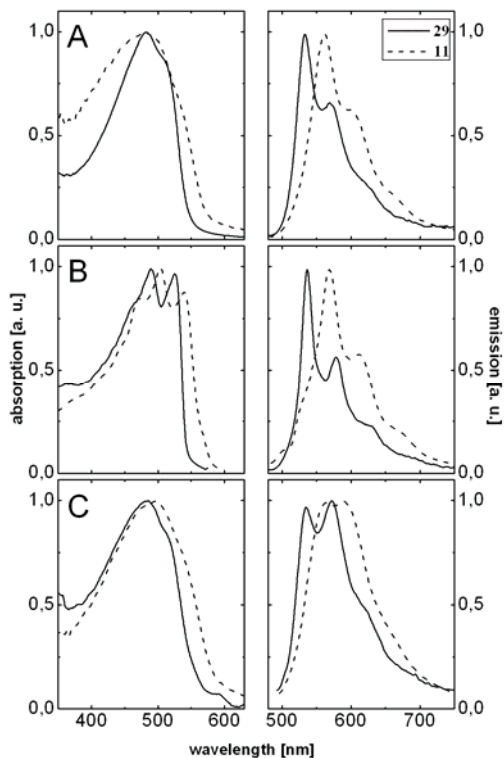


Figure 2.13. Absorption and PL emission spectra for copolymers **29** and **11** in dilute toluene solution at room temperature (A, 293 K), at low temperature (B, 77 K), and as thin films (C). (for the PL spectra: excitation wavelength: 500 nm)

Figure 2.14 shows the transient singlet-triplet difference absorption spectra for the 1,5-naphthylene-based copolymer **29** as well as for the 1,4-phenylene-based copolymer **11** in dilute toluene solution with a time delay of 5.6 μs between excitation and observation. Again the region from 400 to ca. 550 nm shows the expected ground state bleaching and the occurrence of polaronic absorption bands (p^+/p^-) at higher wavelength (~ 600 nm). The barely noticeable maxima for the $T_1 \rightarrow T_n$ transition do not vary upon exchange of the arylene ring system. The poor intensity of the $T_1 \rightarrow T_n$ transition might be due to so-called geminate pair recombination of excited states, which can only be suppressed in low temperature measurements. Further experiments using the copolymer material **29** as active semiconducting layer of OFET devices are under way.

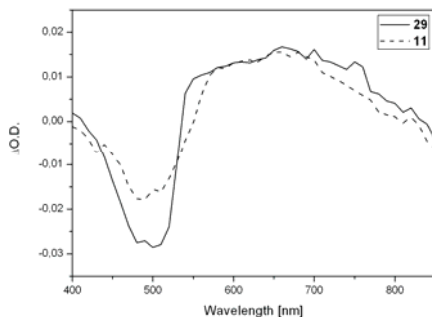


Figure 2.14. Transient singlet-triplet difference absorption spectra for the copolymers **29** and **11** in toluene at room temperature (transient time: 5.6 μs for **29**, 1.8 μs for **11**).

2.5 Conclusion

A series of thiophene-phenylene-based step-ladder copolymers with varying lengths of the oligothiophene segment were synthesized, characterized and tested as the active layers of OFET devices. The copolymers have been synthesized in a Stille-type cross-coupling reaction to give single-stranded precursor polymers. The final ring closure to afford the step-ladder copolymers was performed in a polymer-analogous cyclization sequence. The planar structure of the step-ladder core units was confirmed by X-ray crystallography of a related model compound. The optical spectra were recorded both in dilute solution at different temperatures and in the solid state and revealed a spectral red-shift of the absorption and emission maxima with increasing numbers of thiophene building blocks. The OFET experiments showed the best device performance for copolymer **11**, which had the lowest thiophene content. Moderate on/off ratios of up to 10^5 and mobilities of $8 \cdot 10^{-5} \text{ cm}^2/\text{Vs}$ were found for the step-ladder copolymers.

Additionally, an oligothiophene-naphthalene-based copolymer **29** was generated using a similar synthetic procedure. The greater energy difference between benzoid and quinoid resonance structures for the 1,5-naphthylene-based copolymer leads to a 20 – 30 nm blue shift of its absorption and emission spectra (both in dilute solution at different temperature and in the solid state). Investigations of its electronic properties in OFET devices are currently under way.

2.6 Experimental Section

Materials and Characterization. Unless otherwise indicated, all reagents were obtained from commercial suppliers and were used without further purification. The solvents used were commercial p.a. quality. The reactions were carried out under argon with the use of standard and Schlenk techniques. The vials for the microwave assisted reactions were filled in a glove box. ^1H - and ^{13}C -NMR data were obtained on a Bruker ARX 400-spectrometer. The UV-Vis and fluorescence spectra were recorded on a Jasco V-550 spectrophotometer and a Varian-Cary Eclipse photoluminescence spectrometer, respectively. Gel permeation chromatographic analysis (GPC) utilized PS-columns (two columns, 5 μm gel, pore widths mixed bed linear) connected with UV/Vis and RI detection. All GPC analyses were performed on solutions of the polymers in THF at 30 $^\circ\text{C}$ (concentration of the polymer: approx. 1.5 g/L). The calibration was based on polystyrene standards with narrow molecular weight distribution. Microwave-assisted syntheses were performed using a CEM Discover microwave system.

2.6.1 Monomer Synthesis

2,2':5',2''-Terthiophene (3)



2-bromothiophene (14.7 g, 90 mmol) was added drop-wise to a refluxing mixture of magnesium turnings (2.2 g, 90 mmol) with a trace of iodine in anhydrous diethylether (40 mL). The mixture was refluxed for one hour. After complete dissolution of the magnesium the resulting Grignard compound was transferred to a second three-necked flask containing 2,5-dibromothiophene (9.7 g, 40 mmol) and [1,3-bis(diphenylphosphino)-propane]nickel (II) (Ni(dppp)Cl₂) (48 mg, 0.09 mmol) in anhydrous diethylether and stirred at room temperature for 48 h. The solution was poured into water and extracted with ether. The organic layer was washed with brine and dried over Na₂SO₄. After evaporation of the solvent the remaining residue was recrystallized from ethanol. Yield: 82%. ^1H NMR (400 MHz, C₂D₂Cl₄, 25 $^\circ\text{C}$): δ [ppm] = 7.18 (d, 2H, J = 5.0 Hz, H-a), 7.12 (d, 2H, J = 3.7 Hz, H-c), 7.03 (s, 2H, H-d), 6.97 (dd, 2H, J = 3.7 Hz, J = 5.0 Hz, H-b). ^{13}C NMR (100 MHz, C₂D₂Cl₄, 25 $^\circ\text{C}$): δ [ppm] = 137.2, 136.4, 128.3, 125.0, 124.7, 124.1. LR-MS (EI, 70eV): m/z = 248

[M⁺] (100.0), 249 (16.5), 250 (16.7). Anal. Calcd. for C₁₂H₈S₃: C, 58.03; H, 3.25; S, 38.73. Found: C, 57.88; H, 3.74; S, 38.24.

General procedure for α,ω -distannylated oligothiophenes. The oligothiophene (10 mmol) was dissolved in a mixture of THF (30 ml) and N,N,N',N'-tetramethyl-1,2-ethanediamine (2.56 g, 22 mmol, TMEDA) and cooled to -78 °C. Whilst maintaining the temperature n-butyl lithium (1.25 mL, 18 mmol, 1.6 M in hexane) was added dropwise. The mixture was stirred at -78 °C for 1h, then allowed to warm up to room temperature and stirred for an additional 2 h. The reaction was cooled to -78 °C and trimethyltin chloride (23 ml, 1 M in THF, 23 mmol) was added in one portion. The mixture was again allowed to warm up to room temperature and stirred for 12 h. The reaction was quenched by addition of saturated, aqueous ammonium chloride solution and extracted with chloroform. The organic phases were combined, extensively washed with water and brine and dried over Na₂SO₄. The solvent was removed via rotary evaporation and the crude product recrystallized from ethanol.

5,5'-Bis(trimethylstannyl)-2,2'-bithiophene (4)

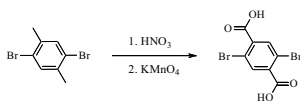


Yield: 77 %. ¹H NMR (400 MHz, C₂D₂Cl₄, 25 °C): δ [ppm] = 7.20 (d, 2H, J = 3.3 Hz), 7.02 (d, 2H, J = 3.3 Hz), 0.32 (s, 18H). ¹³C NMR (100 MHz, C₂D₂Cl₄, 80 °C): δ [ppm] = 143.1, 137.5, 136.3, 125.0, -7.7. FD-MS: 491.8 (100.0). Anal. Calcd. for C₁₄H₂₂S₂Sn₂: C, 34.19; H, 4.51; S, 13.04. Found: C, 34.01; H, 4.46; S, 12.45.

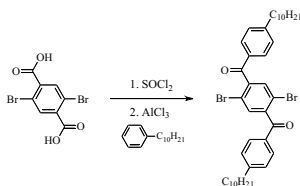
5,5''-Bis(trimethylstannyl)-2,2':5,2''-terthiophene (5)



Yield: 71 %. ¹H NMR (400 MHz, C₂D₂Cl₄, 25 °C): δ [ppm] = 7.21 (d, 2H, J = 3,3 Hz), 7.04 (d, 2H, J = 3.3 Hz), 7.00 (s, 2H), 0.33 (s, 18H, -CH₃). ¹³C NMR (100 MHz, C₂D₂Cl₄, 25 °C): δ [ppm] = 142.5, 138.0, 136.1, 134.9, 125.0, 124.3, -7.9. FD-MS: 573.9 (100.0). Anal. Calcd. for C₁₄H₂₂S₃Sn₂: C, 37.67; H, 4.21; S, 16.76. Found: C, 37.55; H, 4.11; S, 16.74.

2,5-Dibromoterephthalic acid (7)

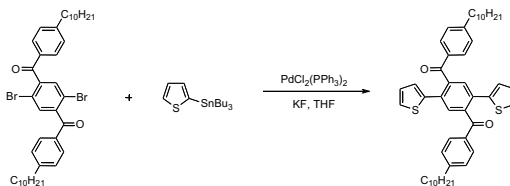
[modification of ref. 22] 2,5-dibromo-1,4-dimethyl-benzene (100 g, 0.38 mol) was stirred in 300 mL of HNO₃ (~40%) and refluxed for 5 days. The reaction mixture was cooled down to room temperature and neutralized with aqueous KOH solution. KMnO₄ (150 g, 0.95 mmol) was added and the mixture refluxed for further 24 h. Then, an additional portion of KMnO₄ (50 g, 0.32 mmol) was added and the reaction refluxed for additional 24 h. The reaction mixture was cooled down to room temperature and acidified with sulphuric acid (pH = 1). After addition of Na₂SO₃ the solution cleared and a colorless precipitate could be separated, washed and dried. Yield: 74 %. ¹H NMR (400 MHz, DMSO-d₆, 80°C): δ [ppm] = 15.3-12.7 (bs, 2H), 7.98 (s, 2H). ¹³C NMR (50 MHz, DMSO-d₆, 80°C): δ [ppm] = 165.8, 137.3, 135.2, 119.0. LR-MS (EI, 70eV): m/z = 307 (43.4), 322 (50.8), 324 [M⁺] (100.0), 326 (47.5).

4',4''-Didecyl-2,5-dibromoterephthalophenone (8)

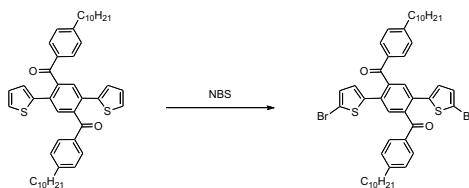
[modification of ref. 9] 2,5-dibromoterephthalic acid (20 g, 0.046 mol) was refluxed in thionyl chloride (30 g, 0.25 mol) for 8 h. The excess of thionyl chloride was distilled off and the residue recrystallized from heptane, filtered and dried. The dichloride was used for the next step without any further purification. To a solution of 2,5-dibromo-terephthaloyl dichloride (3.6g, 10 mmol) in dichloromethane (100 mL) aluminium trichloride (3.4 g, 26 mmol) was added at 0 °C. After 15 min, a solution of *n*-decyl-benzene (9 g, 41 mmol) in dichloromethane (25 mL) was added and stirred for 24 h at room temperature. The reaction was quenched with aqueous HCl (2 N) and the reaction product extracted into dichloromethane. The organic phase was washed with water, brine, dried over Na₂SO₄, and the solvent evaporated to dryness. The crude product was recrystallized from acetone. Yield: 75 %. ¹H NMR (400 MHz, C₂D₂Cl₄, 25°C): δ [ppm] = 7.67 (d, 2H, J = 8.2Hz),

7.52 (s, 2H), 7.25 (d, 2H, $J = 8.2\text{Hz}$), 2.62 (t, 4H, $J = 8.86$), 1.56 (m, 32H), 0.80 (t, 6H, $J = 6.8\text{Hz}$).
 ^{13}C NMR (100 MHz, $\text{C}_2\text{D}_2\text{Cl}_4$, 25°C): δ [ppm] = 193.6 (C=O), 151.0, 143.5, 133.3, 133.1, 130.7, 129.32, 118.8, 36.5, 32.2, 32.2, 31.2, 29.9, 29.8, 29.7, 29.6, 23.0, 14.5. LR-MS (EI, 70eV): m/z = 245 (100.0), 507 (21.5), 724 [M^+] (53.2), 725 (20.5).

4',4''-Didecyl-2,5-bis(2'-thienyl)terephthalophenone (14)



1,4-Bis(4,4'-decylbenzoyl)-2,5-dibromobenzene (2.0 g, 2.76 mmol), 2-(tributyl-stanny)thiophene (2.36 g, 6.34 mmol), potassium fluoride (1.6 g, 27.6 mmol), and bis(triphenylphosphine)-palladium(II)chloride (194 mg, 10 mol%) were mixed in a Schlenk tube under argon atmosphere. THF (50 ml) was added and the reaction mixture was stirred for 2 d at 90°C . Afterwards the reaction mixture was extracted with a mixture of water and chloroform. The organic layer was extensively washed with water, dried with Na_2SO_4 and the solvent was removed *in vacuo*. The crude product was purified by column chromatography on silica (hexane/ethyl acetate : 99/1 v:v) and recrystallized from ethanol to give 1.16 g (58 %) of white crystals. ^1H -NMR (400 MHz, CDCl_3): δ [ppm] = 7.70 (d, 4H, $J=8.2\text{Hz}$), 7.61 (s, 2H), 7.18 (s, 2H), 7.16 (d, 4H, $J=7.9\text{Hz}$), 7.00 (d, 2H, $J=3.5\text{Hz}$), 6.84 (dd, 2H, $J=3.7\text{Hz}$, $J=5.0\text{Hz}$), 2.60 (m, 4H), 1.65 (m, 8H), 1.36 (m, 24H), 0.93 (t, 6H, $J=7.3\text{Hz}$). ^{13}C -NMR (100 MHz, CDCl_3): δ [ppm] = 197.3, 149.5, 140.4, 140.0, 134.2, 131.8, 130.1, 129.4, 128.5, 127.9, 127.6, 126.7, 36.0, 31.8, 30.9, 29.5, 29.5, 29.4, 29.2, 29.1, 22.6, 13.5. FT-mass: m/z (calc) = 730.5 (731.1) Anal. Calcd. for $\text{C}_{48}\text{H}_{58}\text{O}_2\text{S}_2$: C, 78.86; H, 8.00; S, 8.77. Found: C, 78.45; H, 7.70; S, 8.79.

4',4''-Didecyl-2,5-bis(5'-bromothiien-2'-yl)terephthalophenone (15)

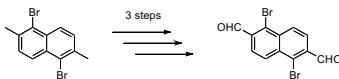
A solution of 4',4''-didecyl-2,5-bis(2'-thienyl)terephthalophenone (1.0 g, 1.4 mmol) in DMF (25 ml) was protected from light and cooled down to $-20\text{ }^{\circ}\text{C}$. To this solution a mixture of NBS (0.61 g, 3.4 mmol, 2.5 eq) in DMF (25 ml) was added dropwise. The mixture was stirred at $-20\text{ }^{\circ}\text{C}$ for 30 min, and then allowed to warm up to room temperature. The mixture was stirred for another 8 h at r.t., and then poured onto ice and extracted with dichloromethane. The combined organic layers were dried over Na_2SO_4 . Afterwards the solvents were removed *in vacuo*. The crude product was purified by column chromatography on silica (hexane/ethyl acetate : 90/10 v:v) and recrystallized from ethanol. Yield: 700 mg. $^1\text{H-NMR}$ (400 MHz, $\text{C}_2\text{D}_2\text{Cl}_4$): δ [ppm] = 7.61 (d, 4H, $J=8.2\text{Hz}$), 7.44 (s, 2H), 7.14 (m, 4H), 6.77 (d, 2H, $J=3.8\text{Hz}$), 6.67 (d, 2H, $J=3.9\text{Hz}$), 2.56 (m, 4H), 1.53 (s, 8H), 1.19 (m, 24H), 0.80 (t, 6H, $J=6.8\text{Hz}$). $^{13}\text{C-NMR}$ (100 MHz, $\text{C}_2\text{D}_2\text{Cl}_4$): δ [ppm] = 197.5, 150.0, 140.5, 140.1, 134.3, 132.1, 130.4, 129.8, 128.9, 128.2, 128.1, 127.2, 36.3, 32.1, 31.1, 29.8, 29.8, 29.7, 29.6, 29.5, 23.0, 14.5. FT-mass: m/z (calc) = 887.6 (888.9). FT-IR (neat): ν [cm^{-1}] = 2920, 2850, 1653, 1603, 1570, 1466, 1432, 1415, 1375, 1310, 1282, 1239, 1178, 1145, 1119, 1078, 997, 963, 921, 894, 846, 808, 757, 718, 699. Anal. Calcd. for $\text{C}_{48}\text{H}_{56}\text{Br}_2\text{O}_2\text{S}_2$: C, 64.84; H, 6.35; S, 7.21. Found: C, 64.76; H, 6.13; S, 7.11.

1,5-Dibromo-2,6-dimethylnaphthalene (24)

2,6-Dimethylnaphthalene (20 g, 128 mmol) was dissolved in acetic acid (500 mL), protected from light and bromine (47.1 g, 297 mmol) diluted in acetic acid was added drop-wise. Thereafter, the mixture was stirred for 3 days at room temperature, after which water (600 ml) was added. The crude product precipitated, this was filtered off and recrystallized from chloroform to give the pure product as white needles. Yield: 28.9 g (72%) $^1\text{H NMR}$ ($\text{C}_2\text{D}_2\text{Cl}_4$, 400 MHz): δ [ppm] = 8.13 (d, $3J= 8.39$, 2H), 7.35 (d, $3J= 8.39$, 2H), 2.58 (s, 6H). $^{13}\text{C NMR}$ ($\text{C}_2\text{D}_2\text{Cl}_4$, 100 MHz): δ [ppm] =

136.3, 132.3, 130.0, 126.7, 124.2, 24.1. FT-mass: m/z (calc) = 313.8 (311.9). Anal. Calcd. for $C_{12}H_{10}Br_3$: C, 46.17 H, 3.20 Found: C, 45.87 H, 2.94.

1,5-Dibromonaphthalene-2,6-dicarbaldehyde (25)



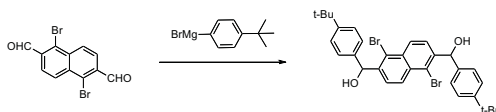
a) 1,5-Dibromo-2,6-dimethylnaphthalene (8 g, 25.6 mmol) and N-bromo-succinimide (13.6 g, 76.8 mmol) were dissolved in tetrachloromethane (200 ml) and heated to reflux. A small amount (tip of a spatula) of benzoyl peroxide was added immediately and another portion 1.5 h later. After stirring for 4 h the reaction mixture was allowed to cool down to room temperature and aq. $NaHCO_3$ -solution added. The white precipitate [1,5-dibromo-2,6-bis(bromomethyl)naphthalene] was filtered off and dried. Yield: 7.7 g (64%) 1H NMR ($C_2D_2Cl_4$, 400 MHz): δ [ppm] = 8.27 (d, J = 8.39, 2H), 7.59 (d, J = 8.39, 2H), 4.78 (s, 4H). FT-mass: m/z (calc) = 467.4 (467.8) Anal. Calcd. for $C_{12}H_8Br_4$: C, 30.81 H, 1.72 Found: C, 30.52 H, 1.90.

b) 1,5-Dibromo-2,6-bis(bromomethyl)naphthalene (8.6 g, 18.4 mmol) and potassium carbonate (40.5 g, 40.5 mmol) suspended in water (150 mL) were dissolved in 1,4-dioxane and refluxed for 48 h. The solvent was carefully removed on a rotary evaporator and 6N aqueous hydrochloric acid added to maintain a pH of 1. The white precipitate was filtered off and extensively washed with water. The product [1,5-dibromo-2,6-bis(hydroxymethyl)naphthalene] was vacuum dried at 50 °C and further used without purification. Yield: 5.7 g (89%) 1H NMR (DMSO- d_6 , 400 MHz): δ [ppm] = 8.27 (d, J = 8.90, 2H), 7.83 (d, J = 8.90, 2H), 4.76 (s, 4H). ^{13}C NMR (DMSO- d_6 , 100 MHz): δ [ppm] = 139.7, 131.3, 126.8, 125.8, 125.5, 120.0. FT-mass: m/z (calc) = 343.4 (343.8). Anal. Calcd. for $C_{12}H_{10}Br_2O_2$: C, 41.91 H, 2.92 Found: C, 41.86 H, 2.78.

c) The dialcohol (5.7 g, 16.5 mmol) obtained from the hydrolysis of 1,5-dibromo-2,6-bis(bromomethyl)naphthalene, pyridinium chlorochromate (7.36 g, 66.0 mmol) and crushed mol sieve (40 g) were suspended in dichloromethane (800 mL) and refluxed for 4 h. The mixture was allowed to cool down to room temperature, diluted with diethyl ether and filtered through a plug of silica and washed extensively with hot chloroform. The organic phases were combined and the solvents evaporated. Recrystallization from chloroform gave the pale yellow product. Yield: 3.5 g (63%) 1H NMR ($C_2D_2Cl_4$, 400 MHz): δ [ppm] = 10.60 (s, 2H), 8.53 (d, J = 8.90, 2H), 8.02 (d, J =

8.90, 2H). ^{13}C NMR ($\text{C}_2\text{D}_2\text{Cl}_4$, 100 MHz): δ [ppm] = 191.9, 136.2, 134.4, 130.1, 128.5, 126.6. FT-mass: m/z (calc) = 342.8 (342). Anal. Calcd. for $\text{C}_{12}\text{H}_6\text{Br}_2\text{O}_2$: C, 42.15; H, 1.77 Found: C, 42.30; H, 1.75.

1,5-Dibromo-2,6-bis(4-*tert*-butylphenyl-hydroxymethyl)naphthalene (26)



1,5-Dibromo-naphthalene-2,6-dicarbaldehyde **25** (2.0 g, 5.8 mmol) was dissolved in 200 mL of dry diethyl ether. The solution was cooled down to 0 °C before 14.5 mL of 4-*tert*-butylphenylmagnesium bromide (2.0 M in diethyl ether) was added dropwise. The reaction mixture was allowed to warm up to room temperature and stirred for an additional 48 h. Afterwards, the reaction mixture was poured into ice-water and treated with 2 N aqueous HCl. The aqueous phase was extracted with diethyl ether and the combined organic phases were washed (water and brine) and dried with MgSO_4 . The solvents were evaporated and the crude product purified by column chromatography on silica with petrol ether/acetic ester (4:1) as eluent (yield: 3.0 g of white crystals, 86%). ^1H NMR (DMSO-d_6 , 400 MHz): δ [ppm] = 8.29 (d, $J=8.9$ Hz, 2H), 8.06 (d, $J=8.9$ Hz, 2H), 7.29 (s, 8H), 6.25 (d, $J=4.4$ Hz, 2H), 6.21 (d, $J=4.4$ Hz, 2H), 1.18 (s, 18H). ^{13}C NMR (DMSO-d_6 , 100 MHz): δ [ppm] = 149.3, 143.2, 140.3, 131.5, 127.3, 126.8, 126.2, 124.7, 120.9, 73.1, 34.0, 30.9, FT-mass: m/z (calc) = 604.4 (608.1): Anal. Calcd. for $\text{C}_{32}\text{H}_{34}\text{Br}_2\text{O}_2$: C, 63.15; H, 5.59; Found: C, 62.52; H, 5.56.

1,5-Dibromo-2,5-bis(4-*tert*-butylbenzoyl)naphthalene (27)



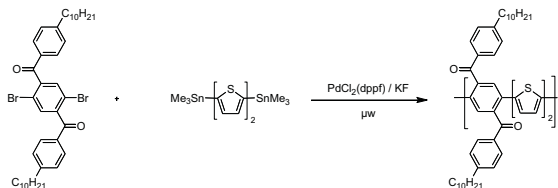
1,5-Dibromo-2,6-bis(4-*tert*-butylphenyl-hydroxymethyl)naphthalene (11.0 g, 5 mmol) was dissolved in 400 mL of toluene. Solid manganese dioxide (>10 micrometers) (32.0 g, 366 mmol)

was added in one portion. The reaction mixture was stirred for 4 d under air. The progress of the reaction was monitored by thin layer chromatography (TLC) with petrol ether/acetic ester (4:1) as eluent. The excess manganese dioxide and other manganese compounds were filtered off (Celite 500). After removing the solvent, **27** was obtained as a white solid (9.5 g, 87%). Mp: 236.8 °C. ^1H NMR ($\text{C}_2\text{D}_2\text{Cl}_4$, 400 MHz): δ [ppm] = 8.39 (d, $J=8.4$ Hz, 2H), 7.68 (d, $J=8.4$ Hz, 4H), 7.47 (d, $J=8.4$ Hz, 2H), 7.41 (d, $J=8.4$ Hz, 4H), 1.27 (s, 18H). ^{13}C NMR ($\text{C}_2\text{D}_2\text{Cl}_4$, 100 MHz): δ [ppm] = 195.6, 158.5, 141.0, 133.3, 133.2, 130.6, 127.9, 127.1, 126.2, 120.2, 35.5, 31.3. FT-mass: m/z (calc) = 606.0 (606.4): Anal. Calcd. for $\text{C}_{32}\text{H}_{30}\text{Br}_2\text{O}_2$: C, 63.62; H, 4.97; Found: C, 64.08; H, 5.06.

2.6.2 Polymer Synthesis

General procedure for microwave-assisted Stille-type polymerizations. Equimolar amounts of the bis(trimethylstannyl)oligothiophene and 4',4''-didecyl-2,5-bis(5'-bromothiophen-2'-yl)terephthalophen-one (**15**), 10 eq. of potassium fluoride, and 10 mol% $\text{PdCl}_2(\text{dppf})$ were mixed in a sealed 10 ml vial under glove box conditions. Dry toluene (2 ml) and dry DMF (1 ml) were added and the solutions irradiated with microwaves (300W, 110 °C) for 15 min. The reaction mixture was diluted with chloroform and washed with aqueous 2N HCl, saturated aqueous NaHCO_3 and NaEDTA solutions and brine. The organic phase was dried over Na_2SO_4 and the solvent removed *in vacuo*. The residue was dissolved in chloroform, re-precipitated into methanol, filtered and dried.

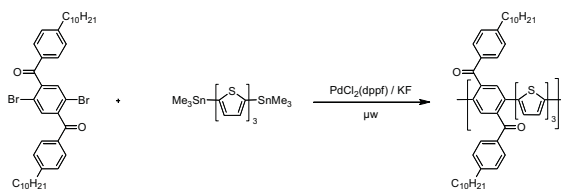
Synthesis of polyketone **9**



Yield: 44 %. GPC (vs polystyrene standards in THF) $M_n = 10,400$ g/mol, $M_w/M_n = 2.8$. ^1H -NMR (400 MHz, $\text{C}_2\text{D}_2\text{Cl}_4$): δ [ppm] = 7.67-7.61 (m, 4H), 7.51-7.48 (bs, 2H), 7.17-7.11 (m, 4H), 6.86-6.75 (m, 4H), 2.61-2.53 (m, 4H), 1.59-1.49 (m, 8H), 1.29-1.17 (m, 24H), 0.87-0.79 (m, 6H). ^{13}C -NMR (100 MHz, $\text{C}_2\text{D}_2\text{Cl}_4$): δ [ppm] = 196.7, 149.9, 140.4, 139.5, 138.3, 134.5, 131.5, 130.3, 129.5, 129.0, 128.8, 124.9, 36.2, 32.0, 30.8, 29.7, 29.6, 29.5, 29.4, 29.3, 22.8, 14.2. UV/VIS (CHCl_3): λ_{max}

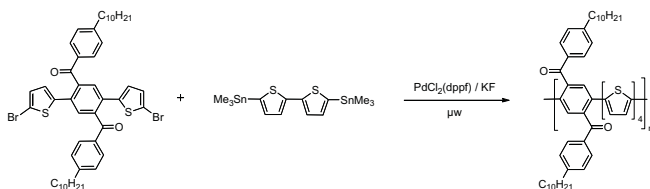
[nm] = 492. FT-IR (neat): ν [cm^{-1}] = 2922, 2851, 1659 (C=O), 1603, 1572, 1529, 1485, 1462, 1414, 1371, 1309, 1279, 1244, 1178, 1146, 1119, 1068, 1019, 984, 928, 893, 849. Anal. Calcd. for $\text{C}_{48}\text{H}_{56}\text{O}_2\text{S}_2$: C, 79.07; H, 7.74; S, 8.80. Found: C, 78.99; H, 7.54; S, 8.49.

Synthesis of polyketone 10



Yield: 47 %. GPC (vs polystyrene standards in THF) $M_n = 14,800$ g/mol, $M_w/M_n = 3.6$. $^1\text{H-NMR}$ (400 MHz, $\text{C}_2\text{D}_2\text{Cl}_4$): δ [ppm] = 7.66-7.59 (m, 4H), 7.49-7.44 (bs, 2H), 7.12-7.01 (m, 6H), 6.82-6.74 (m, 4H), 2.58-2.51 (m, 4H), 1.62-1.47 (m, 8H), 1.33-1.16 (m, 24H), 0.88-0.79 (m, 6H). $^{13}\text{C-NMR}$ (100 MHz, $\text{C}_2\text{D}_2\text{Cl}_4$): δ [ppm] = 194.2, 149.1, 140.4, 140.2, 138.0, 134.6, 134.5, 131.5, 130.1, 129.4, 129.2, 129.1, 128.6, 124.5, 36.2, 32.1, 30.5, 29.7, 29.6, 29.5, 29.4, 29.2, 23.1, 14.3. UV/VIS (CHCl_3): λ_{max} [nm] = 494. FT-IR (neat): ν [cm^{-1}] = 2922, 2849, 1663 (C=O), 1599, 1575, 1538, 1455, 1416, 1371, 1309, 1279, 1256, 1173, 1133, 1075, 990, 927. Anal. Calcd. for $\text{C}_{52}\text{H}_{58}\text{O}_2\text{S}_3$: C, 76.99; H, 7.21; S, 11.86. Found: C, 76.88; H, 6.98; S, 11.42.

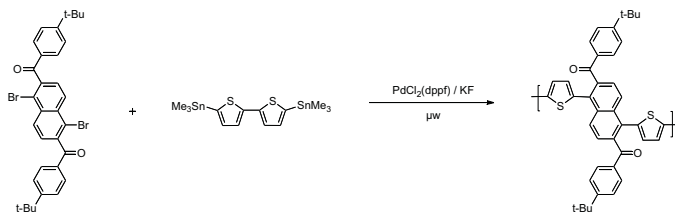
Synthesis of polyketone 16



Yield 52 %. GPC (vs polystyrene standards in THF) $M_n = 12,600$ g/mol, $M_w/M_n = 3.2$. $^1\text{H-NMR}$ (400 MHz, $\text{C}_2\text{D}_2\text{Cl}_4$): δ [ppm] = 7.69-7.60 (m, 4H), 7.56-7.44 (m, 2H), 7.18-7.10 (m, 4H), 7.04-6.71 (m, 8H), 2.59-2.51 (m, 4H), 1.58-1.43 (m, 8H), 1.26-1.11 (m, 24H), 0.85-0.75 (m, 6H). $^{13}\text{C-NMR}$ (100 MHz, $\text{C}_2\text{D}_2\text{Cl}_4$): δ [ppm] = 196.9, 150.0, 140.5, 135.0, 134.6, 131.8, 131.7, 130.3, 129.1, 128.9, 127.9, 127.6, 125.0, 124.9, 124.8, 124.7, 36.2, 32.0, 30.9, 29.8, 29.7, 29.6, 29.5, 29.4, 22.8, 14.2. UV/VIS (CHCl_3): λ_{max} [nm] = 495. FT-IR (neat): ν [cm^{-1}] = 2919, 2850, 1661 (C=O), 1603,

1489, 1456, 1414, 1337, 1280, 1251, 1178, 1146, 1101, 1067, 926, 893, 850, 788. Anal. Calcd. for $C_{56}H_{60}O_2S_4$: C, 75.29; H, 6.77; S, 14.36. Found: C, 75.02; H, 6.55; S, 13.98.

Synthesis of polyketone 28

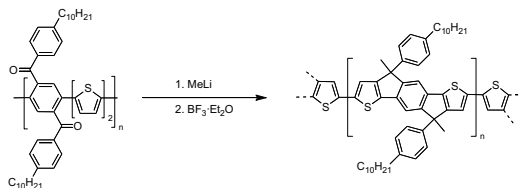


The herein utilized method was slightly modified with respect to the general procedure: 1,5-Dibromo-2,5-bis(4-*tert*-butylbenzoyl)naphthalene (100 mg, 0.16 mmol), 5,5'-bis(trimethylstannyl)-2,2'-bithiophene (81.1 mg, 0.16 mmol), potassium fluoride (95.8 mg, 1.6 mmol) and 1,1-bis(diphenylphosphino)-ferrocenedichloropalladium(II) (12.1 mg, 10 mol%) were transferred into a 10 mL microwave vial. Afterwards the microwave vial was sealed, evacuated and flushed with argon. 2 ml of toluene and 1 ml of DMF were added via a syringe and the mixture irradiated with microwaves (300 W, 120 °C) for 12 min until black palladium metal precipitated out. The mixture was filtered to remove the metallic palladium, diluted with chloroform and washed with aqueous 2N HCl, saturated aqueous NaHCO_3 and NaEDTA solutions and brine. The organic phase was dried over Na_2SO_4 and the solvent removed *in vacuo*. The residue was dissolved in chloroform, reprecipitated into methanol, filtered and dried. Yield: 49 %. GPC (vs polystyrene standards in THF) $M_n = 12,800$ g/mol, $M_w/M_n = 2.4$. ^1H NMR ($\text{C}_2\text{D}_2\text{Cl}_4$, 400 MHz): δ [ppm] = 8.20-8.12 (m, 2H), 7.57-7.52 (m, 4H), 7.33-7.27 (m, 4H), 6.92-6.88 (m, 2H), 6.87-6.83 (m, 2H), 1.27-1.21 (m, 18H). ^{13}C NMR ($\text{C}_2\text{D}_2\text{Cl}_4$, 100 MHz): δ [ppm] = 197.4, 157.3, 140.3, 139.1, 136.7, 135.1, 133.9, 131.5, 130.0, 128.0, 125.9, 125.3, 124.2, 123.9, 35.2, 31.2. FT-IR (neat): ν [cm^{-1}] = 2925, 2852, 1671, 1603, 1461, 1408, 1362, 1332, 1259, 1193, 1164, 1108, 1026, 976, 866, 847, 794, 772, 719, 701. Anal. Calcd. for $\text{C}_{40}\text{H}_{34}\text{O}_2\text{S}_2$: C, 78.65; H, 5.61; S, 10.50; Found C, 78.19; H, 6.23; S, 9.96.

General procedure for the cyclization sequence. A 40-fold excess of MeLi (3.5 mL, 5.6 mmol, 1.6 M) was added at r.t. to a solution of the previously synthesized diketo polymer (0.1 mmol) in toluene (30 ml) and stirred for 30 min. Afterwards THF (20 ml) was added and the mixture stirred at r.t. for additional 12 h. The reaction was quenched with ethanol, chloroform added, and the

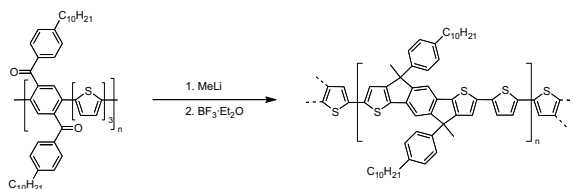
solution washed with aqueous 2N HCl and brine. The organic phase was dried over Na_2SO_4 and the solvent removed *in vacuo*. The crude product was dissolved in dichloromethane (30 ml) and treated with an excess of borontrifluoride etherate (2 mL, 15.9 mmol). The solution was stirred for 3 h and then a mixture of ethanol/water (2:1) added. The organic layer was diluted with chloroform and extracted several times with water. The organic phase was dried over Na_2SO_4 and the solvent removed *in vacuo*. The residue was dissolved in chloroform and precipitated into methanol to give the cyclized step-ladder copolymers.

Synthesis of the step-ladder copolymer 11



Yield: 76 %. GPC (vs polystyrene standards in THF) $M_n = 12,000$ g/mol, $M_w/M_n = 2.0$. $^1\text{H-NMR}$ (400 MHz, $\text{C}_2\text{D}_2\text{Cl}_4$): δ [ppm] = 7.61 (d, 4H, $J = 8$ Hz), 7.45 (s, 2H), 7.11 (d, 4H, $J = 8$ Hz), 6.76 (bs, 2H), 2.58-2.44 (m, 4H), 1.88-1.80 (bs, 6H, CH_3 bridge), 1.52-1.48 (m, 8H), 1.21-1.11 (m, 24H), 0.81-0.75 (m, 6H). $^{13}\text{C-NMR}$ (100 MHz, $\text{C}_2\text{D}_2\text{Cl}_4$): δ [ppm] = 140.9, 140.0, 136.9, 136.3, 133.9, 133.0, 130.9, 128.8, 128.2, 126.1, 125.8, 53.2, 36.1, 32.2, 31.0, 29.7, 29.6, 29.5, 29.4, 29.3, 23.0, 14.2, 13.5. UV/VIS (CHCl_3): λ_{max} [nm] = 492. FT-IR (neat): ν [cm^{-1}] = 2920, 2850, 1510, 1455, 1414, 1374, 1322, 1242, 1187, 1123, 1059, 1018, 990, 960, 871, 822, 720, 698, 674, 658. Anal. Calcd. for $\text{C}_{50}\text{H}_{60}\text{S}_2$: C, 82.82; H, 8.34; S, 8.84. Found: C, 82.60; H, 7.99; S, 8.61.

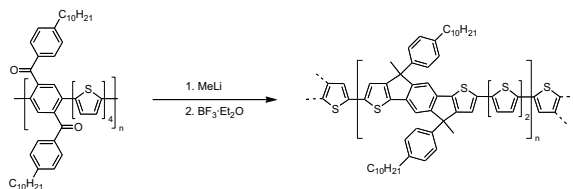
Synthesis of the step-ladder copolymer 12



Yield: 71 %. GPC (vs polystyrene standards in THF) $M_n = 16,200$ g/mol, $M_w/M_n = 2.9$. $^1\text{H-NMR}$ (400 MHz, $\text{C}_2\text{D}_2\text{Cl}_4$): δ [ppm] = 7.25-7.12 (m, 6H), 7.08-6.85 (m, 8H), 2.57-2.42 (m, 4H), 1.95-

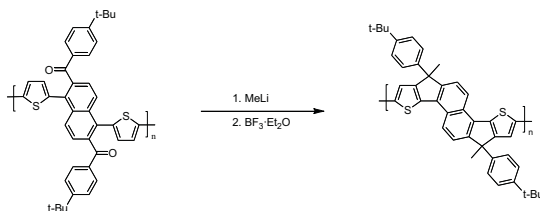
1.75 (m, 6H, CH₃ bridge), 1.65-1.45 (m, 8H), 1.35-1.05 (m, 24H), 0.90-0.74 (m, 6H). ¹³C-NMR (100 MHz, C₂D₂Cl₄): δ [ppm] = 140.2, 138.4, 137.1, 136.5, 136.1, 133.3, 130.7, 129.8, 129.4, 128.7, 128.2, 125.0, 124.9, 54.1, 36.2, 32.0, 31.1, 29.7, 29.6, 29.5, 29.4, 29.3, 22.9, 14.2, 13.5. UV/VIS (CHCl₃): λ_{max} [nm] = 508. FT-IR (neat): ν [cm⁻¹] = 2922, 2851, 1606, 1511, 1455, 1410, 1374, 1293, 1260, 1170, 1064, 1018, 904, 827, 790, 716, 692. Anal. Calcd. for C₅₄H₆₂S₃: C, 80.34; H, 7.74; S, 11.92. Found: C, 79.84; H, 7.26; S, 11.72.

Synthesis of the step-ladder copolymer 17



Yield: 72 %. GPC (vs polystyrene standards in THF) M_n = 14,200 g/mol, M_w/M_n = 3.1. ¹H-NMR (400 MHz, C₂D₂Cl₄): δ [ppm] = 7.23-7.18 (m, 2H), 7.18-7.11 (m, 4H), 7.07-6.97 (m, 6H), 6.97-6.93 (m, 4H), 2.56-2.44 (m, 4H), 1.90-1.77 (m, 6H, CH₃ bridge), 1.58-1.39 (m, 8H), 1.33-1.06 (m, 24H), 0.87-0.74 (m, 6H). ¹³C-NMR (100 MHz, C₂D₂Cl₄): δ [ppm] = 140.4, 138.2, 137.6, 137.0, 136.4, 136.5, 133.7, 133.6, 130.4, 129.9, 128.8, 128.1, 125.4, 125.1, 124.9, 56.3, 36.1, 32.1, 31.4, 29.7, 29.6, 29.5, 29.4, 29.3, 22.8, 14.2, 13.6. UV/VIS (CHCl₃): λ_{max} [nm] = 509. FT-IR (neat): ν [cm⁻¹] = 2920, 2850, 1510, 1455, 1414, 1374, 1322, 1187, 1171, 1122, 1100, 1058, 1018, 871, 825, 787. Anal. Calcd. for C₅₈H₆₄S₄: C, 78.33; H, 7.25; S, 14.42. Found: C, 77.82; H, 6.98; S, 14.11.

Synthesis of the step-ladder copolymer 29

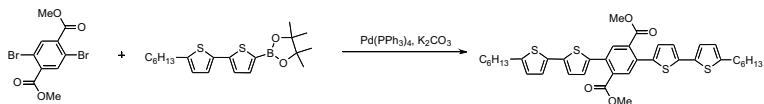


Yield: 82 %. GPC (vs polystyrene standards in THF) M_n = 13,500 g/mol, M_w/M_n = 2.1. ¹H NMR (C₂D₂Cl₄, 400 MHz): δ [ppm] = 8.01-7.94 (m, 4H), 7.92 (s, 2H), 7.56-7.49 (m, 4H), 7.25-7.15 (m,

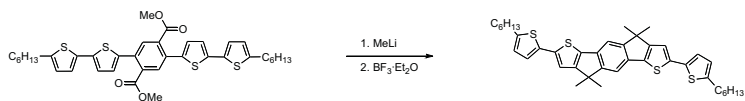
4H), 1.99-1.90 (m, 6H, CH₃ bridge), 1.24 (s, 18H). ¹³C-NMR (100 MHz, C₂D₂Cl₄): δ [ppm] = 149.1, 140.2, 134.4, 133.8, 133.6, 132.8, 131.0, 127.7, 126.1, 126.0, 125.8, 125.7, 125.5, 55.4, 34.5, 31.2, 13.2. UV/VIS (CHCl₃): λ_{max} [nm] = 485. FT-IR (neat): ν [cm⁻¹] = 2959, 2924, 2862, 1674, 1560, 1512, 1455, 1407, 1384, 1361, 1332, 1260, 1217, 1200, 1114, 1087, 1061, 1014, 984, 927, 839, 810, 747, 724, 698, 668, 654. Anal. Calcd. for C₄₂H₃₈S₂: C, 83.12; H, 6.31; S, 10.57; Found: C, 83.01; H, 6.22; S, 10.37.

2.6.3 Synthesis of Model Compounds

2,5-Bis(5-hexyl-2,2'-bithiophene)-5'-yl-dimethylterephthalate (20)



A 250 ml two-neck round bottom flask was charged with 2,5-dibromo-dimethylterephthalate (1.50 g, 4.25 mmol), potassium carbonate (2.9 g, 8.5 mmol, 4 eq), Pd(PPh₃)₄ (0.49g, 10%), THF (60 ml), and water (20 ml). 5-Hexyl-5'-(4,4,5,5-tetramethyl-1,3,2-dioxaborolan-2-yl)-2,2'-bithiophene (4 g, 10.6 mmol, 2.5 eq) was dissolved in degassed THF (20 ml) and added dropwise to the solution via a syringe. The solution was refluxed for 24 h. The reaction mixture was diluted with chloroform and washed with aqueous 2N HCl, saturated aqueous NaHCO₃ and NaEDTA solutions and brine. The organic phase was dried over Na₂SO₄ and the solvent removed *in vacuo*. The crude product was purified by column chromatography on silica (Hex/EA:85/15 v:v) and recrystallized from ethanol. Yield: 76 % ¹H-NMR (400 MHz, CDCl₃): δ [ppm] = 7.72 (s, 2H), 7.01 (d, 2H, J=3.7Hz), 6.96 (d, 2H, J=3.5Hz), 6.92 (d, 2H, J=3.7Hz), 6.64 (d, 2H, J=3.5Hz), 2.73 (t, 4H, J=7.6Hz), 1.64-1.50 (m, 4H), 1.33-1.29 (m, 1H), 1.27-1.18 (m, 12H), 0.83 (t, 6H, J=7.0Hz). ¹³C-NMR (100 MHz, CDCl₃): δ [ppm] = 168.3, 146.4, 139.6, 138.3, 134.3, 133.5, 132.9, 131.8, 128.1, 125.2, 124.1, 123.7, 53.1, 31.8, 31.8, 30.4, 29.0, 22.8, 14.4. FT-mass: m/z (calc) = 690,4 (691) UV/VIS (CHCl₃): λ_{max} [nm] = 384. Anal. Calcd. for C₃₈H₄₂O₄S₄: C, 66.05; H, 6.13; S, 18.56. Found: C, 65.79; H, 5.83; S, 18.09.

Step-ladder model compound 22

22 was generated following the general procedure for the ring closing sequence. Yield: 78 % ¹H-NMR (400 MHz, C₂D₂Cl₄): δ [ppm] = 7.50 (d, 2H, J = 3.7 Hz), 7.25 (s, 2H), 6.98 (s, 2H), 6.63 (d, 2H, J=3.9Hz), 2.72 (m, 12H), 1.66-1.57 (m, 4H, J=7.6Hz), 1.52-1.50 (m, 4H), 1.35-1.21 (m, 12H), 0.82 (t, 6H, J=6.8Hz). ¹³C-NMR (100 MHz, C₂D₂Cl₄): δ [ppm] = 159.1, 155.7, 145.4, 140.0, 138.7, 136.0, 134.3, 125.0, 123.0, 117.1, 113.1, 45.9, 31.7, 31.6, 30.4, 28.9, 26.4, 22.7, 14.2. FD-mass: m/z (calc.) = 654.8 (655.1). UV/VIS (CHCl₃): λ_{max} [nm] = 425, 444 (shoulder). Anal. Calcd. for C₄₀H₄₆S₄: C, 73.34; H, 7.08; S, 19.58. Found: C, 73.04; H, 6.55; S, 19.33.

2.7 References and Notes

1. Kraft, A.; Grimsdale, A. C.; Holmes, A. B., *Angew. Chem. Int. Ed.* **1998**, 37, (4), 402.
2. Anthony, J. E., *Chem. Rev.* **2006**, 106, (12), 5028.
3. McGehee, M. D.; Heeger, A. J., *Adv. Mater.* **2000**, 12, (22), 1655.
4. Dimitrakopoulos, C. D.; Malenfant, P. R. L., *Adv. Mater.* **2002**, 14, (2), 99.
5. Brabec, C. J.; Shaheen, S. E.; Fromherz, T.; Padinger, F.; Hummelen, J. C.; Dhanabalan, A.; Janssen, R. A. J.; Sariciftci, N. S., *Synth. Met.* **2001**, 121, (1-3), 1517.
6. Brabec, C. J.; Sariciftci, N. S.; Hummelen, J. C., *Adv. Funct. Mater.* **2001**, 11, (1), 15.
7. Sheats, J. R., *J. Mater. Res.* **2004**, 19, (7), 1974.
8. Grimsdale, A. C.; Müllen, K., *Macromol. Rapid Commun.* **2007**, 28, (17), 1676.
9. Scherf, U.; Müllen, K., *Macromol. Rapid Commun.* **1991**, 12, 489.
10. Pietrangelo, A.; MacLachlan, M. J.; Wolf, M. O.; Patrick, B. O., *Org. Lett.* **2007**, 9, (18), 3571.
11. Cicoira, F.; Santato, C.; Melucci, M.; Favaretto, L.; Gazzano, M.; Muccini, M.; Barbarella, G., *Adv. Mater.* **2006**, 18, (2), 169.
12. Li, X. C.; Siringhaus, H.; Garnier, F.; Holmes, A. B.; Moratti, S. C.; Feeder, N.; Clegg, W.; Teat, S. J.; Friend, R. H., *J. Am. Chem. Soc.* **1998**, 120, (9), 2206.
13. Takimiya, K.; Kunugi, Y.; Konda, Y.; Niihara, N.; Otsubo, T., *J. Am. Chem. Soc.* **2004**, 126, (16), 5084.
14. Wex, B.; Kaafarani, B. R.; Schroeder, R.; Majewski, L. A.; Burckel, P.; Grell, M.; Neckers, D. C., *J. Mater. Chem.* **2006**, 16, (12), 1121.
15. Xiao, K.; Liu, Y.; Qi, T.; Zhang, W.; Wang, F.; Gao, J.; Qiu, W.; Ma, Y.; Cui, G.; Chen, S.; Zhan, X.; Yu, G.; Qin, J.; Hu, W.; Zhu, D., *J. Am. Chem. Soc.* **2005**, 127, (38), 13281.
16. Yamamoto, T.; Takimiya, K., *J. Am. Chem. Soc.* **2007**, 129, (8), 2224.
17. Li, Y. N.; Wu, Y. L.; Gardner, S.; Ong, B. S., *Adv. Mater.* **2005**, 17, (7), 849.

18. Wu, Y. L.; Li, Y. N.; Gardner, S.; Ong, B. S., *J. Am. Chem. Soc.* **2005**, 127, (2), 614.
19. Kalinin, A. V.; Reed, M. A.; Norman, B. H.; Snieckus, V., *J. Org. Chem.* **2003**, 68, (15), 5992.
20. Behnisch, B.; Martinez-Ruiz, P.; Schweikart, K. H.; Hanack, M., *Eu. J. Org. Chem.* **2000**, (14), 2541.
21. Melucci, M.; Barbarella, G.; Zambianchi, M.; DiPietro, P.; Bongini, A., *J. Org. Chem.* **2004**, 69, (14), 4821.
22. Naylor, J. R., *J. Chem. Soc.* **1952**, 408.
23. Nehls, B. S.; Fuldner, S.; Preis, E.; Farrell, T.; Scherf, U., *Macromolecules* **2005**, 38, (3), 687.
24. Schlüter, A. D., *J. Polym. Sci. Part A: Polym. Chem.* **2001**, 39, (10), 1533.
25. Scherf, U., *J. Mater. Chem.* **1999**, 9, (9), 1853.
26. Scherf, U.; Bohnen, A.; Müllen, K., *Macromol. Chem.* **1992**, 193, (5), 1127.
27. Melucci, M.; Barbarella, G.; Sotgiu, G., *J. Org. Chem.* **2002**, 67, (25), 8877.
28. Chaloner, P. A.; Gunatunga, S. R.; Hitchcock, P. B., *J. Chem. Soc., Perkin Trans. 2* **1997**, (8), 1597.
29. Schweitzer, B.; Arkhipov, V. I.; Scherf, U.; Bäessler, H., *Chem. Phys. Lett.* **1999**, 313, (1-2), 57.
30. Romanovskii, Y. V.; Gerhard, A.; Schweitzer, B.; Personov, R. I.; Bäessler, H., *Chem. Phys.* **1999**, 249, (1), 29.
31. Sinha, S.; Monkman, A. P.; Güntner, R.; Scherf, U., *Appl. Phys. Lett.* **2003**, 82, (26), 4693.
32. Sinha, S.; Rothe, C.; Güntner, R.; Scherf, U.; Monkman, A. P., *Phys. Rev. Lett.* **2003**, 90, (12).
33. Hertel, D.; Soh, E. V.; Bassler, H.; Rothberg, L. J., *Chem. Phys. Lett.* **2002**, 361, (1-2), 99.
34. Sasaki, S.; Yamamoto, T.; Kanbara, T.; Morita, A.; Yamamoto, T., *J. Polym. Sci., Part B* **1992**, 30, (3), 293.

35. Kobashi, M.; Takeuchi, H., *Macromolecules* **1998**, 31, (21), 7273.
36. Chen, S. A.; Lee, S. J., *Synth. Met.* **1995**, 72, (3), 253.
37. Sirringhaus, H.; Tessler, N.; Friend, R. H., *Science* **1998**, 280, (5370), 1741.
38. Thompson, B. C.; Kim, Y. G.; Reynolds, J. R., *Macromolecules* **2005**, 38, (13), 5359.
39. Preis, E.; Scherf, U., *Macromol. Rapid Commun.* **2006**, 27, (14), 1105.
40. Anton, U.; Adam, M.; Wagner, M.; Zhou, Q. L.; Müllen, K., *Chem. Ber. - Recueil* **1993**, 126, (2), 517.
41. Thibault, M. E.; Closson, T. L. L.; Manning, S. C.; Dibble, P. W., *J. Org. Chem.* **2003**, 68, (22), 8373.

3 Phenylene-Thienylene-Vinylene-Based Oligomers

3.1 Introduction and Motivation

Organic field effect transistors (OFET) based on π -conjugated polymers^[1-6] and other small molecules^[7-13] have attracted a lot of attention over the past few decades as they have many advantages over their inorganic counterparts. The properties of individual molecules can be tailored by variation of the molecular structures, e.g., by changing the degree of conjugation^[14] or via introduction of electron-rich or -deficient substituents.^[15] Even though most of the oligomeric materials are still processed via vacuum deposition,^[1-6] upon introduction of suitable solubilizing substituents such oligomers can be made solution-processable, providing the opportunity to coat thin organic layers onto the OFET substrates with well-established printing techniques like ink-jet, offset, and screen printing. Low production costs due to the application of commercially available synthetic building blocks and simple processing make such solubilized oligomers possible candidates for displays, radio-frequency identification devices (RFID tags), and electronic circuits. The performance of these devices has been continually improving towards the state-of-the-art and is now becoming attractive for a growing number of commercial applications.

The electronic and optoelectronic properties of thin solid films, the state in which organic semiconductors are applied in devices, is determined to a large extent by intermolecular π -interactions.^[16] Since charge and exciton transport, two factors of critical importance for electronic applications, generally involves multiple molecules, the organization of the material on a supramolecular scale plays an important role. From a preparative point of view, the improvement of the materials to foster a defined molecular self-assembly is seen as the most obvious strategy to control the order.^[17-21]

A series of linear oligomers combining phenylene, thienylene and vinylene building blocks have been designed, synthesized and investigated to determine the influence of the different structural features on the charge mobility in organic thin-film transistors. (Oligo)thienylene units were chosen as the terminal groups of the newly synthesized oligomers due to their ability to allow coplanarity of the molecular structure, which is related to the small torsion angle between neighboring thiophene units.^[22, 23] Furthermore, in order to maximize the organization of the oligomers in the solid state, vinylene units were introduced, which is a well-known strategy in the formation of coplanar oligomers with extended π -conjugation.^[24] Finally, the utilization of central *para*-phenylene units should introduce symmetry and linearity into the molecules. Such planar oligomers

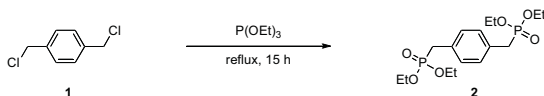
should form complex self-organized structures through intermolecular interactions, such as π -stacking and/or electrostatic interactions. The optical properties of the oligomers were investigated by UV/Vis absorption and photoluminescence (PL) spectroscopy. Vacuum-deposited thin films were investigated by AFM and the oligomers tested as *p*-type semiconducting layers of organic thin-film transistors (OFETs).

3.2 Results and Discussion

3.2.1 Precursor Synthesis

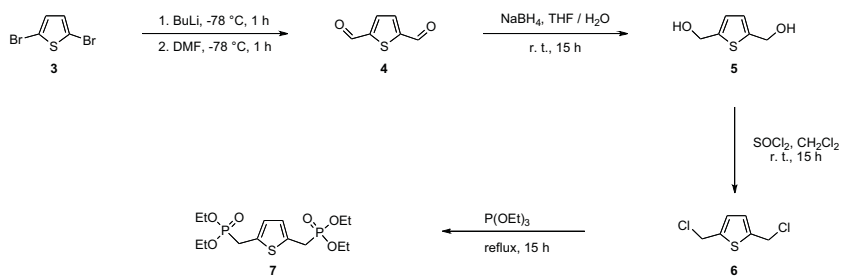
The synthesis of the different oligomers utilized several well known synthetic methods for the formation of C=C and C=N double bonds including Horner-Wittig-type and Knoevenagel-type condensation reactions.

The generation of the 1,4-phenylene-based Horner-Wittig reagent starts from the commercially available 1,4-xylylene dichloride **1**, which was converted in a single reaction step by refluxing with triethyl phosphite to give 1,4-bis(diethyl-phosphono-methylene)benzene **2** in high yields (Scheme 3.1).^[25]



Scheme 3.1. Arbusov-type reaction towards the precursor molecule **2** for the use as central building block in the following oligomer synthesis.

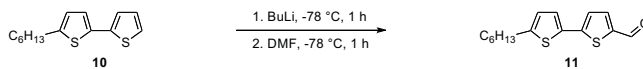
Synthesis of the thienylene-based Horner-Wittig reagent **7** afforded a more complicated multi-step procedure (Scheme 3.2). Starting from 2,5-dibromo-thiophene **3** the reaction involves a Vilsmeier-type formylation via lithiation of the dibromide at low temperature and subsequent reaction with an excess of dimethyl formamide (DMF).^[26] The resulting dialdehyde **4** was then reduced to the corresponding dialcohol **5**, followed by reaction with thionyl chloride to give 2,5-bis(chloromethyl)thiophene **6**.^[27] The dichloride **6** was then converted to the corresponding Horner-Wittig reagent **7** in an Arbusov-type reaction following the procedure described before.^[25]



Scheme 3.2. Synthetic pathway towards the central building block **7**; the commercially available *para*-phenylenediamine **8** and 1,4-bis(cyanomethyl)benzene **9** are listed for completeness.

The two precursor molecules which are used to built up the central segments, *para*-phenylenediamine **8** for the Schiff-base formation and 1,4-bis(cyano-methyl)benzene **9** for Knoevenagel-type reactions are both commercially available and were used without further purification.

The bithiophene molecule which forms the two terminal groups of the oligomers (Scheme 3.3) was obtained starting from 5'-*n*-hexyl-2,2'-bithiophene **10** which was converted in a Vilsmeier-type formylation to 5-formyl-5'-*n*-hexyl-2,2'-bithiophene **11**.^[26, 28-30]

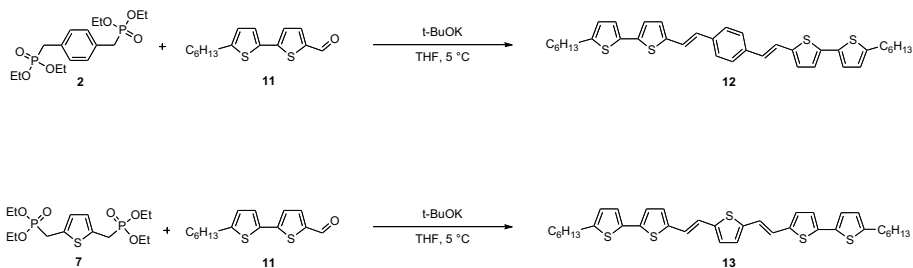


Scheme 3.3. Bithiophene precursor **11** synthesized in a Vilsmeier-type reaction.

3.2.2 Oligomer Synthesis

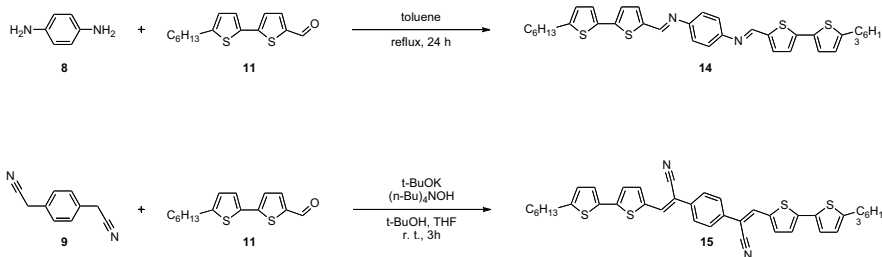
The synthesis of the oligomers **12** and **13** (depicted in Scheme 3.4) was achieved in a single reaction step through double Horner-Wittig-type olefination of the corresponding central building block (**2** or **7**) with 5-formyl-5'-*n*-hexyl-2,2'-bithiophene **11** under basic conditions. After aqueous work-up and repeated recrystallization, the oligomers could be obtained as orange powders in moderate to good yields of 65 and 78 %, respectively, and excellent purities of more than 99 % by

HPLC. The chemical structures were verified by ^1H and ^{13}C NMR spectroscopy, as well as mass spectrometry. Moreover, no residual signs of diethylphosphonomethylene groups were found in the IR spectra of **12** and **13**.



Scheme 3.4. Oligomers **12** and **13** generated in Horner-Wittig-type olefinations.

Oligomers **14** and **15** (Scheme 3.5) were synthesized starting from 5'-hexyl-2,2'-bithiophene-5-carbaldehyde **11** in a Schiff-base formation reaction at room temperature for **14** and a Knoevenagel-type condensation in refluxing toluene for **15**, respectively. The resulting orange products were purified by repeated recrystallizations and gave the expected oligomers in good yields and purities of >98 % by HPLC. The molecules were fully characterized by IR, mass spectrometry, and ^1H and ^{13}C -NMR spectroscopic measurements.



Scheme 3.5. Synthesis of the oligomers **14** and **15**.

3.2.3 Optical Spectroscopy

The absorption and emission spectra of **12** and **13** in dilute chloroform solution are depicted in Figure 3.2. Compound **12** shows a broad and slightly structured long wavelength absorption band with a long wavelength absorption maximum at $\lambda_{\text{max}} = 436$ nm with signs of vibronic fine splitting (long wavelength shoulder at ca. 460 nm for the 0-0-transition). The steep absorption edge points to

a rather planar arrangement of the oligomer backbone with a limited degree of conformational freedom. Upon exchange of the central 1,4-phenylene for a 2,5-thienylene core in oligomer **13**, the absorption maximum experiences a bathochromic shift of 35 nm to $\lambda_{\text{max}} = 471$ nm with a vibronic side band (shoulder) at 498 nm (0-0-transition). This result reflects the lower aromaticity of **13** and the increased participation of quinoid resonance structures, especially in the excited state.^[22, 23, 31, 32]

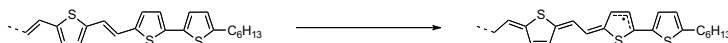


Figure 3.1. Benzoid and one possible quinoid resonance structure for the oligomer **13**.

The PL emission spectrum of compound **12** exhibits the highest energy PL band with a maximum at 495 nm and a well-resolved 0-1 transition at 521 nm. The relatively small Stokes shift of only 1,540 cm^{-1} indicates minimal geometrical variations between the electronic ground and first excited state.

Oligomer **13** demonstrates a rather broad PL emission spectrum with a PL maximum at 571 nm (shoulder for the 0-0 transition at 535 nm). The thienylene-based oligomer **13** shows a Stokes shift of 1,390 cm^{-1} . All optical data are summarized in Table 3.2.

Absorption and PL emission spectra of the oligomers **12** and **13** were further investigated (especially at low temperature) in the group of Prof. H. Burrows, University of Coimbra, Portugal. Figure 3.3 shows the normalized absorption spectra of **12** and **13** in dilute toluene solution with essentially similar findings to the room temperature spectra as in dilute chloroform solutions, with broad and poorly resolved absorption bands. Measurements of oligomer **12** in dilute toluene

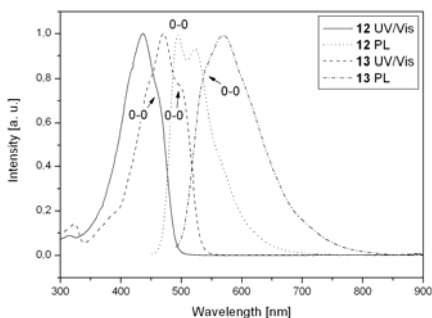


Figure 3.2. Normalized UV/Vis absorption and PL emission spectra of oligomers **12** and **13**.

solution at 77K reveals much better resolved 0-0, 0-1 (max), and 0-2 transitions at 424, 450, and 480 nm, respectively. The increased resolution can be ascribed to an increase of the rigidity at low temperature.

Figure 3.4 shows the PL emission spectra of the two oligomers **12** and **13** in dilute toluene solution. At room temperature **12** exhibits a series of well-resolved transitions at 488 (0-0), 522 nm (0-1) and 560 nm (0-2, shoulder), respectively. Upon cooling to liquid nitrogen temperature (77 K) the spectrum is better resolved and shows a weak bathochromic shift for the 0-0 and 0-1 transition to 494 and 530 nm, respectively. In addition, the 0-2 vibronic transition, which at room temperature presented as a shoulder at 560 nm, now becomes well-resolved and peaks at 570 nm. A further side-band assigned to the 0-3 transition is observed at 620 nm (shoulder).

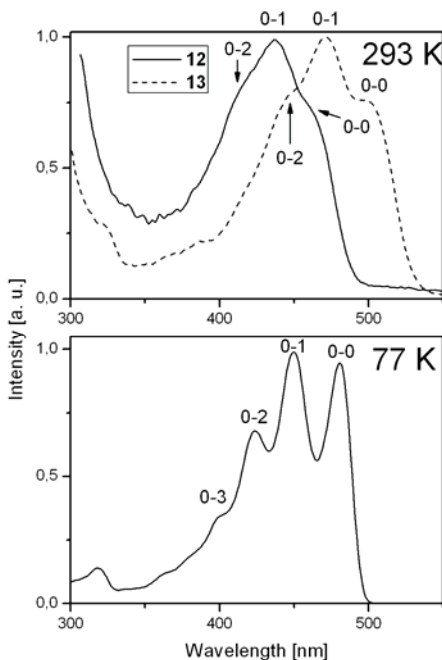


Figure 3.3. Normalized UV/Vis absorption spectra for **12** and **13** at room temperature and at 77 K for **12**, respectively (dilute toluene solution).

Oligomer **13** shows essentially similar room temperature emission spectra both in dilute chloroform and toluene solution. The PL at 77 K is better resolved with the 0-0 transition peaking at 537, and vibronic progressions at 570 and 610 nm. An additional low intensity emission band found at 490 nm is of higher energy than the 0-0 transition of the absorption spectrum of **13**. Therefore, the band cannot be intrinsic and might be induced by decomposition products or impurities during the measurement (possibly contamination by **12**). The spectroscopic data for the oligomers **12** and **13** are summarized in Table 3.1.

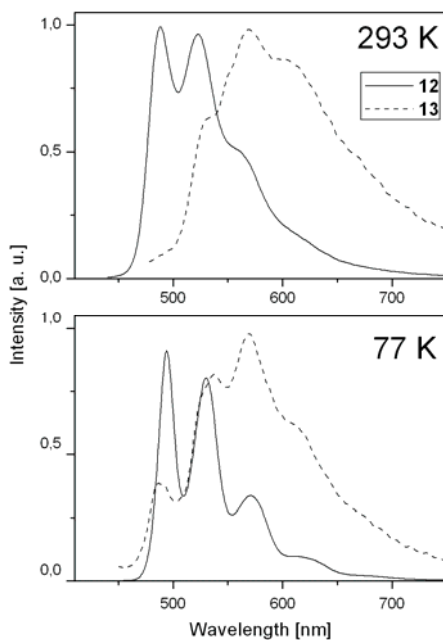


Figure 3.4. Normalized PL emission at room temperature and 77 K for **12** and **13** in dilute toluene solution.

Table 3.1. Spectroscopic data for oligomers **12** and **13** in dilute toluene solution at room temperature (293 K) and low temperature (77 K).

Oligomer	$\lambda_{\max}^{\text{Abs}}$	$\lambda_{\max}^{\text{Abs}}$	$\lambda_{\max}^{\text{Fluo}}$	$\lambda_{\max}^{\text{Fluo}}$	$\lambda_{\max}^{T_1 \rightarrow T_n}$
	[nm], 293 K	[nm], 77 K	[nm], 293 K	[nm], 77 K	[nm]
12	413, <u>437</u> , 461	399, 424, <u>450</u> , 480	<u>488</u> , 522, 560	<u>494</u> , 530, 570, 620	655
13	447, <u>470</u> , 499	n. m.	530, <u>570</u> , 605	537, <u>570</u> , 610	645

The transient singlet-triplet difference absorption spectra of the oligomers **12** and **13** recorded with a time delay of 12 μs between excitation and observation are depicted in Figure 3.5. Both materials experience an initial ground state bleaching and the occurrence of polaronic absorption bands (p^+/p^-) at higher wavelength (~ 500 nm). The $T_1 \rightarrow T_n$ transitions are clearly visible and peak at $\lambda_{\max} = 655$ (**12**) and 645 nm (**13**), respectively.

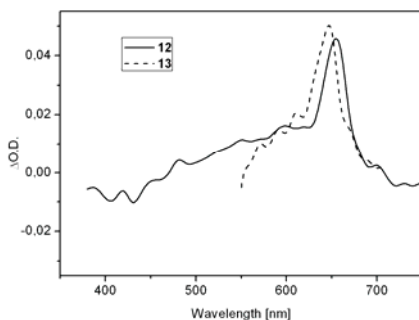


Figure 3.5. Transient singlet-triplet difference absorption spectra for oligomers **12** and **13** in toluene at room temperature (delay interval between excitation and observation: 12 μs).

Figure 3.6 shows the absorption spectra of the oligomers **14** and **15** in dilute chloroform solution. In compound **14** the vinylene groups of oligomer **12** have been exchanged by $\text{C}=\text{N}$ groups, while in oligomer **15** the vinylenes are substituted with additional cyano groups. The absorption spectrum of **14** shows a featureless absorption with an absorption maximum λ_{\max} at 425 nm, which is blue-shifted by 11 nm compared to its vinylene counterpart **12**. The cyano-substituted oligomer **15** also shows a structureless long wavelength absorption band and experiences a bathochromic shift of 8 nm compared to its non-substituted counterpart with an absorption maximum λ_{\max} peaking at 468 nm. The shift results from the introduction of the electron-withdrawing cyano group (slight push-pull effect).

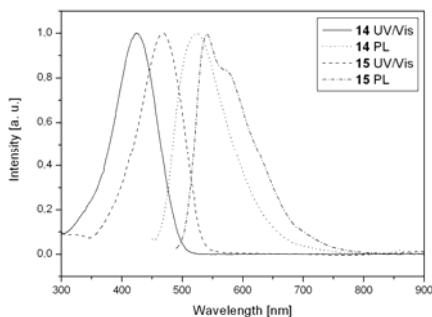


Figure 3.6. Normalized UV/Vis absorption and PL emission spectra for **14** and **15** in dilute chloroform solution.

Table 3.2. Spectroscopic data of oligomers **12-15** in dilute chloroform solution.

oligomer	$\lambda_{\max}(\text{abs.})$ [nm]	$\lambda_{\max}(\text{em.})$ [nm]	Stokes shift [cm^{-1}]
12	436, 460	495, 521	1,537
13	471, 498	535, 571	1,389
14	425	525	4,482
15	468	540, 570	2,849

The oligomers **14** and **15** exhibit PL emission maxima at 525 and 540 nm, respectively, while the latter also shows a vibronic side band at 570 nm. While the cyano-substituted oligomer **15** shows a moderate Stokes shift of $2,849 \text{ cm}^{-1}$, the Schiff-base derivative **14** exhibits a quite larger shift of $4,482 \text{ cm}^{-1}$, probably indicating some charge-transfer character in the excited state.

3.2.4 OFET Investigations

The OFET properties of vacuum-deposited thin layers of the synthesized oligomers **12-15** were investigated in the group of Prof. Z. Bao, Stanford University, CA, USA in bottom gate/top contact transistors utilizing silicon gate and gold source/drain electrodes. As the conducting channel is formed by the first few deposited monolayers the device performance may be dependent on the pre-

treatment of the silicon oxide dielectric layer prior to organic-semiconductor deposition by vacuum deposition. Three types of substrates were used for the fabrication: a) plain silicon wafers with thermally grown SiO₂ layer, b) silicon wafers treated with octadecyltrichlorosilane (OTS), and c) silicon wafers treated with hexamethyldisilazane (HMDS). OTS and HMDS are used in the fabrication of transistors to generate a hydrophobic smooth and continuous surface. Thus, the contact between the SiO₂ layer and the deposited organic material is improved and therefore, the film formation ability enhanced. In contrast to the hydroxyl-terminated SiO₂ surface, treatment with OTS or HMDS generates a hydrophobic surface without dipole moment.^[33] In this case the alkyl side chains of the silanes are covalently bound to the substrate surface. Thus, a higher ordered structure of the semiconducting layer may be achieved, resulting in a high hole mobility.^[34] The semiconducting oligomers **12-15** were vacuum-deposited onto the substrates at room or elevated temperature, respectively.

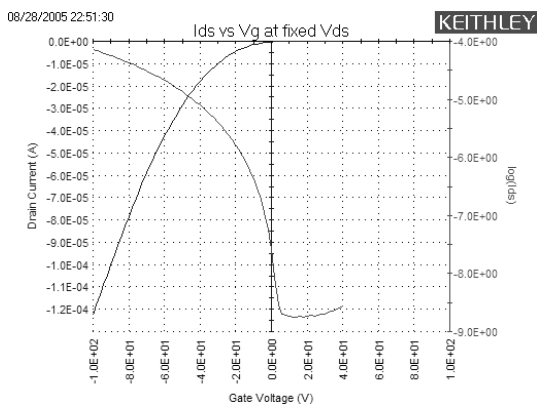


Figure 3.7. Drain current vs. gate voltage plot for an OFET device with vacuum-deposited **13** as semiconducting layer (OTS-treatment, substrate temperature: 60 °C).

The OFET device parameters for the oligomers **12** and **13** are listed in Table 3.3. The compounds show typical *p*-channel transistor properties. One representative current/voltage-characteristic of **12** is depicted in Figure 3.7. Both oligomers showed a higher hole mobility at elevated substrate temperature during deposition (60 °C). The best results were obtained for the phenylene-thiophene-vinylene oligomer **12**, which reached hole mobilities of up to $1.0 \cdot 10^{-1} \text{ cm}^2/\text{Vs}$.

Table 3.3. OFET properties for the oligomers **12** and **13** on different substrates and for different substrate temperatures during the deposition of the organic layer.

oligomer	substrate temperature	surface treatment	mobility [cm ² /Vs]	on/off ratio	threshold voltage V _t [V]
12	r.t.	plain	5.1•10 ⁻²	2,870	-6.1
		OTS	1.2•10 ⁻¹	12,220	-5.8
		HMDS	1.0•10 ⁻¹	4,470	-11.9
	60 °C	plain	1.0•10 ⁻¹	8,370	-13.3
		OTS	1.3•10 ⁻¹	10,250	-3.2
		HMDS	1.1•10 ⁻¹	520	-3.3
13	r.t.	plain	1.1•10 ⁻²	120	n/a
		OTS	2.3•10 ⁻²	430	-31.4
		HMDS	1.7•10 ⁻²	420	-30.9
	60 °C	plain	3.5•10 ⁻²	550	-12.4
		OTS	5.5•10 ⁻²	5,420	-6.4
		HMDS	4.7•10 ⁻²	920	-7.3

The measured mobilities, on/off ratios and threshold voltages V_t of all devices are listed in Table 3.3. It was observed that OTS-treated substrates led to the best results with high on/off-ratios of up to 12,000 and threshold voltages low as V_t = -3.2 V for **12**. Comparison of **12** with the thienylene-vinylene-based material **13** revealed mobilities one order of magnitude lower for **13** together with reduced on/off-ratios and increased threshold voltages.

Table 3.4 lists OFET device parameters for the oligomers **14** and **15**. No field effect was observed for oligomer **14** for room temperature deposition due to incomplete film formation. Upon deposition of **14** at elevated substrate temperature a slight to moderate field effect was observed with a mobility three order of magnitudes lower than for **12** but comparable on/off-ratio and V_t values with the best devices on HMDS-treated Si/SiO₂ wafers. The cyano-substituted derivative **15** showed only moderate OFET results with the best device parameters for OTS- and HMDS-treated substrates being obtained at a deposition temperature of 60 °C.

Table 3.4. OFET properties for the oligomers **14** and **15** on different substrates and for different substrate temperatures during deposition of the organic layers.

oligomer	substrate temperature	surface treatment	mobility [cm ² /Vs]	on/off ratio	threshold voltage V _t [V]
14	r.t.	plain	n/a	n/a	n/a
		OTS	1.6•10 ⁻⁶	n/a	n/a
		HMDS	n/a	n/a	n/a
	60 °C	plain	2.0•10 ⁻⁵	810	-13.3
		OTS	1.1•10 ⁻⁴	6,870	-3.2
		HMDS	1.2•10 ⁻³	7,160	-3.0
15	r.t.	plain	1.8•10 ⁻⁵	320	-13.4
		OTS	1.2•10 ⁻³	170	-3.5
		HMDS	3.7•10 ⁻⁴	n/a	n/a
	60 °C	plain	4.2•10 ⁻⁴	4,120	-18.4
		OTS	3.5•10 ⁻³	4,110	-29.2
		HMDS	1.5•10 ⁻³	5,790	-17.8

In conclusion, oligomer **12** vacuum-deposited at 60 °C onto OTS-treated Si/SiO₂ wafers gave the highest OFET mobility and on/off ratio as well as the lowest threshold voltage, closely followed by oligomer **13** under similar conditions. The other two oligomers **14** and **15** performed very poorly for room temperature deposition and poorly for elevated substrate temperature.

3.2.5 AFM Investigations

Atomic force microscopy (AFM) investigation of vacuum-deposited thin oligomer films may provide complementary information about the thin-film properties. Previous studies into the time-dependent mechanism of vacuum-deposited quaterthiophene and alkyl-substituted quaterthiophene films have shown that incorporation of alkyl substituents on the semiconductors' backbone shifts the growth mechanism from three dimensional (3D) island to layer-by-layer growth.^[35-40] This is a result of the lowered substrate-molecule interaction and a decrease of the interlayer interactions between adjacent layers caused by the increased interlayer distance induced by the alkyl substitution. This should then lead to larger, interconnected grains, which may enhance the charge transport within the semiconductive layer near the dielectric interface.

AFM investigations showed that oligomer **12** forms very large aggregates and therefore showed a large surface roughness of up to 110 nm when vacuum-deposited at room temperature (Figure 3.8, left). In contrast to this, very smooth films with an average surface roughness of only ~ 7 nm were observed for thin films prepared from the other oligomers at room temperature (Figure 3.8, right shows an AFM image for a thin layer of **13** as an example).

Further investigations of the deposition process of **12** revealed, that the formation of islands occurs whose size increases with the substrate deposition temperature (Figure 3.9). At $T_{\text{sub}} = 125$ °C a terrace-like morphology is clearly observed for oligomers **12** and **13** with an average step height of

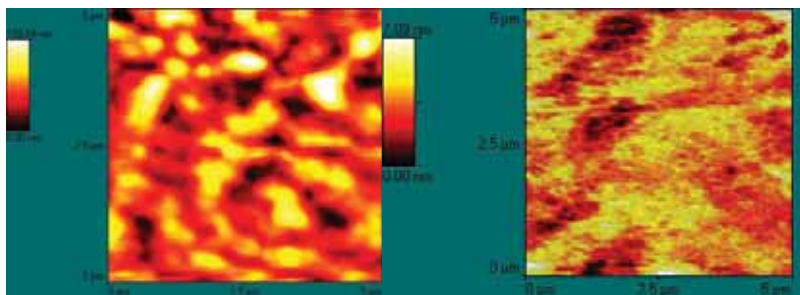


Figure 3.8. AFM images of thin films of **12** (left) and **13** (right) (AFM conditions: contact-mode, plain Si/SiO₂ substrate, room temperature).

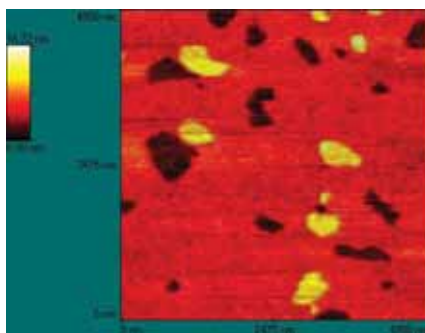


Figure 3.9. Island formation for oligomer **12** (AFM conditions: contact-mode, plain Si/SiO₂ substrate, 125 °C).

4.9 - 5.0 nm (Figure 3.9), which corresponds to the molecular length and indicates an orientation of the molecules with their long molecular axis normal to the substrate.

In the case of oligomers **14** and **15** the formation of such islands is strongly suppressed even though a few can be found at a deposition temperature T_{sub} of 125 °C. These islands also show an average step height of about 5.0 nm.

It could be concluded that, the formation of terrace-like morphologies and a molecular orientation of the type observed for **12** is favorable for efficient charge transport across the semiconducting layer.

3.3 Conclusion

This chapter has outlined the synthesis of four novel, phenylene-thienylene-vinylene-based oligomers. All oligomers have been synthesized in multi-step reaction sequences utilizing common and well-known synthetic methods, giving the products in good yields and excellent purities. Oligomer **12** shows the highest potential as vacuum-deposited oligomeric semiconductor in OFET devices with field-effect mobilities up to 0.1 cm²/Vs and on/off ratios up to 10⁵ at an optimum substrate deposition temperature of 60 °C. Attempts to improve the OFET performance of **12** by variation of the initial structure through incorporation of hetero atoms, thienylene as the central core unit or additional functional groups (-CN) lowered the OFET device performance. This initial study with only a few structural variations should be extended by the generation of a broader variety of derivatives in order to derive reliable structure-property-relations.

3.4 Experimental Section

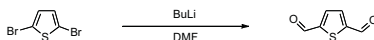
Materials and Characterization. Unless otherwise indicated, all reagents were obtained from commercial suppliers and were used without further purification. The solvents were used as commercial p.a. quality. The reactions were carried out under argon with the use of standard and Schlenk techniques. The vials for the microwave assisted reactions were filled in a glove box. ^1H - and ^{13}C -NMR data were obtained on a Bruker ARX 400-spectrometer. The UV-Vis and fluorescence spectra were recorded on a Jasco V-550 spectrophotometer and a Varian-Cary Eclipse photoluminescence spectrometer, respectively. Microwave-assisted syntheses were performed using a CEM Discover microwave system.

1,4-Bis(diethylphosphonomethyl)benzene (2)



1,4-Xylylene dichloride (5 g, 28.6 mmol) and triethyl phosphite (31.2 mL, 180 mmol) were mixed and stirred for 15 h at 120 °C. Afterwards the excess triethyl phosphite was distilled off at 180 °C. The residue was recrystallized from hexane and dried in vacuo. Yield: 9.95 g, 92 %. ^1H NMR (400.1 MHz, $\text{C}_2\text{D}_2\text{Cl}_4$): δ [ppm] = 7.18 (s, 4H), 4.03 (m, 8H), 3.06 (d, 4H, $J_{\text{P,H}}=19.8$ Hz), 1.17 (d, 12H, $J=6.9$ Hz). ^{13}C NMR (100.6 MHz, $\text{C}_2\text{D}_2\text{Cl}_4$): δ [ppm] = 129.8, 129.6, 61.9, 33.2 (d, $J_{\text{C,P}}=137.3$ Hz), 16.2. LS-MS (EI, 70 eV): m/z = 378 [M^+] (6.4), 364 (2.6), 305 (2.4), 240 (60.0), 227 (15.2), 213 (55.4), 153 (37.3), 109 (56.6), 104 (96.7), 45 (14.9). Anal. Calcd. for $\text{C}_{14}\text{H}_{26}\text{O}_6\text{P}_2\text{S}$: C, 43.75; H, 6.82; S, 8.34. Found: C, 43.49; H, 6.47; S, 8.39.

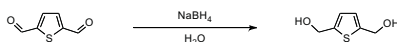
2,5-Thiophenedicarboxaldehyde. (4)



To a solution of 2,5-dibromothiophene (9.0 g, 37.2 mmol) in diethyl ether (300 mL) a solution of butyl lithium in hexane (62 mL, 1.6 M) was added dropwise at -78 °C under an argon atmosphere. The mixture was stirred at -78 °C for 1 h. To the solution DMF (30 mL) was added and stirred at -78 °C for 1 h. Afterwards the reaction was allowed to warm up to room temperature and stirring was continued for 30 min. The suspension was then poured into a mixture of conc. aqueous HCl

and ice under vigorous stirring. Saturated NaHCO_3 solution was added dropwise until the aqueous layer reached pH 6. The layers were separated and the aqueous layer extensively extracted with diethyl ether. The combined organic layers were dried over Na_2SO_4 and the solvent was removed in vacuo. The crude product was recrystallized from THF/ Et_2O (4:1) to afford the pure product. Yield: 4.6 g, 89 %. ^1H NMR (400.1 MHz, $\text{C}_2\text{D}_2\text{Cl}_4$): τ^{M} [ppm] = 9.44 (s, 2H), 7.26 (s, 2H). ^{13}C NMR (100.6 MHz, $\text{C}_2\text{D}_2\text{Cl}_4$): τ^{M} [ppm] = 194.5, 146.3, 140.2. LR-MS (EI, 70 eV): m/z = 140 [M^+] (100), 112 (36.5), 84 (48.2). FT-IR (neat): ν [cm^{-1}] = 3072, 1669, 1520, 1462, 1186, 1053, 825, 775, 686, 474. Anal. Calcd. for $\text{C}_6\text{H}_4\text{O}_2\text{S}$: C, 51.42; H, 2.88; S, 22.88. Found: C, 51.38; H, 3.10, S, 22.62.

2,5-Bis(hydroxymethyl)thiophene. (5)



To a stirred solution of 2,5-thiophene dicarboxaldehyde (3.3 g, 23.6 mmol) in THF (47 mL) sodium borohydride (1.96 g, 5.2 mmol) diluted in water (51 mL) was added dropwise. The mixture was stirred at room temperature for 15 h and the phases separated. The aqueous phase was saturated with NaCl, and afterwards filtered and extensively extracted with diethyl ether. The combined organic phases were dried over Na_2SO_4 and filtered. The solvent was removed in vacuo and the product isolated as a yellow oil. Yield: 3.24 g, 95 %. ^1H NMR (400.1 MHz, $\text{DMSO}-d_6$): τ^{M} [ppm] = 6.74 (s, 4H), 5.29 (t, 2H), 4.54 (d, 4H, J = 5.5 Hz). ^{13}C NMR (100.6 MHz, $\text{C}_2\text{D}_2\text{Cl}_4$): τ^{M} [ppm] = 150.6, 126.9, 59.1. LR-MS (EI, 70 eV): m/z = 144 [M^+] (100), 112 (64.2), 84 (21.7). Anal. Calcd. for $\text{C}_6\text{H}_8\text{O}_2\text{S}$: C, 49.98; H, 5.59; S, 22.24. Found: C, 49.88; H, 5.44; S, 22.17.

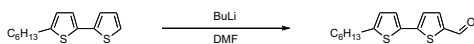
2,5-Bis(chloromethyl)thiophene. (6)



2,5-Bis(hydroxymethyl)thiophene (3.17 g, 22 mmol) was diluted in dry dichloromethane under argon atmosphere and thionyl chloride (7.85 g, 66 mmol) was added at once. The mixture was stirred at room temperature overnight. The solvent was removed in vacuo to give the product without further purification as a colorless oil. Yield: 3.0 g, 75 %. ^1H NMR (400.1 MHz, $\text{C}_2\text{D}_2\text{Cl}_4$): τ^{M} [ppm] = 6.86 (s, 2H), 4.69 (s, 4H). ^{13}C NMR (100.6 MHz, $\text{C}_2\text{D}_2\text{Cl}_4$): τ^{M} [ppm] = 141.9, 127.8, 40.9. LR-MS (EI, 70 eV): m/z = 181 [M^+] (42.2), 112 (100), 84 (16.1). Anal. Calcd. for $\text{C}_6\text{H}_6\text{Cl}_2\text{S}$: C, 39.80; H, 3.34; S, 17.71. Found: C, 39.85; H, 3.59; S, 17.75.

2,5-Bis(diethylphosphonomethyl)thiophene (7)

2,5-Bis(chloromethyl)thiophene (4.2 g, 23.2 mmol) and triethyl phosphite (30.0 mL, 173 mmol) were mixed and stirred for 15 h at 120 °C. Afterwards the excess triethyl phosphite was distilled off at 180 °C. The residue was recrystallized from hexane and dried in vacuo. Yield: 6.1 g, 68 %. ¹H NMR (400.1 MHz, C2D2Cl4): δ [ppm] = 6.55 (s, 2H), 4.28 (m, 8H), 3.00 (d, 4H, JP,H=20.2 Hz), 1.30 (d, 12H, J=6.9 Hz). ¹³C NMR (100.6 MHz, C2D2Cl4): δ [ppm] = 137.9, 138.9, 62.2, 26.1 (d, JC,P=128.4 Hz), 16.0. LR-MS (EI, 70 eV): m/z = 384 [M⁺] (60.4), 248 (15.2), 112 (100), 84 (20.9). Anal. Calcd. for C₁₄H₂₆O₆P₂S: C, 43.75; H, 6.82; S, 8.34. Found: C, 43.49; H, 6.47; S, 8.39.

5-Formyl-5'-n-hexyl-2,2'-bithiophene (11)

To a solution of 5'-n-hexyl-2,2'-bithiophene (3.0 g, 12.9 mmol) and DMF (0.25 mL) in 25 mL of dry dichloroethane butyl lithium in hexane (7.6 mL, 12.1 mmol, 1.6 M) was added dropwise under an argon atmosphere. The mixture was then refluxed for 8 h. After cooling down to room temperature, aqueous sodium acetate (1 M) was added until pH=7 was reached and the mixture stirred vigorously for 1 h. The solution was extracted with dichloromethane, and the organic phase dried over Na₂SO₄. After evaporation of the solvent, the crude product was purified by column chromatography on silica (eluent: hexane/ethyl acetate : 98/2). 3.0 g of violet crystals were isolated (85% yield); ¹H-NMR (400 MHz, CDCl₃): TM [ppm] = 9.73 (s, 1H), 7.57 (d, 1H, J=4.0 Hz), 7.12 (d, 1H, J=3.6 Hz), 7.10 (d, 1H, J=4.0 Hz), 6.68 (d, 1H, J=3.6 Hz), 2.73 (t, 2H, J=7.6 Hz), 1.64-1.53 (m, 2H), 1.33-1.2 (m, 6H), 0.82 (t, 3H, J=6.8 Hz). ¹³C NMR (100.6 MHz, CDCl₃): TM [ppm] = 182.9, 149.2, 148.1, 141.1, 138.0, 133.5, 126.5, 125.8, 123.8, 31.7, 31.7, 30.5, 29.0, 22.8, 14.4. FT-MS m/z = 278.8 (278.4). FT-IR (neat): ν [cm⁻¹] = 2923, 2851, 1653, 1604, 1559, 1464, 1436, 1375, 1283, 1242, 1216, 1180, 1146, 1105, 1048, 998, 924, 894, 879, 847, 813, 798, 751, 725, 703, 688, 663. Anal. Calcd. for C₁₅H₁₈OS₂: C, 64.71; H, 6.52; S, 23.03. Found: C, 64.53; H, 6.44; S, 22.97.

1,4-Bis[2-(5'-hexyl-2,2'-bithiophen-5-yl)vinyl]benzene (12)

1,4-Bis(diethylphosphonomethyl)benzene (163 mg, 0.43 mmol) and 5'-hexyl-2,2'-bithiophene-5-carboxaldehyde (300 mg, 1.1 mmol) were mixed in a Schlenk flask and dissolved in dry THF (20 mL) under argon atmosphere. To ensure complete removal of oxygen, the flask was evacuated and again flushed with argon several times. The mixture was cooled down to 5 °C, and potassium *tert*-butoxide (100 mg, 0.86 mmol in THF) added dropwise. The mixture was stirred for 1 h at 5 °C. Afterwards the mixture was allowed to warm up to room temperature and stirred for another 10 h. The orange precipitate was filtered off and recrystallized from toluene to give **12**. Yield: 175 mg, 65 %. ¹H NMR (400.1 MHz, C₂D₂Cl₄): TM [ppm] = 7.38 (s, 4H), 7.11 (d, 2H, J = 15.99 Hz), 6.96 (d, 4H, J = 3.56 Hz), 6.91 (d, 2H, J = 3.82 Hz), 6.82 (d, 2H, J = 16.03 Hz), 6.65 (d, 2H, J = 3.56 Hz), 2.76 (t, 4H), 1.66 (m, 4H), 1.47 – 1.19 (m, 12H), 0.87 (t, 6H). ¹³C NMR (100.6 MHz, C₂D₂Cl₄):

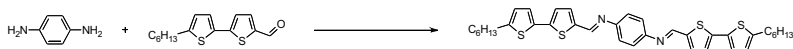
TM [ppm] = 146.2, 141.6, 137.3, 136.7, 135.0, 128.0, 127.3, 127.0, 125.1, 123.9, 123.8, 122.0, 31.7, 31.6, 30.4, 28.9, 22.7, 14.2. FT-mass: m/z (calc) = 626.1 (627.0). FT-IR (neat): ν [cm⁻¹] = 2959, 2918, 2851, 1608, 1559, 1540, 1520, 1464, 1436, 1373, 1337, 1306, 1283, 1256, 1221, 1205, 1130, 1114, 1049, 1212, 958, 957, 880, 865, 758, 744, 734, 727, 656. Anal. Calcd. for C₃₈H₄₂S₄: C, 72.79; H, 6.75; S, 20.46. Found: C, 72.81; H, 6.62; S, 20.37.

2,5-Bis[2-(5'-hexyl-2,2'-bithiophen-5-yl)vinyl]thiophene (13)

2,5-Bis(diethylphosphonomethyl)thiophene (163 mg, 0.43 mmol) and 5'-hexyl-2,2'-bithiophene-5-carboxaldehyde (300 mg, 1.1 mmol) were mixed in a Schlenk flask and dissolved in dry THF (20 mL) under argon atmosphere. To ensure complete removal of oxygen, the flask was evacuated and again flushed with argon several times. The mixture was cooled down to 5 °C, and potassium *tert*-butoxide (100 mg, 0.86 mmol in THF) added dropwise. The mixture was stirred for 1 h at 5 °C. Afterwards the mixture was allowed to warm to room temperature and stirred for another 10 h. The orange precipitate was filtered off and recrystallized from toluene to give the **13**. Yield: 171 mg, 63 %. ¹H NMR (400.1 MHz, C₂D₂Cl₄): TM [ppm] = 6.97 – 6.92 (m, 4H), 6.91 – 6.85 (m, 8H), 6.68 –

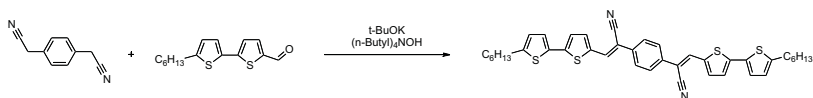
6.62 (m, 2H), 2.75 (m, 4H), 1.65 (m, 4H), 1.39 – 1.26 (m, 12H), 0.87 (t, 6H). ^{13}C NMR (100.6 MHz, $\text{C}_2\text{D}_2\text{Cl}_4$): δ [ppm] = 146.3, 141.8, 141.0, 137.4, 135.0, 127.4, 127.3, 125.2, 124.0, 123.9, 121.9, 121.4, 31.7, 31.6, 30.4, 28.9, 22.7, 14.2. FT-mass: m/z (calc) = 632.4 (633.0). FT-IR (neat): ν [cm^{-1}] = 2918, 2853, 1597, 1558, 1532, 1510, 1435, 1373, 1319, 1288, 1244, 1227, 1191, 1117, 1043, 875, 742, 755, 723, 703, 684, 662. Anal. Calcd. for $\text{C}_{36}\text{H}_{40}\text{S}_5$: C, 68.30; H, 6.37; S, 25.33. Found: C, 68.15; H, 6.52; S, 25.86.

1,4-Bis[(5'-hexyl-2,2'-bithiophene-5-yl)methylene]phenylenediamine (14)



1,4-Phenylenediamine (60 mg, 0.55 mmol) was dissolved in toluene (20 mL) and 5'-hexyl-2,2'-bithiophene-5-carbaldehyde (324 mg, 1.16 mmol) dissolved in toluene (20 mL) added dropwise at room temperature. The mixture was refluxed in a Dean-Stark apparatus for 24 h. Afterwards the precipitate was filtered off and recrystallized from toluene to give an orange product. Yield: 249 mg, 73 %. ^1H NMR (400.1 MHz, $\text{C}_2\text{D}_2\text{Cl}_4$): δ [ppm] = 8.5 (s, 2H), 7.3 (d, 2H, $J = 3.94$ Hz), 7.2 (s, 4H), 7.06 (d, 2H, $J = 3.35$ Hz), 7.05 (d, 2H, $J = 3.45$ Hz), 6.7 (d, 2H, $J = 3.60$ Hz), 2.7 (t, 4H), 1.6 (m, 4H), 1.4 – 1.2 (m, 12H), 0.8 (t, 6H). ^{13}C NMR (100.6 MHz, $\text{C}_2\text{D}_2\text{Cl}_4$): δ [ppm] = 151.7, 149.6, 147.5, 143.0, 141.3, 134.6, 132.9, 125.4, 125.1, 123.6, 122.2, 31.7, 31.6, 30.5, 28.9, 22.7, 14.2. FT-mass: m/z (calc) = 628.2 (629.0). FT-IR (neat): ν [cm^{-1}] = 2959, 2923, 2852, 1592, 1553, 1524, 1469, 1446, 1369, 1344, 1324, 1287, 1245, 1227, 1200, 1172, 1108, 1059, 1040, 951, 883, 847, 823, 787, 777, 748, 724, 707, 661. Anal. Calcd. for $\text{C}_{36}\text{H}_{40}\text{N}_2\text{S}_4$: C, 68.74; H, 6.41; N, 4.45; S, 20.39. Found: C, 68.73; H, 6.73; N, 4.37; S, 20.05.

1,4-Bis[(5'-hexyl-2,2'-bithiophene-5-yl)-1-cyanovinyl]benzene (15)



5'-Hexyl-2,2'-bithiophene-5-carbaldehyde (300 mg, 1.1 mmol) and 1,4-bis(cyanomethyl)benzene (67 g, 0.43 mmol) were dissolved in a solvent mixture of *tert*-butanol (10 mL) and THF (10 mL). To this solution potassium *tert*-butoxide (1M in THF, 1.1 mL) and tetrabutylammonium hydroxide

(1M in methanol, 1.1 mL) were added. The mixture was stirred at ambient temperature for 3 h. The orange precipitate was collected by filtration and washed with methanol (3x50 mL). Yield: 160 mg, 55 % of orange crystals after drying *in vacuo* for 24 h. ^1H NMR (400.1 MHz, $\text{C}_2\text{D}_2\text{Cl}_4$, T = 353.15K): δ [ppm] = 7.63 (s, 4H), 7.55 (s, 2H), 7.50 (d, 2H, $J = 4.07$ Hz), 7.11 (d, 2H, $J = 3.56$ Hz), 7.10 (d, 2H, $J = 4.07$ Hz), 6.70 (d, 2H, $J = 3.56$ Hz), 2.78 (t, 4H), 1.67 (m, 4H), 1.32–1.16 (m, 12H), 0.87 (t, 6H). ^{13}C NMR (100.6 MHz, $\text{C}_2\text{D}_2\text{Cl}_4$): δ [ppm] = 147.7, 143.5, 136.2, 134.8, 133.8, 133.6, 130.3, 127.2, 126.1, 125.2, 123.4, 117.5, 106.9, 31.4, 30.2, 29.7, 28.7, 22.4, 13.7. FT-mass: m/z (calc) = 676.1 (677.0). FT-IR (neat): ν [cm^{-1}] = 2953, 2922, 2851, 2206, 1902, 1830, 1752, 1653, 1550, 1517, 1506, 1463, 1420, 1369, 1354, 1329, 1305, 1285, 1273, 1238, 1192, 1178, 1146, 1110, 1092, 1060, 1043, 1022, 983, 958, 877, 806, 750, 735, 726, 699, 679. Anal. Calcd. for $\text{C}_{40}\text{H}_{40}\text{N}_2\text{S}_4$: C, 70.96; H, 5.96; N, 4.14; S, 18.94. Found: C, 70.79; H, 6.09; N, 4.03; S, 18.82.

3.5 References and Notes

1. Tsumura, A.; Koezuka, H.; Ando, T., *Appl. Phys. Lett.* **1986**, 49, (18), 1210.
2. Tsumura, A.; Koezuka, H.; Tsunoda, S.; Ando, T., *Chem. Lett.* **1986**, (6), 863.
3. Burroughes, J. H.; Jones, C. A.; Friend, R. H., *Nature* **1988**, 335, (6186), 137.
4. Bao, Z.; Lovinger, A. J.; Dodabalapur, A., *Appl. Phys. Lett.* **1996**, 69, (20), 3066.
5. Stutzmann, N.; Friend, R. H.; Sirringhaus, H., *Science* **2003**, 299, (5614), 1881.
6. Ong, B. S.; Wu, Y. L.; Liu, P.; Gardner, S., *J. Am. Chem. Soc.* **2004**, 126, (11), 3378.
7. Clarisse, C.; Riou, M. T.; Gauneau, M.; Lecontellec, M., *Electron. Lett.* **1988**, 24, (11), 674.
8. Horowitz, G.; Fichou, D.; Peng, X. Z.; Xu, Z. G.; Garnier, F., *Solid State Commun.* **1989**, 72, (4), 381.
9. Lin, Y. Y.; Gundlach, D. J.; Nelson, S. F.; Jackson, T. N., *IEEE Trans. on Electron Dev.* **1997**, 44, (8), 1325.
10. Meng, H.; Bao, Z. N.; Lovinger, A. J.; Wang, B. C.; Mujsce, A. M., *J. Am. Chem. Soc.* **2001**, 123, (37), 9214.
11. Gorjanc, T. C.; Levesque, I.; D'iorio, M., *J. Vac. Sci. Technol. A* **2004**, 22, (3), 760.
12. Gorjanc, T. C.; Levesque, I.; D'iorio, M., *Appl. Phys. Lett.* **2004**, 84, (6), 930.
13. Wakim, S.; Bouchard, J.; Simard, M.; Drolet, N.; Tao, Y.; Leclerc, M., *Chem. Mater.* **2004**, 16, (23), 4386.

14. Padmanaban, G.; Ramakrishnan, S., *J. Am. Chem. Soc.* **2000**, 122, (10), 2244.
15. van Hutten, P. F.; Krasnikov, V. V.; Hadziioannou, G., *Acc. Chem. Res.* **1999**, 32, (3), 257.
16. Kim, J., *Pure Appl. Chem.* **2002**, 74, (11), 2031.
17. Schenning, A. P. H. J.; Jonkheijm, P.; Hoeben, F. J. M.; van Herrikhuyzen, J.; Meskers, S. C. J.; Meijer, E. W.; Herz, L. M.; Daniel, C.; Silva, C.; Phillips, R. T.; Friend, R. H.; Beljonne, D.; Miura, A.; De Feyter, S.; Zdanowska, M.; Uji-i, H.; De Schryver, F. C.; Chen, Z.; Wurthner, F.; Mas-Torrent, M.; den Boer, D.; Durkut, M.; Hadley, P., *Synth. Met.* **2004**, 147, (1-3), 43.
18. Leclere, P.; Surin, M.; Lazzaroni, R.; Kilbinger, A. F. M.; Henze, O.; Jonkheijm, P.; Biscarini, F.; Cavallini, M.; Feast, W. J.; Meijer, E. W.; Schenning, A. P. H. J., *J. Mater. Chem.* **2004**, 14, (13), 1959.
19. Leclere, P.; Surin, M.; Jonkheijm, P.; Henze, O.; Schenning, A. P. H. J.; Biscarini, F.; Grimsdale, A. C.; Feast, W. J.; Meijer, E. W.; Müllen, K.; Bredas, J. L.; Lazzaroni, R., *Eur. Polym. J.* **2004**, 40, (5), 885.
20. Lehn, J. M., *Polym. Int.* **2002**, 51, (10), 825.
21. Lehn, J. M., *Rep. Prog. Phys.* **2004**, 67, (3), 249.
22. Drolet, N.; Morin, J. F.; Leclerc, N.; Wakim, S.; Tao, Y.; Leclerc, M., *Adv. Funct. Mater.* **2005**, 15, (10), 1671.
23. Leclerc, M.; Faid, K., *Adv. Mater.* **1997**, 9, (14), 1087.
24. Roncali, J., *Chem. Rev.* **1997**, 97, (1), 173.
25. Kauffman, J. M.; Moyna, G., *J. Org. Chem.* **2003**, 68, (3), 839.
26. Feringa, B. L.; Hulst, R.; Rikers, R.; Brandsma, L., *Synthesis* **1988**, (4), 316.
27. Garrigues, B., *Phosphorus, Sulfur, Silicon Relat. Elem.* **1990**, 53, (1-4), 75.
28. Frere, P.; Raimundo, J. M.; Blanchard, P.; Delaunay, J.; Richomme, P.; Sauvajol, J. L.; Orduna, J.; Garin, J.; Roncali, J., *J. Org. Chem.* **2003**, 68, (19), 7254.
29. Elandaloussi, E. H.; Frere, P.; Roncali, J.; Richomme, P.; Jubault, M.; Gorgues, A., *Adv. Mater.* **1995**, 7, (4), 390.
30. Nakayama, J.; Fujimori, T., *Sulfur Lett.* **1990**, 11, 29.
31. Cao, H.; Ma, J.; Zhang, G. L.; Jiang, Y. S., *Macromolecules* **2005**, 38, (4), 1123.
32. Egbe, D. A. M.; Nguyen, L. H.; Schmidtke, K.; Wild, A.; Sieber, C.; Guenes, S.; Sariciftci, N. S., *J. Polym. Sci., Part A* **2007**, 45, (9), 1619.
33. Reese, C.; Bao, Z. N., *Materials Today* **2007**, 10, (3), 20.
34. Koyanagi, T.; Muratsubaki, M.; Hosoi, Y.; Shibata, T.; Tsutsui, K.; Wada, Y.; Furukawa, Y., *Chem. Lett.* **2006**, 35, (1), 20.

35. Locklin, J.; Roberts, M. E.; Mannsfeld, S. C. B.; Bao, Z. N., *Poly. Rev.* **2006**, 46, (1), 79.
36. Locklin, J.; Bao, Z. N., *Anal. Bioanal. Chem.* **2006**, 384, (2), 336.
37. Verlaak, S.; Steudel, S.; Heremans, P.; Janssen, D.; Deleuze, M. S., *Phys. Rev.* **2003**, 68, (19).
38. Ruiz, R.; Choudhary, D.; Nickel, B.; Toccoli, T.; Chang, K. C.; Mayer, A. C.; Clancy, P.; Blakely, J. M.; Headrick, R. L.; Iannotta, S.; Malliaras, G. G., *Chem. Mater.* **2004**, 16, (23), 4497.
39. Campione, M.; Borghesi, A.; Moret, M.; Sassella, A., *J. Mater. Chem.* **2003**, 13, (7), 1669.
40. Ackermann, J.; Videlot, C.; Raynal, P.; El Kassmi, A.; Dumas, P., *Appl. Surf. Sci.* **2003**, 212, 26.

4 Alkylidencyclopentadithiophene - Homopolymers

4.1 Introduction and Motivation

Concerns over global warming and the need to develop inexpensive renewable energy sources stimulates the research for efficient, low-cost photovoltaic devices.^[1] The conversion of solar energy, along with other alternative technologies, has proved to have the potential to be cheap and easy method to produce energy utilizing organic, polymer-based photovoltaic devices.^[2] Along with their advantages in weight and cost over their traditional silicon-based counterparts, which have been developed since the early 1950's,^[3-5] the organic photovoltaics offer a high potential through tuning of their chemical, physical, and optical properties. The main reasons for the reduction in costs are: a) the low-cost synthesis, b) the effective deposition technologies for the polymer materials, which are mostly soluble in organic solvents and can be applied via solution cast or printing techniques, and c) the prospect of applying these techniques to high-throughput manufacturing using reel-to-reel deposition on flexible substrates.

The organic electronic materials that are used are conjugated solids which are capable to absorb sunlight, generate photoinduced charge carriers, and ensure charge transport within the delocalized π -electron system. Today's best organic semiconductors have high absorption coefficients,^[6] exceeding 10^5 cm^{-1} and charge carrier mobilities^[7] as high as $10 \text{ cm}^2/\text{Vs}$, making them competitive with amorphous silicon.^[8] Poly(3-alkylthiophene)s (P3AT) are worthy of note, with their good solubility, processability, and environmental stability.^[9, 10] Conjugated polymer/fullerene bulk heterojunction solar cells utilizing regioregular poly(3-hexylthiophene) (P3HT) as light absorbing donor and the fullerene derivative PCBM as acceptor gave record power conversion efficiencies of up to 5% and realized external quantum efficiencies (EQE) of approx. 75%.^[11, 12] The high efficiencies are mainly achieved by the microcrystalline, π -stacked morphology of P3HT in the solid state. The hole mobilities observed in regioregular P3HT can be up to $0.1 \text{ cm}^2/\text{Vs}$.

In order to optimize the device performance it is crucial to control the energy levels of the donor and acceptor components and the phase-separated morphology of the active layers.^[13-16] Therefore, it is a challenge of great interest to find the synergy between a suitable solubility of the organic materials required for low-cost "wet"-processing into thin layers, and the ordered structure of the organic semiconductor in the solid state necessary for the sufficient transport of charge carriers.^[13]

This chapter is focused on novel cyclopentadithiophene (*4H*-cyclopenta[2,1-b:3,4-b']-dithiophene, CPDT)-based donor polymers (PCPDT) containing the heteroaromatic, electron-rich analogue of fluorene as the building block of the polymer backbones. Essentially, the aryl-aryl coupling of CPDT-type monomers as methylene-bridged bithiophenes results in the generation of so-called step-ladder polymers. Special effort was devoted to variation of the substitution pattern in the 4-position of the CPDT ring system, for example in dialkyl or alkylidene-substituted derivatives. In contrast to the already known 4,4-dialkylated CPDT, in which the side-chains are arranged orthogonally to the molecular plane (“out-of-plane”),^[17, 18] the introduction of an olefinic dialkylmethylene group in 4-position results in a rotation of the alkyl substituents into the plane (“in-plane”).

The homopolymer composed of 4-dialkylmethylene CPDT building blocks **7** shows an enhanced interchain solid-state interaction similar to regioregular P3HT. As a result of the increased π -stacking ability the homopolymer **8** possesses a reduced band gap energy in relation to P3HT (1.59 vs. 2.17 eV).

4.2 Results and Discussion

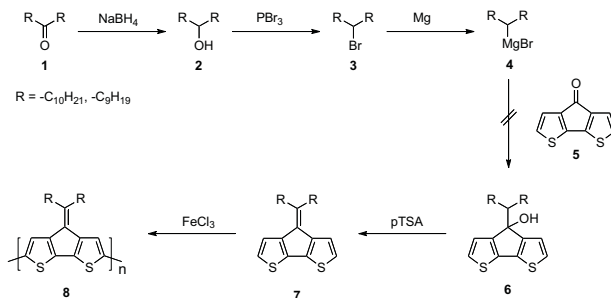
4.2.1 Monomer and Polymer Synthesis

The synthesis of planar alkylidenecyclopentadithiophene (*4H*-cyclopenta[2,1-b:3,4-b']-dithiophene, CPDT) derivatives was approached via four different synthetic pathways.

4.2.2 Alkylidenecyclopentadithiophene monomers via a *Gignard-type reaction.*

The first synthetic strategy toward the desired monomer is depicted in Scheme 4.1 and started from a dialkyl ketone **1**, which was reduced to the corresponding alcohol **2** by reduction with sodium borohydride and subsequently brominated with phosphorous tribromide to yield the symmetric monobrominated species **3**. Afterwards the intermediate **3** was used in a Grignard-type reaction with *4H*-cyclopenta-[2,1-b:3,4-b]dithiophen-4-one (CDT) **5**, which was prepared according to the literature.^[19-24] The Grignard-type reaction was found to give yields of only 16-20% and attempted an optimization of the reaction conditions did not show any improvement. The low yields of the coupling reaction may be explained by the low reactivity of the carbonyl group. Subsequent

dehydration of the resulting alcohol with *para*-toluenesulfonic acid as a catalyst then led to the target molecule **7** in an overall yield of 4%. Due to the low yields, this route was not continued.

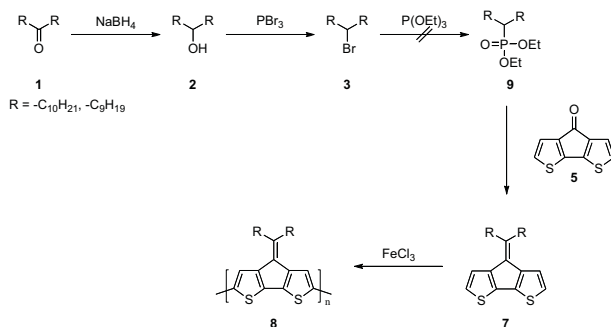


Scheme 4.1. Grignard-type strategy towards the CPDT-type monomer **7** and polymer **8**.

4.2.3 Alkylidencyclopentadithiophene via a Horner-Wittig-type reaction.

In the second route it was planned that the bromo compound **3** would be reacted in an Arbuzov-reaction to the corresponding phosphonic ester **9**, followed by a Horner-Wittig-type reaction with 4*H*-cyclopenta-[2,1-b:3,4-b]dithiophen-4-one (CDT) **5** to give the target monomer **7** (Scheme 4.2).

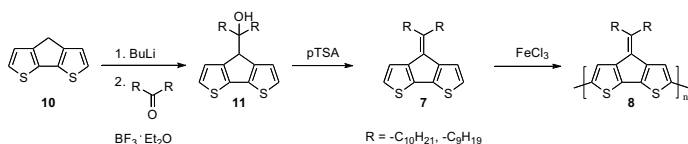
Bromo compound **3** showed low reactivity with triethyl phosphite, and gave a product mixture which could not be purified by column chromatography or recrystallization. This route was also not continued.



Scheme 4.2. Horner-Wittig-type reaction towards CPDT-type monomer **7** and polymer **8**.

4.2.4 Alkylidenecyclopentadithiophene via a Knoevenagel-type reaction.

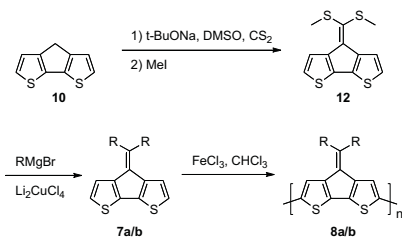
The third route started from cyclopentadithiophene (4*H*-cyclopenta[2,1-*b*:3,4-*b'*]-dithiophene, CPDT, **10**), which was synthesized following procedures well-known from the literature.^[25] Taking advantage of the acidic hydrogens of **10**, it was planned that commercially available keto compounds **1** would be coupled with **10** in a piperidine-catalyzed Knoevenagel-condensation protocol (Scheme 4.3).^[26] Even though the reaction works in medium yields with short-chain ketones as acetone,^[27] no reaction was observed with **1** bearing two long alkyl side-chains (R: -C₉H₁₉, -C₁₀H₂₁).



Scheme 4.3. Knoevenagel-type reaction towards CPDT-type monomer **7** and polymer **8**.

4.2.5 Successful Synthesis of Alkylidenecyclopentadithiophene via a Dimethylated Thioacetal Intermediate

In a first reaction step towards the envisaged polymer **8**, CPDT **10** was deprotonated and reacted with CS₂ resulting in a ketene dithiolate anion, followed by an *in situ* alkylation with methyl iodide to yield the dimethylated thioacetal **12** (Scheme 4.4).^[28] In the next reaction step **12** was treated with 2 eq. of an alkyl Grignard reagent in THF at -5° C for 4 h to give the 4-dialkylmethylene-CPDT derivative **7**. Using this method, monomers with both hexyl (**7a**) and decyl side-chains (**7b**) were synthesized.



Scheme 4.4 Synthetic route towards poly[2,6-(4-dialkylmethylene cyclopentadithiophene)] polymers **8a** (R = hexyl) and **8b** (R = decyl).

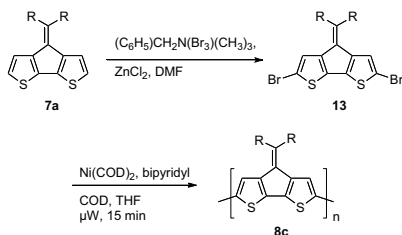
The resulting monomers could be oxidatively polymerized to the polymers **8a/b** using FeCl₃ as oxidizing agent as extensively described for poly(alkylthiophene)s.^[29, 30] Hereby, a mixture of FeCl₃ and monomer **7a/b**, respectively, was stirred in chloroform for 48 h in a light stream of argon.^[18, 29, 31] After dedoping treatment with hydrazine hydrate a dark blue polymer was isolated by precipitation into methanol. The crude product was purified by Soxhlet extraction with methanol and acetone and reprecipitation from chloroform into methanol. The resulting polymer was fully soluble in chloroform. GPC analysis using polystyrene standards showed the polymer to have reasonably high mean average molecular weights M_n (Table 4.1) of 4,200 for polymer **8a** and 5,700 for polymer **8b**. The polymer structure was confirmed by ¹H-NMR spectroscopy.

Table 4.1. Synthesis, yields, molecular weight data and optical properties of polymers **8a-c** and **14**.

Polymer	Coupling agent	Yield [%]	M_n/M_w	Absorption
				maximum λ_{max} chloroform solution/film [nm]
8a	FeCl ₃	32	4,200/9,700	593/n.m.
8b	FeCl ₃	44	5,700/10,400	621/699
8c	Ni(COD) ₂	14	1,600/3,300	570/n.m.
14	NiCl ₂ /Zn	40	9,000/16,300	566/567

8a,c: R = hexyl; **8b**: R = decyl

An alternate route towards polymer **8** followed a standard Yamamoto-type aryl-aryl coupling protocol (Scheme 4.5). First, compound **7a** was brominated with a mixture of benzyltrimethylammonium tribromide and zinc chloride, yielding the dibromo monomer **13**. The Ni(COD)₂-catalyzed polycondensation was carried out utilizing a microwave-assisted heating protocol. This method is known to give polymers in reasonable yields and high molecular weights.^[32] However, for monomer **13** polymer **8c** was achieved only in low yields (14 %) indicating that the dibromo derivative **13** is not well-suited for Yamamoto-type aryl-aryl couplings. The polymer **8c** obtained via Yamamoto-type coupling was purified by Soxhlet extraction of the precipitate with methanol, acetone, and chloroform, respectively, while an insoluble part remained as a dark colored powder. GPC measurements of the chloroform-soluble fraction against polystyrene standards showed a mean average molecular weight M_n of only 1,600 g/mol.



Scheme 4.5. Preparation of polymer **8c** via a Yamamoto-type coupling.

4.2.6 Optical Spectroscopy

As mentioned before, polymer **8** is expected to form π -stacked solid-state aggregates due to the in-plane arrangement of the alkyl side-chains. The observed distinct red shift of the absorption maximum of the solid-state UV-Vis spectrum of **8b** (Figure 4.1) compared to the solution spectrum (dilute solution in chloroform) suggests a significant face-to-face interchain stacking of the polymer chains in the solid state. A dilute chloroform solution of **8b** (R: n-decyl) shows a long-wavelength UV-Vis maximum at 621 nm. The solid-state absorption maximum is red-shifted to 699 nm indicating the formation of electronically interacting, π -stacked aggregates. This observation is supported by the presence of a vibronic side-band (shoulder at 645 nm) in the solid-state UV-Vis spectrum, a total quenching of the fluorescence emission and the decreased solubility of **8b** when stored in solution for several days (due to aggregate formation).

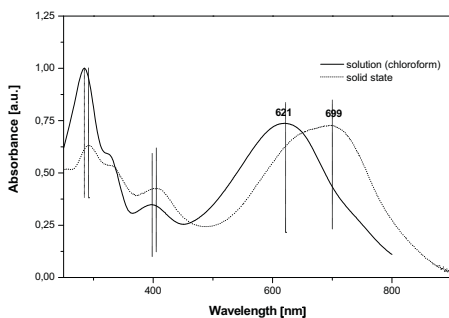


Figure 4.1. UV-Vis spectra of poly(didecylmethylene-CPDT) **8b** in solution (chloroform) and in the solid state.

For comparison, Figure 4.2 shows the absorption spectra of poly(dialkyl-CPDT) **14** bearing out-of-plane alkyl substituents.^[17] **14** shows a solution absorption maximum peaking at 566 nm (dilute chloroform solution, Figure 4.2). The solid-state UV-Vis spectrum of **14** does not exhibit any red shift of the absorption maximum. The comparison of the absorption spectra of **8** and **14** (Figures 5.1 and 5.2) illustrates the dominant role that the positioning of the substituents (in-plane vs. out-of-plane) plays in permitting efficient π -stacking in the solid state. Only the presence of in-plane substituents allows for a π -stacked face-to-face packing of the conjugated polythiophene backbones.

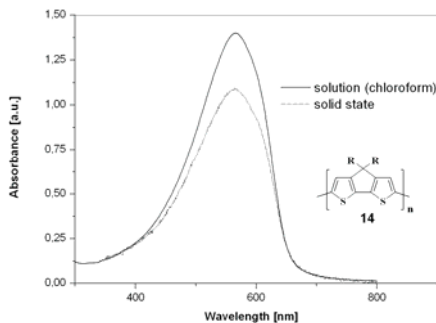


Figure 4.2. UV-Vis spectra of poly(dialkyl-CPDT) **14** in dilute solution (chloroform) and in the solid state.

4.2.7 Electrical Properties

The polymer **8** was tested in a bulk heterojunction solar cell setup with polymer **8** as an electron donor material and the C₆₀ derivative PCBM as an electron acceptor in the group of Dr. C. Brabec, Konarka Technologies, Linz, Austria.

The optimal orbital energies for an electron donor are determined by the energy thresholds that ensure air stability and a sufficient charge transfer to the fullerene acceptor.^[33] In order to ensure air stability, the HOMO level of the donor polymer donor has to be 5.2 eV or lower.^[34] Simultaneously, the LUMO level of the donor should have an offset of approximately 0.3 - 0.4 eV relative to the LUMO level of the acceptor material to allow effective charge transfer (LUMO PCBM: 4.2 eV).

One of the best performing polymers in bulk heterojunction solar cells is poly(3-hexyl- thiophene) (P3HT) and although the HOMO (5.12 eV) is close to stability limit the LUMO level (2.95 eV)

needs to be reduced further to circumvent energy losses. The energy levels of P3HT are compared to those of polymer **8** in Table 4.2.

Table 4.2. Comparison of the energy levels of P3HT, **8b**, and PCBM.

polymer	P3HT	8b	PCBM
LUMO level	2.95 eV	3.25 eV	4.2 eV
HOMO level	5.12 eV	4.84 eV	6.0 eV
energy gap E_g	2.17 eV	1.59 eV	1.8 eV

In comparison to P3HT the LUMO level of polymer **8** is reduced by 0.3 eV (2.95 eV vs. 3.25 eV). At the same time the HOMO level is affected as well and rises from 5.12 eV to 4.84 eV. Therefore, polymer **8** should show a low oxidative stability. Moreover, polymer **8** also shows a reduced offset between the HOMO level of the donor polymer and the LUMO level of the PCBM acceptor. Therefore, the open circuit voltage of an **8**/PCBM bulk heterojunction photovoltaic device was only about 300 mV, insufficient for commercial applications.

4.3 Conclusion

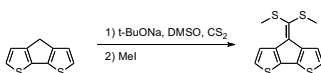
Two novel 4-dialkylmethylene-CPDT monomers were synthesized and oxidatively coupled using FeCl_3 . Comparison of the UV-Vis absorption spectra of poly(cyclopentadithiophene)s with either in-plane (4-dialkylmethylene-CPDT) or out-of-plane (4,4-dialkyl-CPDT) alkyl chains revealed a strong preference for intermolecular π -stacking for the poly(CPDT)s composed of planar building blocks. This result defines an important design rule for semiconducting polymers with optimized solid-state π -stacking: “in-plane” alkyl chains are superior over an “out-of-plane” arrangement of the solubilizing substituents.

4.4 Experimental Section

Materials and Characterization. Unless otherwise indicated, all reagents were obtained from commercial suppliers and were used without further purification. The solvents used were commercial p.a. quality. The reactions were carried out under argon with the use of standard and Schlenk techniques. The vials for the microwave assisted reactions were filled in a glove box. ^1H - and ^{13}C -NMR data were obtained on a Bruker ARX 400-spectrometer. The UV-Vis and fluorescence spectra were recorded on a Jasco V-550 spectrophotometer and a Varian-Cary Eclipse

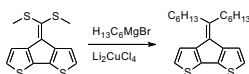
photoluminescence spectrometer, respectively. Gel permeation chromatographic analysis (GPC) utilized PS-columns (two columns, 5 μm gel, pore widths mixed bed linear) connected with UV/Vis and RI detection. All GPC analyses were performed on solutions of the polymers in THF at 30 $^{\circ}\text{C}$ (concentration of the polymer: approx. 1.5 g/L). The calibration was based on polystyrene standards with narrow molecular weight distribution. Microwave-assisted syntheses were performed using a CEM Discover microwave system.

4-[Bis(methylsulfanyl)methylene]-4*H*-cyclopenta[2,1-*b*:3,4-*b'*]dithiophene (**12**)



To a solution of cyclopentadithiophene **10** (1 g, 5.6 mmol) in dry DMSO sodium *tert*-butoxide (1.13 g, 11.8 mmol, 2.1 eq) was added in small portions at r.t. under argon followed by carbon disulfide (472 mg, 6.2 mmol, 1.1 eq) and the reaction mixture stirred for 10 min. Afterwards, methyl iodide (0.74 ml, 11.8 mmol, 2.1 eq) was added via a syringe and the reaction mixture stirred for additional 4 h. The reaction mixture was poured into ice-water and mixed with an aqueous solution of ammonia to bind the remaining methyl iodide. The resulting precipitate was extracted with *tert*-butyl ethyl ether and washed with water. The combined organic layers were dried over Na_2SO_4 and the solvent removed *in vacuo*. The crude product was purified by column chromatography on silica (eluent: hexane) to afford the product as a dark red oil (yield: 1.28 g, 81%). $^1\text{H-NMR}$ (400 MHz, CDCl_3): δ [ppm] = 7.81 (d, 1H, $J=5.1\text{Hz}$), 7.07 (d, 1H, $J=5.1\text{Hz}$), 2.54 (s, 6 H). $^{13}\text{C-NMR}$ (100MHz, CDCl_3): δ [ppm] = 143.6, 141.3, 138.0, 133.6, 125.0, 123.3, 17.9. mass: m/z (%) = 282 (M^+ , 100), 252 (10), 220 (43), 203 (31), 176 (17), 132 (7), 110 (12), 69 (6), 45 (11). Anal. Calcd. for $\text{C}_{12}\text{H}_{10}\text{S}_4$: C, 51.02; H, 3.57; S, 45.41; Found: C, 50.97; H, 3.82; S, 45.12.

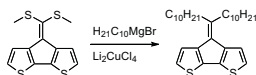
4-(Dihexylmethylene)-4*H*-cyclopenta[2,1-*b*:3,4-*b'*]dithiophene (**7a**)



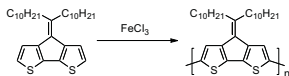
To a stirred solution of 4[bis(methylsulfanyl)methylene]-4*H*-cyclopenta[2,1-*b*:3,4-*b'*]dithiophene **12** (400 mg, 1.4 mmol) in THF (10 ml) at -5°C under nitrogen lithium tetrabromocuprate (0.35 ml, 2.5 mol%, 0.1 M in THF) was added, followed by a dropwise addition of hexylmagnesium bromide (3.1 ml, 3.1 mmol, 1 M in Et_2O), keeping the temperature below 0°C . The reaction was stirred

for further 4 h at -5°C and then quenched by the addition of a conc. aqueous solution of sodium hydroxide (10 ml). The mixture was stirred for 10 min, then filtered through celite and extracted with ethyl acetate until the organic solution was clear. The combined organic phases were washed with a conc. aqueous solution of sodium hydroxide, saturated sodium bisulfite, and brine. The organic layer was dried over sodium sulfate and the solvent removed *in vacuo*. The crude product was purified by column chromatography on silica (eluent: hexane) to afford the product as a yellow oil (yield: 266 mg, 53%). $^1\text{H-NMR}$ (400 MHz, CDCl_3): δ [ppm] = 7.13 (d, 2H, $J=5.0\text{Hz}$), 7.07 (d, 2H, $J=5.0\text{Hz}$), 2.58 (m, 4H), 1.56 (m, 4H), 1.39 (m, 4H), 1.27 (m, 8H), 0.84 (m, 6H). $^{13}\text{C-NMR}$ (100MHz, CDCl_3): δ [ppm] = 149.9, 143.6, 136.8, 127.9, 123.7, 123.1, 35.8, 34.1, 31.8, 29.9, 29.7, 29.1, 22.6, 22.3, 14.1. mass: m/z (%) = 358 (100), 274 (8), 217 (17), 203 (17), 189 (12), 43 (16). Anal. Calcd. for $\text{C}_{22}\text{H}_{30}\text{S}_2$: C, 73.68; H, 8.43; S, 17.88; Found: C, 73.21; H, 7.99; S, 17.69.

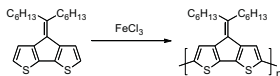
4-(Didecylmethylene)-4H-cyclopenta[2,1-b:3,4-b']dithiophene (7b)



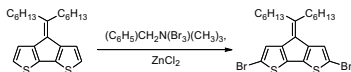
To a stirred solution of lithium tetrachlorocuprate (1.8 ml, 2.5 mol%, 0.1 M in THF) in THF (10 ml) at -5°C under nitrogen 4[bis(methylsulfanyl)methylene]-4H-cyclopenta[2,1-b:3,4-b']-dithiophene **12** (2.0 g, 7.1 mmol) in THF (20 ml) was added, followed by a dropwise addition of decylmagnesium bromide (20.0 ml, 20.0 mmol, 1 M in Et_2O) under keeping the temperature below 0°C . The reaction was stirred for further 9 h at -5°C and then quenched by the addition of a conc. aqueous solution of sodium hydroxide (10 ml). The mixture was stirred for 10 min, then filtered through celite and extracted with ethyl acetate until the organic solution was clear. The combined organic phases were washed with a conc. aqueous solution of sodium hydroxide, saturated sodium bisulfite, and brine. The organic layer was dried over sodium sulfate and the solvent was removed *in vacuo*. The crude product was purified by column chromatography on silica (eluent: hexane) to afford the product as a yellow oil (yield: 2.07 g, 62 %). $^1\text{H-NMR}$ (400 MHz, $\text{C}_2\text{D}_2\text{Cl}_4$): δ [ppm] = 7.14 (d, 2H, $J=5.0\text{Hz}$), 7.07 (d, 2H, $J=4.9\text{Hz}$), 2.59 (m, 4H), 1.56 (m, 4H), 1.39 (m, 4H), 1.22 (m, 12H), 0.83 (t, 6H, $J=6.8\text{Hz}$). $^{13}\text{C-NMR}$ (100MHz, $\text{C}_2\text{D}_2\text{Cl}_4$): δ [ppm] = 151.0, 143.8, 136.8, 127.8, 124.3, 123.5, 36.0, 32.1, 30.5, 29.9, 29.8, 29.8, 29.6, 29.4, 23.0, 14.5. mass: m/z (%) = 470 (M^+ , 100), 329 (6), 216 (27), 202 (21), 189 (12), 184 (9), 176 (7), 43 (15). Anal. Calcd. for $\text{C}_{30}\text{H}_{46}\text{S}_2$: C, 76.53; H, 9.85; S, 13.62; Found: C, 76.92; H, 9.43; S, 14.01.

Poly{2,6-[(4-(didecylmethylene)-4*H*-cyclopenta[2,1-*b*:3,4-*b'*]*dithiophene*)]} (8b**)**

In a two-neck round-bottom flask 4-(didecylmethylene)-4*H*-cyclopenta[2,1-*b*:3,4-*b'*]*dithiophene* **7b** (750 mg, 1.6 mmol) was mixed with dry chlorobenzene (50 ml). To this solution anhydrous FeCl₃ (1.04 g, 6.4 mmol) in dry chlorobenzene was added and the mixture stirred for 48 h at r.t. under a gentle stream of argon. The (oxidized) polymer was precipitated into methanol and the crude product was dedoped by refluxing it in chloroform/hydrazine hydrate for 24 h. Soxhlet extraction with methanol and acetone, and further precipitation from a chloroform solution into methanol gave the blue colored polymer **8b** (yield: 329 mg, 44%). ¹H-NMR (400 MHz, toluene-*d*₈, 353 K): δ [ppm] = 7.06 (br, s, 2H); 1.79-0.87 (br, m, 42H). UV/VIS: λ_{max} [nm]: 621 (chloroform), 699 (film). Anal. Calcd. for C₃₀H₄₄S₂: C, 76.86; H, 9.46; S, 13.68; Found: C, 76.43; H, 9.33; S, 13.44. GPC [g/mol]: M_n: 5,900; M_w 10,400.

Poly{2,6-[(4-(dihexylmethylene)-4*H*-cyclopenta[2,1-*b*:3,4-*b'*]*dithiophene*)]} (8a**)**

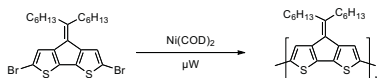
8a was prepared as described for polymer **8b** (yield: 32%). ¹H-NMR (400 MHz, C₂D₂Cl₄, 353 K): δ [ppm] = 7.13 (br, s, 2H), 2.49 (m, 4H), 1.65 (br, m, 4H), 1.49 (br, m, 4H), 1.32 (br, m, 8H), 0.80 (br, m, 6H). UV/VIS: λ_{max} [nm]: 593 (chloroform). Anal. Calcd. for C₂₂H₂₈S₂: C, 74.10; H, 7.91; S, 17.98; Found: C, 73.33; H, 7.54; S, 17.84. GPC [g/mol]: M_n: 4,200; M_w 9,700.

2,6-Dibromo-4-(dihexylmethylene)-4*H*-cyclopenta[2,1-*b*:3,4-*b'*]*dithiophene* (13**)**

To a mixture of benzyltrimethylammonium tribromide (2.06 g, 5.3 mmol) and zinc chloride (0.75 g, 5.5 mmol) a solution of 4-(dihexylmethylene)-4*H*-cyclopenta[2,1-*b*:3,4-*b'*]*dithiophene* **7a** (0.9 g, 2.5 mmol) in DMF (40 ml) was added via a syringe and the mixture stirred at r. t. for 2.5 h.

Afterwards water (20 ml) and an aqueous solution of NaHSO₃ (20 ml) were added dropwise. After removing the solvents, the crude product was purified by column chromatography on silica (eluent: hexane/ethyl acetate : 95/5) to give an orange solid (yield: 1.6 g, 56 %). ¹H-NMR (400 MHz, C₂D₂Cl₄): δ [ppm] = 7.11 (s, 2H), 2.52 (m, 4H), 1.51 (m, 4H), 1.37 (m, 1H), 1.26 (m, 1H), 0.84 (t, 1H, J=7.0Hz). ¹³C-NMR (100MHz, C₂D₂Cl₄): δ [ppm] = 152.8, 141.0, 136.4, 127.4, 126.0, 110.0, 35.7, 31.7, 29.7, 29.1, 22.5, 14.0. mass: m/z (%) = 516 (42), 498 (11), 279 (82), 217 (24). Anal. Calcd. for C₂₂H₂₈Br₂S₂: C, 51.17; H, 5.47; S, 12.42; Found: C, 50.97; H, 5.18; S, 12.03.

Poly{2,6-[(4-(dihexylmethylene)-4*H*-cyclopenta[2,1-b:3,4-b']dithiophene)]} (8c)



2,6-Dibromo-4-(dihexylmethylene)-4*H*-cyclopenta[2,1-b:3,4-b']dithiophene **13** (55 mg, 0.1 mmol), Ni(COD)₂ (70.3 mg, 0.26 mmol) and 2,2'-bipyridyl (36.6 mg, 0.23 mmol) were mixed in a 10 ml microwave tube in the glovebox. Afterwards THF (2 ml) and COD (25.3 mg, 0.23 mmol) were added via a syringe. The mixture was heated in a microwave reactor to a maximum temperature of 110 °C for 15 min. The precipitate was isolated and Soxhlet extracted with chloroform. The chloroform solution was concentrated and re-precipitated into methanol, yielding a blue colored solid (yield: 5 mg, 14%). ¹H NMR (400 MHz, C₂D₂Cl₄, 353 K): δ [ppm] = 7.11 (br, s, 2H), 2.53 (m, 4H), 1.62 (br, m, 4H), 1.45 (br, m, 4H), 1.32 (br, m, 8H), 0.84 (br, m, 6H). UV/VIS: λ_{max} [nm]: 570 (chloroform). C₂₂H₂₈S₂: C, 74.10; H, 7.91; S, 17.98; Found: C, 73.54; H, 7.21; S, 17.44. GPC [g/mol]: M_n: 1,600; M_w 3.300.

4.5 References and Notes

1. Tang, C. W., *Appl. Phys. Lett.* **1986**, 48, (2), 183.
2. Sariciftci, N. S.; Smilowitz, L.; Heeger, A. J.; Wudl, F., *Science* **1992**, 258, (5087), 1474.
3. Archer, M. D.; Hill, R.; Archer, M. D.; Hill, R., *Clean Electricity From Photovoltaics, Series on Photoconversion of Solar Energy*. Imperial College Press, London: 2001.
4. Chapin, D. M.; Fuller, C. S.; Pearson, G. L., *J. Appl. Phys.* **1954**, 25, (5), 676.
5. Goetzberger, A.; Hebling, C., *Sol. Energy Mater. Sol. Cells* **2000**, 62, (1-2), 1.
6. Roncali, J., *Chem. Rev.* **1997**, 97, (1), 173.
7. Dimitrakopoulos, C. D.; Malenfant, P. R. L., *Adv. Mater.* **2002**, 14, (2), 99.
8. Hoppe, H.; Sariciftci, N. S., *J. Mater. Res.* **2004**, 19, (7), 1924.
9. Chirvase, D.; Chiguvare, Z.; Knipper, M.; Parisi, J.; Dyakonov, V.; Hummelen, J. C., *J. Appl. Phys.* **2003**, 93, (6), 3376.
10. Chirvase, D.; Parisi, J.; Hummelen, J. C.; Dyakonov, V., *Nanotechnology* **2004**, 15, (9), 1317.
11. Reyes-Reyes, M.; Kim, K.; Carroll, D. L., *Appl. Phys. Lett.* **2005**, 87, (8), 083506.
12. Padinger, F.; Rittberger, R. S.; Sariciftci, N. S., *Adv. Funct. Mater.* **2003**, 13, (1), 85.
13. Sirringhaus, H.; Brown, P. J.; Friend, R. H.; Nielsen, M. M.; Bechgaard, K.; Langeveld-Voss, B. M. W.; Spiering, A. J. H.; Janssen, R. A. J.; Meijer, E. W.; Herwig, P.; de Leeuw, D. M., *Nature* **1999**, 401, (6754), 685.
14. Aasmundtveit, K. E.; Samuelsen, E. J.; Guldstein, M.; Steinsland, C.; Flornes, O.; Fagermo, C.; Seeberg, T. M.; Pettersson, L. A. A.; Inganäs, O.; Feidenhans'l, R.; Ferrer, S., *Macromolecules* **2000**, 33, (8), 3120.
15. Breiby, D. W.; Samuelsen, E. J., *J. Polym. Sci., Part B* **2003**, 41, (20), 2375.
16. Mc Cullough, R. D.; Tristram-Nagle, S.; Williams, S. P.; Lowe, R. D.; Jayaraman, M., *J. Am. Chem. Soc.* **1993**, 115, (11), 4910.
17. Asawapirom, U.; Scherf, U., *Macromol. Rapid Commun.* **2001**, 22, (10), 746.
18. Coppo, P.; Cupertino, D. C.; Yeates, S. G.; Turner, M. L., *Macromolecules* **2003**, 36, (8), 2705.
19. Tsunoda, T.; Suzuki, M.; Noyori, R., *Tetrahedron Lett.* **1980**, 21, (14), 1357.
20. Beyer, R.; Kalaji, M.; Kingscote-Burton, G.; Murphy, P. J.; Pereira, V. M. S. C.; Taylor, D. M.; Williams, G. O., *Synth. Met.* **1998**, 92, (1), 25.
21. Ferraris, J. P.; Henderson, C.; Torres, D.; Meeker, D., *Synth. Met.* **1995**, 72, (2), 147.

22. Jordens, P.; Rawson, G.; Wynberg, H., *J. Chem. Soc.* **1970**, (2), 273.
23. Noyori, R.; Murata, S.; Suzuki, M., *Tetrahedron* **1981**, 37, (23), 3899.
24. Michael, U.; Hornfeld, A., *Tetrahedron Lett.* **1970**, (60), 5219.
25. Brenna, M. E., *PhD thesis*. Università degli Studi, Milano: 1993.
26. Kozaki, M.; Yonezawa, Y.; Okada, K., *Org. Lett.* **2002**, 4, (25), 4535.
27. Benincori, T.; Consonni, V.; Gramatica, P.; Pilati, T.; Rizzo, S.; Sannicola, F.; Todeschini, R.; Zotti, G., *Chem. Mater.* **2001**, 13, (5), 1665.
28. Heeney, M.; Bailey, C.; Giles, M.; Shkunov, M.; Sparrowe, D.; Tierney, S.; Zhang, W. M.; McCulloch, I., *Macromolecules* **2004**, 37, (14), 5250.
29. Coppo, P.; Cupertino, D. C.; Yeates, S. G.; Turner, M. L., *J. Mater. Chem.* **2002**, 12, (9), 2597.
30. Sugimoto, R.; Takeda, S.; Gu, H. B.; Yoshino, K., *Chem. Express* **1986**, (1), 635.
31. Coppo, P.; Adams, H.; Cupertino, D. C.; Yeates, S. G.; Turner, M. L., *Chem. Commun.* **2003**, (20), 2548.
32. Galbrecht, F.; Yang, X. H.; Nehls, B. S.; Neher, D.; Farrell, T.; Scherf, U., *Chem. Commun.* **2005**, (18), 2378.
33. Thompson, B. C.; Kim, Y. G.; Reynolds, J. R., *Macromolecules* **2005**, 38, (13), 5359.
34. deLeeuw, D. M.; Simenon, M. M. J.; Brown, A. R.; Einerhand, R. E. F., *Synth. Met.* **1997**, 87, (1), 53.

5 Fused-Ring Dithiophenes – Alternating Donor- Acceptor Copolymers – an outlook

5.1 Introduction and Motivation

Poly(carbazole-2,7-diyl)s show similar optical and electronic properties to their fluorine-2,7-diyl counterparts. They exhibit high photo- and electroluminescence quantum yields, are not sensitive to the formation of keto defects and do not show excimer emission. Poly(carbazole-2,7-diyl)s are promising semiconducting materials for OLED device applications showing high EL efficiencies. The 2,7-connection provides an uninterrupted conjugation along the main chain. A range of related polycarbazole homopolymers and copolymers have been synthesized by Leclerc *et al.*^[1, 2] and Iraqi *et al.*^[3-5]

The nitrogen of the carbazole units allows functionalization with alkyl or aryl groups.^[6-8] Also, due to the electron-rich nature of the 9*H*-carbazole system, polycarbazoles show good hole-transporting properties. Similar properties could be also expected for dithienopyrrole (**1**)-related polymers; the synthesis of such monomers will be outlined in the following chapter. Combination of such electron-rich, hole-transporting building blocks with electron-poor 2,1,3-benzothiadiazole **2** moieties will result in alternating donor-acceptor copolymers. These polymers can be generated in transition metal catalyzed cross-coupling reactions such as Stille- or Suzuki-type reactions, leading to novel materials with tunable electronic and optical properties. Related donor-acceptor copolymers can be also made starting from the electron-rich 4-dialkylmethylene-cyclopentadithiophene **3** building blocks (as described in Chapter 4).

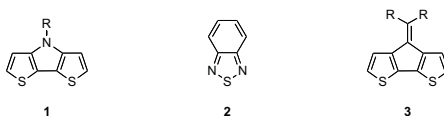
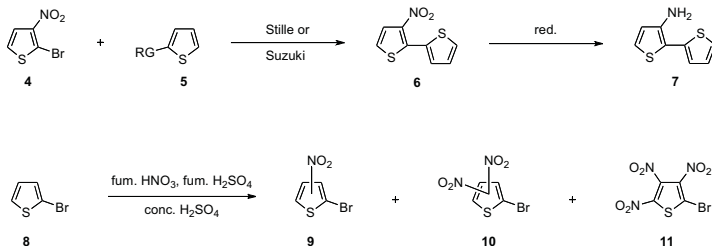


Figure 5.1. Structure of dithieno[3,2-b:2',3'-d]pyrrole **1**, 2,1,3-benzothiadiazole **2**, and 4-dialkylmethylene-cyclopentadithiophene **3**.

5.2 Results and Discussion

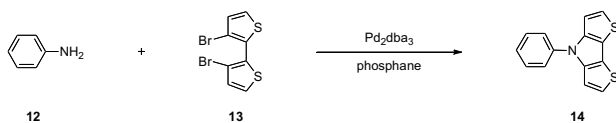
5.2.1 Monomer and Polymer Synthesis

The synthesis of carbazoles usually starts from *ortho*-aminobiphenyl compounds,^[9-17] followed by a later functionalization of the –NH–nitrogen after cyclization. However, most of these synthetic pathways require the use of strong acids to accomplish the *ortho*-cyclization. The transfer of this sequence to bithiophenes would start with 2-bromo-3-nitrothiophene **4** and its coupling to **6**. However, trial reactions for the nitration of 2-bromothiophene **8** following a protocol by Rasmussen *et al.* resulted in a complex mixture of reaction products with various substitution patterns (Scheme 5.1).^[18]



Scheme 5.1. Approach towards *ortho*-aminobithiophene via 2-bromo-3-nitrothiophene **4** (RG: –SnR₃, –B(OH)₂).

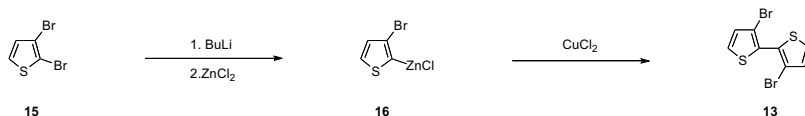
In a second synthetic approach a double *N*-arylation strategy is adopted. Although the double arylation of primary amines was successfully accomplished by Buchwald and others for the synthesis of triaryl amines^[12] the first synthesis of carbazole and dithienopyrrole systems utilizing a Buchwald-type reaction was recently reported by Tamao *et al.* in 2003 (Scheme 5.2).^[19]



Scheme 5.2. Double *N*-arylation in the synthesis of dithienopyrrole **14** after Tamao *et al.*

The starting molecule for this sequence is the commercially available 2,3-dibromo-thiophene **15** which is coupled to 3,3'-dibromo-2,2'-bithiophene **13** due to the much higher reactivity in the 2-positions. Derived from the classical synthesis of dialkyl and diaryl compounds in Wurtz- or

Ullmann-type reactions,^[20-26] the reductive dimerization of aryl halides can be also catalyzed by nickel or palladium complexes in the presence of reducing agents such as zinc powder.^[27, 28]

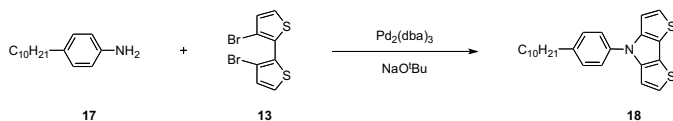
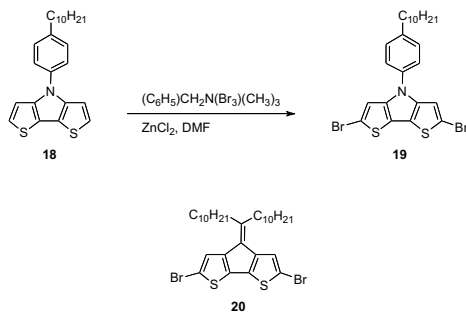


Scheme 5.3. Copper(II)-catalyzed oxidative coupling towards 3,3'-dibromo-2,2'-bithiophene **13**.

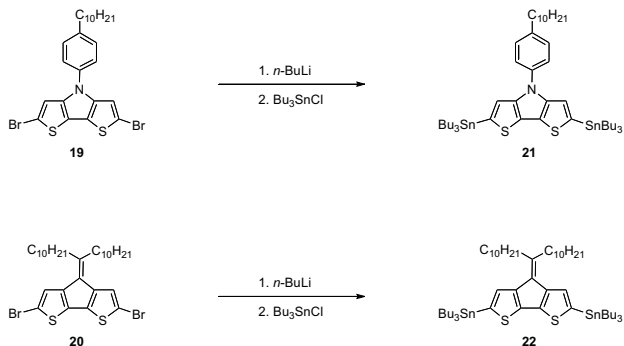
Despite the recent advances in palladium catalysis,^[29-33] copper- or nickel-mediated couplings are still often preferred. High yields have been found for the oxidative coupling of organocuprates. While lithium organocuprates show a poor functional group tolerance,^[34-36] magnesium organocuprates improved the reliability of the method.^[37-39] However, such reactions are limited by the requirement to have an electronically activated aryl precursor and the use of stoichiometric amounts of copper reagents. Further improvement of the reaction system led to the copper-catalyzed coupling of organozinc reagents, which show an improved functional group tolerance,^[40] undergo a rapid transmetalation with copper salts,^[41] and can be synthesized under mild conditions.^[42-45] The organozinc reagents can be obtained from the reaction of aryl bromides, which are often commercially available.

The actual synthesis of the bithiophene **13** follows a method reported by Iyoda *et al.* for the dimerization of arylzinc intermediates in a reaction sequence involving halogen-lithium exchange, transmetalation with $ZnCl_2$, and copper-catalyzed dimerization (Scheme 5.3).^[46, 47] Hereby, 2,3-dibromothiophene **15** was lithiated with *n*-BuLi in THF at $-78\text{ }^\circ\text{C}$, followed by treatment with $ZnCl_2$ at $-50\text{ }^\circ\text{C}$. The resulting zinc compound **16** was then treated with $CuCl_2$ at $-78\text{ }^\circ\text{C}$ and allowed to warm up to complete the coupling.^[46] Filtration and recrystallization from hexane gave the product **13** with excellent purity in 65 % yield. The purity of **13** was found to be crucial for the following reaction step as impurities reduce the yield of the target dithienopyrrole significantly.

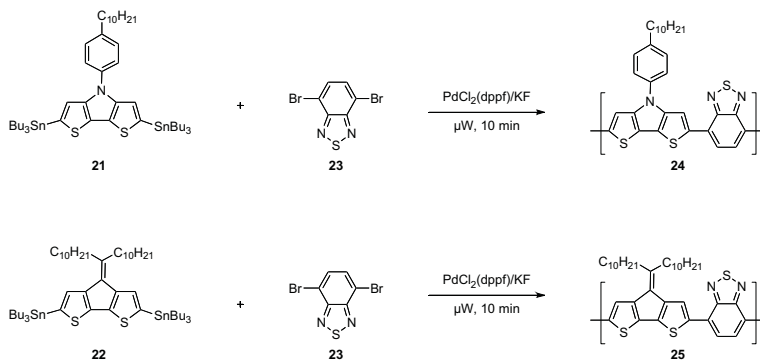
The next reaction step was a twofold palladium-catalyzed Buchwald-Hartwig-type reaction of the bithiophene **13** with 4-decylaniline **17** utilizing a $Pd(dba)_2 / NaO^tBu$ catalytic system (Scheme 5.4). Purification by column chromatography and recrystallization from hexane gave the product **18** in 42 % yield.^[19] Treatment of the “carbazole-analogue” **18** with benzyltrimethylammonium tribromide and zinc chloride in DMF gave the 2,6-dibrominated derivative **19** in 94 % yield.^[48] The reaction sequence used to obtain 2,6-dibromo-4-dialkylmethylene-cyclopentadithiophene **20** was described in Chapter 4.

Scheme 5.4. Double *N*-arylation in the synthesis of *N*-(4-decylphenyl)dithienopyrrole **18**.Scheme 5.5. Dibromo monomers **19** and **20**.

Two possible sequences may lead to the corresponding alternating donor-acceptor copolymers utilizing a Stille-type cross-coupling.^[49-51] Reaction of **19** with *n*-butyl lithium followed by treatment with tributyltin chloride gives the corresponding bis(tributylstannyl) monomer **21** in 91% yield, following a protocol reported by Yeh *et al.* (Scheme 5.6)^[52, 53] A similar procedure can be adopted for the conversion of **20** to **22**.^[54] Several attempts to copolymerize **21** or **22** with 4,7-dibromo-2,1,3-benzothiadiazole **23** following a Stille-type, microwave-assisted coupling protocol utilizing a $\text{PdCl}_2(\text{dppf})/\text{KF}$ catalytic system failed. Only low molecular weight oligomers with an

Scheme 5.6. Stannylation of 2,6-dibromodithienopyrrole **19** and 2,6-dibromo-4-didecyl-alkylmethylene-cyclopentadithiophene **20**.

average molecular weight (M_n) of about 1,500 g/mol could be obtained (Scheme 5.7). The low conversion might be due to the low reactivity of the electron-poor 4,7-dibromo-2,1,3-benzothiadiazole **23** in the Stille-type cross-couplings.



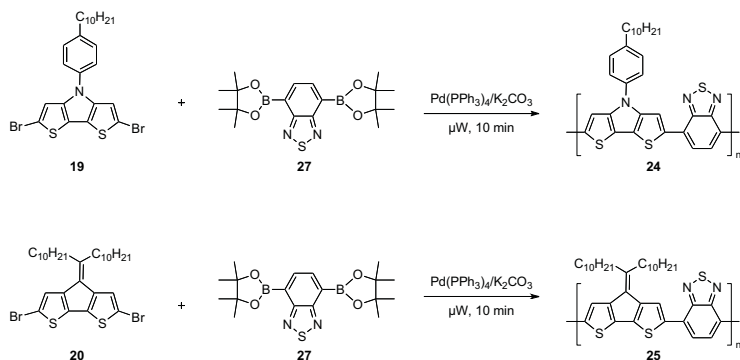
Scheme 5.7. Attempts to polymerize the distannylated monomers **21** and **22** with 4,7-dibromo-2,1,3-benzothiadiazole **23** in a microwave-assisted Stille-type coupling protocol.

To overcome the reactivity problem it was decided to invert the positions of the functional groups and to switch to a Suzuki-type cross-coupling starting from a 2,1,3-benzothiadiazole-4,7-diboronic ester **27** (Scheme 5.8).^[55, 56] Monomer **27** was generated by conversion of the dibromide **23** in a Suzuki-Miyaura-type reaction utilizing bis(pinacolato)diboron **26**.^[57, 58] **27** could be afforded in reasonable yields of 76 % but still contained ca. 8 % of the mono-boronic ester as revealed by HPLC analysis (92% bis /8% mono). Attempts to purify the material by column chromatography or recrystallization have been unsuccessful.

Therefore, it was not surprising that the initial, alternating copolymers made from **27** and the dibromo monomers **19** or **20**, respectively, in Suzuki-type, microwave-assisted cross-coupling reactions showed rather low mean average molecular weights (M_n) of only 1,000 g/mol.



Scheme 5.8. Generation of a 2,1,3-benzothiadiazole-4,7-bis(pinacolato)diboronate **27**.



Scheme 5.9. First attempts to polymerize the monomers **19** and **20** with 2,1,3-benzo-thiadiazole-4,7-diboronic ester **27** in a microwave-assisted Suzuki-type cross-coupling.

5.3 Conclusion

In conclusion, a novel dibromodithienopyrrole monomer was synthesized. In a subsequent reaction sequence the dibromodithienopyrrole was converted into the corresponding distannylated monomer. Initial attempts at Stille-type cross-coupling reactions of this monomer with 4,7-dibromo-2,1,3-benzothiadiazole only yielded low molecular weight oligomers.

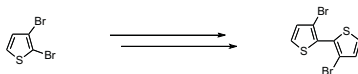
Changing to Suzuki-type cross-coupling conditions and using a 2,1,3-benzothiadiazole-4,7-diboronic ester monomer may be a promising alternative but could not be successfully completed until now. Improvement of the purity of the diboronic ester monomer seems necessary for the generation of high molecular weight donor-acceptor copolymers, and may be the target of further studies.

5.4 Experimental Section

Materials and Characterization. Unless otherwise indicated, all reagents were obtained from commercial suppliers and were used without further purification. The solvents used were commercial p.a. quality. The reactions were carried out under argon with the use of standard and Schlenk techniques. The vials for the microwave assisted reactions were filled in a glove box. ¹H- and ¹³C-NMR data were obtained on a Bruker ARX 400-spectrometer. The UV-Vis and fluorescence spectra were recorded on a Jasco V-550 spectrophotometer and a Varian-Cary Eclipse photoluminescence spectrometer, respectively. Gel permeation chromatographic analysis (GPC)

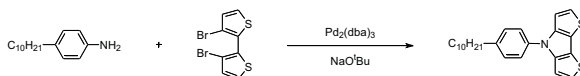
utilized PS-columns (two columns, 5 μm gel, pore widths mixed bed linear) connected with UV/Vis and RI detection. All GPC analyses were performed on solutions of the polymers in THF at 30 $^{\circ}\text{C}$ (concentration of the polymer: approx. 1.5 g/L). The calibration was based on polystyrene standards with narrow molecular weight distribution. Microwave-assisted syntheses were performed using a CEM Discover microwave system.

3,3'-dibromo-2,2'-bithiophene (13)



To a solution of 2,3-dibromothiophene (4.5 g, 18.6 mmol) in dry THF (150 ml) *n*-butyl lithium (13.2 ml, 20.5 mmol, 1.6 M) was added at -78°C and the mixture was stirred for 3 h. A solution of ZnCl_2 (2.79 g, 20.5 mmol) in dry THF (25 ml) was added to the reaction mixture at -50°C and the resulting mixture was stirred for 2 h. The reaction mixture was cooled to -78°C and copper(II)chloride (3.75 g, 27.9 mmol) added. After stirring for 2 h at -78°C , the reaction mixture was allowed to warm up to r. t. and stirred overnight. The organic phase was extracted with aq. HCl, aq. NaHCO_3 , aq. EDTA, and brine to give a crude product which was purified by column chromatography on silica (eluent: hexane), followed by recrystallization from hexane to give 3,3'-dibromo-2,2'-bithiophene in 80 % yield. ^1H NMR (400.1 MHz, $\text{C}_2\text{D}_2\text{Cl}_4$): δ [ppm] = 7.44 (d, 2H, J = 5.2 Hz), 7.11 (d, 2H, J = 5.2). ^{13}C NMR (100.6 MHz, $\text{C}_2\text{D}_2\text{Cl}_4$): δ [ppm] = 130.5, 125.9, 123.2, 112.5. LR-MS (EI, 70 eV): m/z = 324 [M^+] (90.8), 245 (42.8), 164 (100), 120 (35.1). Anal. Calcd. for $\text{C}_8\text{H}_4\text{Br}_2\text{S}_2$: C, 29.65; H, 1.24; S, 19.79. Found: C, 28.99; H, 1.11; S, 19.35.

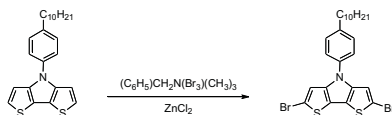
N-(4-Decylphenyl)-4H-dithieno[3,2-b;2',3'-d]pyrrole (18)



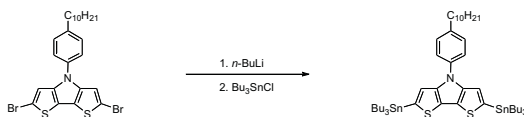
A mixture of 3,3'-dibromo-2,2'-bithiophene (324 mg, 1 mmol), sodium *tert*-butoxide (288.3 mg, 3 mmol), and $\text{Pd}_2(\text{dba})_3$ (9.5 mg, 0.01 mmol) in toluene (0.5 mL) was stirred at room temperature. A solution of 4-decylaniline (77.2 mg, 0.50 mmol) and tri(*tert*-butyl)phosphine (0.04 ml, 0.04 mmol) in toluene (0.5 mL) was then added under argon. The reaction mixture was heated to 80 $^{\circ}\text{C}$ for 16 h. The solvent was removed *in vacuo*, the crude product redissolved in hexane/toluene

(80/20), and filtered through a silica plug. Purification was accomplished by column chromatography on silica (eluent: hexane) to afford *N*-phenyl-4H-dithieno[3,2-b;2',3'-d]pyrrole) as pale yellow solid in 42 % yield (166 mg). R_f 0.15 (hexane) $^1\text{H NMR}$ (400.1 MHz, $\text{C}_2\text{D}_2\text{Cl}_4$): δ [ppm] = 7.40 (d, 2H, J = 5.5 Hz), 7.27 (d, 2H, J = 8.3 Hz), 7.18 (d, 2H, J = 8.3 Hz), 7.08 (d, 2H, J = 5.5 Hz), 2.64-2.57 (m, 2 H), 1.33-1.24 (m, 6 H), 0.89 (t, 3 H, J = 6.5 Hz) $^{13}\text{C NMR}$ (100.6 MHz, $\text{C}_2\text{D}_2\text{Cl}_4$): δ [ppm] = 149.3, 144.3, 137.5, 126.8, 123.5, 123.4, 116.9, 112.0, 35.6, 31.8, 31.1, 29.6, 29.5, 29.3, 29.2, 29.1, 22.6, 14.0. FD-MS: m/z = 395.1 (calcd. 395.6). Anal. Calcd. for $\text{C}_{24}\text{H}_{29}\text{NS}_2$: C, 72.86; H, 7.39; S, 16.21. Found: C, 72.35; H, 7.11; S, 16.04.

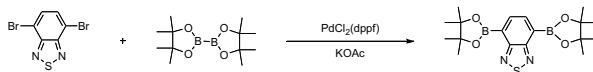
2,6-Dibromo- $\{N$ -(4-decylphenyl)-4H-dithieno[3,2-b;2',3'-d]pyrrole $\}$ (19)



Benzyltrimethylammonium tribromide (869 mg, 2.2 mmol) and zinc chloride (318 mg, 2.3 mmol) were mixed in a Schenk tube under argon atmosphere. Afterwards *N*-(4-decylphenyl)-4H-dithieno[3,2-b;2',3'-d]pyrrole (420 mg, 1.1 mmol) in DMF (40 ml) was added via a syringe and the mixture stirred at r. t. for 2.5 h. Afterwards water (20 ml) and aqueous NaHSO_3 -solution (20 ml) were added dropwise. The solvents were removed *in vacuo*. The crude product was purified by column chromatography on silica (eluent: hexane). Yield: 560 mg, 92 %. $^1\text{H NMR}$ (400.1 MHz, $\text{C}_2\text{D}_2\text{Cl}_4$): δ [ppm] = 7.55 (d, 2H, J = 5.6 Hz), 7.42 (d, 2H, J = 5.6), 7.19 (s, 2H), 2.69-2.62 (m, 2 H), 1.39-1.31 (m, 6 H), 0.89 (t, 3 H, J = 6.5 Hz) $^{13}\text{C NMR}$ (100.6 MHz, $\text{C}_2\text{D}_2\text{Cl}_4$): δ [ppm] = 150.2, 141.1, 136.5, 127.0, 122.7, 116.7, 115.7, 110.5, 35.6, 31.6, 31.0, 29.8, 29.5, 29.4, 29.4, 29.2, 22.5, 14.1. FD-MS: m/z = 552.8 (calcd. 553.4). Anal. Calcd. for $\text{C}_{24}\text{H}_{27}\text{Br}_2\text{NS}_2$: C, 52.09; H, 4.92; S, 11.59. Found: C, 51.89; H, 4.63; S, 11.32.

2,6-bis(tri-*n*-butylstannyl)-*N*-(4-decylphenyl)-4H-dithieno[3,2-b;2',3'-d]pyrrole (21)

2,6-Dibromo-*N*-(4-decylphenyl)-4H-dithieno[3,2-b;2',3'-d]pyrrole (486 mg, 0.88 mmol) was dissolved in dry THF (20 mL) under nitrogen and cooled to -78°C . *n*-BuLi in THF was added dropwise (1.16 mL, 1.86 mmol) and the reaction mixture stirred for 30 min. The solution was allowed to warm up to room temperature and stirred for an additional 1.5 h. The resulting thick brown suspension was cooled to -78°C and tri-*n*-butyltin chloride (0.50 mL, 1.86 mmol) added. The stirred solution was warmed up to room temperature. The mixture was quenched with 100 mL H_2O and extracted with hexane. The organic layer was washed with H_2O (6 x 50 mL) and dried over MgSO_4 . After filtration and evaporation of the solvent a brown oil was isolated (780 mg, 91 % yield) ^1H NMR (400.1 MHz, $\text{C}_2\text{D}_2\text{Cl}_4$): τ^{M} [ppm] = 7.50 (d, 2H, $J = 5.4$ Hz), 7.38 (d, 2H, $J = 5.4$), 6.98 (s, 2H), 2.73-2.66 (m, 2 H), 2.02 (m, 2H), 1.57 (m, 12H), 1.38-1.30 (m, 18H), 1.12 (m, 12H), 0.90 (m, 30H). ^{13}C NMR (100.6 MHz, $\text{C}_2\text{D}_2\text{Cl}_4$): τ^{M} [ppm] = 147.1 (t, $J = 113.4$ Hz), 146.3, 140.1 (t, $J = 498.0$ Hz), 127.0, 122.7, 117.0, (t, $J = 976.3$ Hz), 115.9, 110.7, 35.7, 31.8, 31.0, 29.7, 29.5, 29.4, 29.4, 29.2, 28.9 (m), 27.1 (m), 22.6, 14.1, 11.0 (m). FD-MS: $m/z = 973.9$ (calcd. 973.71). Anal. Calcd. for $\text{C}_{48}\text{H}_{81}\text{NS}_2\text{Sn}_2$: C, 59.21; H, 8.38; S, 6.59. Found: C, 58.99; H, 8.11; S, 6.55.

2,1,3-benzothiadiazole-4,7-bis(pinacolato) boronate (27)

A solution of 4,7-dibromo-2,1,3-benzothiadiazole (1 g, 3.41 mmol), bis(pinacolato) diboron (2 g, 7.8 mmol), $\text{PdCl}_2(\text{dppf})$ (500 mg, 0.6 mmol), and KOAc (2 g, 20 mmol) in degassed 1,4-dioxane (10 mL) was stirred at 80°C overnight. The reaction was quenched by addition of water, and the resulting mixture washed with ethyl acetate (3x 30 mL). The organic layer was washed with brine, dried over Na_2SO_4 , and concentrated *in vacuo* to yield a dark red solid. The solid was purified by column chromatography on silica (eluent: hexane/ethyl acetate : 97/3) to give the desired compound as a pink solid (600 mg, 46%). ^1H NMR (300 MHz, CD_2Cl_2): δ 8.10 (s, 2H), 1.41 (s, 24H).

^{13}C NMR (100.6 MHz, CD_2Cl_2): δ [ppm] = 157.6, 138.1, 120.3, 84.9, 25.3. FD-MS: m/z = 387.8 (calcd. 388.1).

5.5 References and Notes

1. Blouin, N.; Michaud, A.; Leclerc, M., *Adv. Mater.* **2007**, 19, (17), 2295.
2. Morin, J. F.; Leclerc, M.; Ades, D.; Siove, A., *Macrom. Rapid Commun.* **2005**, 26, (10), 761.
3. Iraqi, A.; Wataru, I., *Synth. Met.* **2001**, 119, (1-3), 159.
4. Iraqi, A.; Wataru, I., *J. Polym. Sci. Part A* **2004**, 42, (23), 6041.
5. Iraqi, A.; Wataru, I., *Chem. Mater.* **2004**, 16, (3), 442.
6. Iraqi, A.; Pegington, R. C.; Simmance, T. G., *J. Polym. Sci. Part A* **2006**, 44, (10), 3336.
7. Iraqi, A.; Pickup, D. F.; Yi, H. N., *Chem. Mater.* **2006**, 18, (4), 1007.
8. Iraqi, A.; Simmance, T. G.; Yi, H. N.; Stevenson, M.; Lidzey, D. G., *Chem. Mater.* **2006**, 18, (24), 5789.
9. Boger, D. L.; Duff, S. R.; Panek, J. S.; Yasuda, M., *J. Org. Chem.* **1985**, 50, (26), 5782.
10. Cadogan, J. I. G.; Cameron, M.; Mackie, R. K.; Searle, R. J. G., *J. Chem. Soc.* **1965**, (SEP), 4831.
11. Driver, M. S.; Hartwig, J. F., *J. Am. Chem. Soc.* **1995**, 117, (16), 4708.
12. Harris, M. C.; Buchwald, S. L., *J. Org. Chem.* **2000**, 65, (17), 5327.
13. Liu, Z. J.; Larock, R. C., *Org. Lett.* **2004**, 6, (21), 3739.
14. Soderberg, B. C. G., *Curr. Org. Chem.* **2000**, 4, (7), 727.
15. Wood, J. L.; Stoltz, B. M.; Dietrich, H. J.; Pflum, D. A.; Petsch, D. T., *J. Am. Chem. Soc.* **1997**, 119, (41), 9641.
16. Yamato, T.; Hideshima, C.; Suehiro, K.; Tashiro, M.; Prakash, G. K. S.; Olah, G. A., *J. Org. Chem.* **1991**, 56, (21), 6248.
17. Thayumanavan, S.; Basu, A.; Beak, P., *J. Am. Chem. Soc.* **1997**, 119, (35), 8209.
18. Kenning, D. D.; Mitchell, K. A.; Calhoun, T. R.; Funfar, M. R.; Sattler, D. J.; Rasmussen, S. C., *J. Org. Chem.* **2002**, 67, (25), 9073.
19. Nozaki, K.; Takahashi, K.; Nakano, K.; Hiyama, T.; Tang, H. Z.; Fujiki, M.; Yamaguchi, S.; Tamao, K., *Angew. Chem. Int. Ed.* **2003**, 42, (18), 2051.

20. Wurtz, A., *Ann. Chem. Phys.* **1855**, 275.
21. Wurtz, A., *Ann.* **1885**, 364.
22. Ullmann, F., *Ber.* **1903**, 2389.
23. Ullmann, F.; Spongel, P., *Ber.* **1905**, 2211.
24. Fanta, P. E., *Chem. Rev.* **1964**, 613.
25. Fanta, P. E., *Synthesis* **1974**, (1), 9.
26. Semmelhack, M. F.; Helquist, P.; Jones, L. D.; Keller, L.; Mendelson, L.; Ryono, L. S.; Smith, J. G.; Stauffer, R. D., *J. Am. Chem. Soc.* **1981**, 103, (21), 6460.
27. Kang, S. K.; Kim, T. H.; Pyun, S. J., *J. Chem. Soc., Perkin Trans. 1* **1997**, (6), 797.
28. Kondo, Y.; Matsudaira, T.; Sato, J.; Murata, N.; Sakamoto, T., *Angew. Chem. Int. Ed.* **1996**, 35, (7), 736.
29. Dai, C. Y.; Fu, G. C., *J. Am. Chem. Soc.* **2001**, 123, (12), 2719.
30. Cammidge, A. N.; Crepy, K. V. L., *Tetrahedron* **2004**, 60, (20), 4377.
31. Milne, J. E.; Buchwald, S. L., *J. Am. Chem. Soc.* **2004**, 126, (40), 13028.
32. Altenhoff, G.; Goddard, R.; Lehmann, C. W.; Glorius, F., *J. Am. Chem. Soc.* **2004**, 126, (46), 15195.
33. Su, W. P.; Urgaonkar, S.; McLaughlin, P. A.; Verkade, J. G., *J. Am. Chem. Soc.* **2004**, 126, (50), 16433.
34. Coleman, R. S.; Gurralla, S. R., *Org. Lett.* **2005**, 7, (9), 1849.
35. Dieter, R. K.; Li, S. J.; Chen, N. Y., *J. Org. Chem.* **2004**, 69, (8), 2867.
36. Surry, D. S.; Spring, D. R., *Chem. Soc. Rev.* **2006**, 35, (3), 218.
37. Ila, H.; Baron, O.; Wagner, A. J.; Knochel, P., *Chem. Commun.* **2006**, (6), 583.
38. Surry, D. S.; Fox, D. J.; MacDonald, S. J. F.; Spring, D. R., *Chem. Commun.* **2005**, (20), 2589.
39. Surry, D. S.; Su, X. B.; Fox, D. J.; Franckevicius, V.; Macdonald, S. J. F.; Spring, D. R., *Angew. Chem. Int. Ed.* **2005**, 44, (12), 1870.
40. Knochel, P.; Singer, R. D., *Chem. Rev.* **1993**, 93, (6), 2117.
41. Wipf, P., *Synthesis* **1993**, (6), 537.
42. Ikegami, R.; Koresawa, A.; Shibata, T.; Takagi, K., *J. Org. Chem.* **2003**, 68, (6), 2195.
43. Majid, T. N.; Knochel, P., *Tetrahedon Lett.* **1990**, 31, (31), 4413.
44. Fillon, H.; Gosmini, C.; Perichon, J., *J. Am. Chem. Soc.* **2003**, 125, (13), 3867.

45. Zhu, L.; Wehmeyer, R. M.; Rieke, R. D., *J. Org. Chem.* **1991**, 56, (4), 1445.
46. Kabir, S. M. H.; Miura, M.; Sasaki, S.; Harada, G.; Kuwatani, Y.; Yoshida, M.; Iyoda, M., *Heterocycles* **2000**, 52, (2), 761.
47. Kabir, S. M. H.; Hasegawa, M.; Kuwatani, Y.; Yoshida, M.; Matsuyama, H.; Iyoda, M., *J. Chem. Soc., Perkin Trans. 1* **2001**, (2), 159.
48. Asawapirom, U.; Scherf, U., *Macrom. Rapid Commun.* **2001**, 22, (10), 746.
49. Stille, J. K., *Angew. Chem. Int. Ed.* **1986**, 25, (6), 508.
50. Delnoye, D. A. P.; Sijbesma, R. P.; Vekemans, J. A. J. M.; Meijer, E. W., *J. Am. Chem. Soc.* **1996**, 118, (36), 8717.
51. Zhang, C. Y.; Tour, J. M., *J. Am. Chem. Soc.* **1999**, 121, (38), 8783.
52. Yoon, M. H.; DiBenedetto, S. A.; Facchetti, A.; Marks, T. J., *J. Am. Chem. Soc.* **2005**, 127, (5), 1348.
53. Wei, Y.; Yang, Y.; Yeh, J. M., *Chem. Mater.* **1996**, 8, (11), 2659.
54. Zhu, Z.; Waller, D.; Gaudiana, R.; Morana, M.; Muhlbacher, D.; Scharber, M.; Brabec, C., *Macromolecules* **2007**, 40, (6), 1981.
55. Suzuki, A., *J. Organomet. Chem.* **1999**, 576, (1-2), 147.
56. Miyaura, N.; Suzuki, A., *Chem. Rev.* **1995**, 95, (7), 2457.
57. Ishiyama, T.; Murata, M.; Miyaura, N., *J. Org. Chem.* **1995**, 60, (23), 7508.
58. Zhang, M.; Tsao, H. N.; Pisula, W.; Yang, C. D.; Mishra, A. K.; Müllen, K., *J. Am. Chem. Soc.* **2007**, 129, (12), 3472.

6 Acknowledgements

Mein größter Dank gilt meiner Familie, die mich auf meinem bisherigen Lebensweg jederzeit unterstützt hat. Ohne ihren Rückhalt wäre ich heute nicht der Mensch, der ich bin.

Ich möchte Herrn Professor Ullrich Scherf für die hilfreiche Unterstützung, zahlreich gebotene Möglichkeiten – sei es Mitarbeit an Projekten oder Teilnahme an Konferenzen – und hervorragende Ausbildung in Hinblick auf die zukünftige Laufbahn danken.

Ebenso möchte ich Herrn Professor Manfred Schneider danken, der mir durch seine unnachahmliche ihm zu eigene Art eine der größten und wichtigsten Lektionen meines Lebens gelehrt hat.

Den Bewohnern des Musiklabors möchte ich für die angenehme Atmosphäre, großartige Gemeinschaft, wunderbaren Touren rund um die Welt und die wummernden Bässe danken. Im Besonderen sind dabei folgende Personen zu nennen: Frank „Cluster-Stefan“ Galbrecht, Benjamin „Le Stefan“ Souharce, Christof „Pierogi-Stefan“ Kudla, Sven „Schweden-Stefan“ Weber, Benjamin Nehls und Nachwuchs-DJ Nils Koenen. Mit Euch lässt sich Laborarbeit in einer neuen Dimension erleben.

Weiterhin haben Argiri Tsami, Askin Bilge, Richard Charvet, Tony Farrell, Eduard Preis und Michael Forster als häufige Besucher des Musiklabors sehr zur angenehmen Atmosphäre und mit viel Erfahrung dem hohen Lernerfolg beigetragen. Letzterem möchte ich im Besonderen für die Korrekturen meiner Arbeit und dem schärfsten Essen nach Udom Asawapirom danken.

Ohne besondere Reihenfolge danke ich Sylwia Adameczyk, Anke Helfer, Sybille Allard, Dieter Belle, Udom Asawapirom, Roland Güntner, Swapna und Jitendra Kadam, Guoli Tu, Deqing Gao für viele Messungen, herzlichen Empfang in der Arbeitsgruppe und interkulturelle Erfahrungen.

Außerdem danke ich meinen Studenten Kristina Schottler, Stefan Stelljes, Felix Fuge, Daniel Gallenkamp und Ren Yi.

Bianca Enz, Du bist und bleibst die Gute Seele des AK Scherf.

I would like to thank the people at Cambridge Display Technology, who turned the hard part – the writing up – into a joyful experience. For their help and understanding I thank Richard Wilson and Thomas Pounds, and for the manifold distractions Ian Warburton, Ruth Pegington, James Wiltshire, Sheena Elliott and all other members of the Curry Club. Martin Humphries, many thanks for giving my thesis a good read-through.

Last but not least, I would like to thank all fellow students and colleagues from the different projects for the fruitful collaborations and equally important the great time in Wuppertal and elsewhere.

Nebenbei sollte ich noch den Herrn Suzuki vom Herrn Yamamoto grüßen.

Torsten „Stefan-Delüx“ Bünnagel